TOWARD PRACTICE OF COOPERATIVE WIRELESS NETWORKS: ENERGY SAVING AND INCENTIVE DESIGN

BY

A-LONG JIN

B.E., Nanjing University of Posts and Telecommunications, 2012

THESIS

Submitted in partial fulfillment of the requirements
for the degree of Master of Science in Computer Science
in the Graduate School of the
University of New Brunswick, 2014

Master's Committee:

Supervisor: Dr. Wei Song
Chairperson: Dr. Huajie Zhang
Internal: Dr. Michael W. Fleming
External Reader: Dr. Donglei Du

Abstract

Cooperative communications have been considered as a promising technique to deal with signal fading in wireless networks, and thereby increase the channel capacity. However, many practical issues remain to be addressed, especially in the medium access control (MAC) layer. In this thesis, we study two important issues toward the practice of cooperative wireless networks, i.e., energy saving and incentive design for cooperative MAC.

First, we propose an energy-efficient cooperative scheme for the widely studied scenario with a single source-destination (S-D) pair. Extending the classic model to multiple S-D pairs, we further propose an effective and scalable cooperative scheme. Theoretical analysis is conducted for both schemes, and simulation results show that both schemes can achieve significant energy saving.

In practice, due to the lack of incentives for wireless devices to serve as relay nodes, cooperative communications are still not widely applied. Hence, in addition to energy saving, we also design an auction-based incentive mechanism to coordinate cooperative transmission between S-D pairs and relays. Both theoretical analysis and numerical results show that the proposed mechanism guarantees desirable properties.

to Anqi and my parents

Acknowledgements

It is a great pleasure to express my respect to the many people who have supported me throughout my study at UNB.

Foremost, I would like to express my deep and sincere gratitude to my supervisor, Dr. Wei Song. Ever since I started working with Dr. Song, she has been giving me enough freedom to explore my own interests, and has generously and patiently spent much time discussing research ideas with me. Most importantly, her enthusiasm and vision in research has greatly inspired me, and her constant guidance and encouragement has made this work possible.

Furthermore, I would like to thank all the other thesis committee members, Dr. Huajie Zhang, Dr. Michael W. Fleming, and Dr. Donglei Du, for their generous time and commitment. Their constructive comments and invaluable suggestions are really appreciated.

Many thanks to my fellows Dizhi Zhou, Peijian Ju, Xiaojing Li, Qing Shen, and Kai Dong for the various valuable discussions I had with them as well as the joyful time we spent together.

Finally, I am grateful to my wife Anqi and my parents, whose unceasing love and support has helped me go through all the difficulties to complete the venture. I dedicate this thesis to them.

Contents

List of Tables

List of Figures

List of Symbols

Symbols in Chapter 3

S	Source node
D	Destination node
L	Distance between S and D
ν	Path-loss exponent
P_0	Transmit power
N_0	Power of additive white Gaussian noise
T_0	SNR threshold of signal decoding
R_i	Relay node
r_i	Distance of relay R_i to destination D
T_i	Backoff time of relay R_i
L_i	Distance of relay R_i to source S
λ	Relay intensity
$\lambda^{'}$	Potential relay intensity after thinning process
$\widetilde{\lambda}$	Estimated relay intensity
$\Delta\lambda$	Estimation error of relay intensity
Ω_L	The circle region with a diameter L, as shown in Fig. 3.1
Ω_r	The part of the circle centered at D of a radius r within Ω_L
$\mathcal{A}_r$	The area of region Ω_r
Λ_r / $\Lambda_r^{'}$	Intensity measure of potential relays in Ω_r with respect to λ / $\lambda^{'}$
ϱ_i	Sleeping probability of relay R_i
ζ_i	Active probability of relay R_i
$r_{(1)}$ / $r_{(2)}$	Distance of the first / second nearest potential relay to D
$f(r)$	The probability density function (PDF) of $r_{(1)}$
$F(r)$	The cumulative distribution function (CDF) of $r_{(1)}$
$\widetilde{F}(r)$	Estimated CDF of $r_{(1)}$
ΔF	Estimation error of $F(r)$
F_B	The bound of estimation error ΔF
E	Average energy consumption of a successful transmission
E_t	Energy consumption for transmitting a packet
E_r	Energy consumption for listening and receiving a packet
L_0	Threshold that determines the active / sleeping probability
P_{1^+} / P_{2^+}	The probability that at least one / two potential relay(s) in Ω_{L_0}
$g(r_1, r_2)/h(r_1)$	Joint PDF of $r_{(1)}$ and $r_{(2)}$
P_c	Collision probability
P_c^U	Upper bound for P_c
c	Collision window (time interval)
ϖ	Collision window (distance interval)
τ_i	Forwarding probability of R_i in probability-based scheme

Symbols in Chapter 4

S_j	Source node
D_j	Destination node
R_i	Relay node
n	Total number of S-D pairs
m	Total number of relay nodes
ν	Path-loss exponent
P_0	Transmit power
N_0	Power of additive white Gaussian noise
T_0	SNR threshold of signal decoding
$P_{S_j R_i}$	Transmission success probability of packets from S_j to R_i
$P_{R_i D_j}$	Transmission success probability of packets from R_i to D_j
$\mathcal{D}$	Packet delay
$\overline{\mathcal{D}}$	Average packet delay
$\mathcal{D}_{max}$	Acceptable upper bound of packet delay
P_{out}	Delay outage probability
ε	A small probability that is allowed for QoS violation
d_{ij}	Distance between relay R_i and destination D_j
l	Maximum distance of potential relays to a destination
W_{ij}^d	Cooperation capability of R_i for D_j with respect to d_{ij}
E_i	Energy level of R_i
E_c	Energy upper limit
W_{ij}^e	Cooperation capability of R_i for D_j with respect to E_i
$U(0,\ 1)$	Uniform distribution between 0 and 1
W_{ij}	Overall cooperation capability of R_i for D_j
ρ	Trade-off parameter between energy status and distance metric
χ_j	Set of relays that correctly overhear packet from S_j
$\mathbf{1}_{\chi_j}(\cdot)$	Indicator function
T_{ij}	Backoff time of R_i for the S_j-D_j pair
κ	Update step length
$f(d)$	The probability density function (PDF) of distance d_{ij}
$f_w(w)$	The PDF of the overall cooperation capacity
$f_T(t)$	The PDF of the backoff time
$F_T(t)$	The cumulative distribution function (CDF) of the backoff time
c	Collision window (time interval)
P_c	Collision probability
P_c^U	Upper bound for P_c
P_{suc}	Transmission success probability
P_{ij}	The probability that W_{ij} is the largest for D_j
Q_j	The probability that at least one potential relay forwards packet for S_j
$\overline{P_{ij}}$	The probability that R_i transmits packets for S_j in the long term
P_{suc}^L	Lower bound for P_{suc}
P_{suc}^U	Upper bound for P_{suc}
$\widetilde{P_{suc}^U}$	Relaxed upper bound for P_{suc}
$P_\tau^{(i)}$	Normalized relaying probability of R_i in probability-based scheme

Symbols in Chapter 5

b_i	Buyer (S-D pair)
s_j	Seller (relay)
n	Total number of buyers
m	Total number of sellers
$\mathcal{B}$	Set of buyers (S-D pairs)
b_{ij}	Buyer b_i with positive valuation toward seller s_j
$\mathcal{B}'$	Extended set of buyers with positive valuations
$\mathcal{S}$	Set of sellers (relays)
$\mathbb{B}$	Sorted buyer list of $\mathcal{B}'$ in a descending order of positive valuations
$\mathbb{S}$	Sorted seller list of $\mathcal{S}$ in an ascending order of asks
$\mathcal{B}_c$	Set of winning buyer candidates ($\mathcal{B}_c \subseteq \mathcal{B}$)
$\mathcal{S}_c$	Set of winning seller candidates ($\mathcal{S}_c \subseteq \mathcal{S}$)
$\mathcal{B}_a$	Set of winning buyers before elimination ($\mathcal{B}_a \subseteq \mathcal{B}_c$)
$\mathcal{S}_a$	Set of winning sellers before elimination ($\mathcal{S}_a = \mathcal{S}_c$)
$\mathcal{B}_w$	Set of winning buyers ($\mathcal{B}_w = \mathcal{B}_a$)
$\mathcal{S}_w$	Set of winning sellers ($\mathcal{S}_w \subseteq \mathcal{S}_a$)
$\hat{\sigma}(\cdot)$	Mapping function from the indices of $\mathcal{S}_a$ to $\mathcal{B}_a$
$\sigma(\cdot)$	Mapping function from the indices of $\mathcal{S}_w$ to $\mathcal{B}_w$
D_i^j	Bid of buyer b_i on seller s_j
$\mathbf{D}_i$	Bid vector of buyer b_i
$\mathbf{D}$	Bid matrix of all buyers
A_j	Ask of seller s_j
$\mathbf{A}$	Ask vector of all sellers
$\mathbf{A}_{-j}$	Ask vector of all sellers except s_j
V_i^j	Valuation of buyer b_i on relaying service from seller s_j
$\mathbf{V}_i$	Valuation vector of buyer b_i
C_j	Cost of seller s_j for providing relaying service
ϕ / φ	Parameters that determine the winning candidates
P_i^{b}	Price charged to buyer b_i
P_j^{s}	Payment rewarded to seller s_j
P_{ij}^{b}	Price charged to buyer b_i for relaying service of seller s_j
P_{ij}^{s}	Payment rewarded to seller s_j with assigned buyer b_i
U_i^{b}	Utility of buyer b_i
U_j^{s}	Utility of seller s_j
U_{ij}^{b}	Utility of buyer b_i with assigned seller s_j
U_{ij}^{s}	Utility of seller s_j with assigned buyer b_i

Chapter 1

Introduction

In the past decade, wireless networks [1] have been widely studied and used. However, wireless communications face several challenging issues which are not imposed in wired networks, such as mobility, power consumption, interference and reliability. Besides, signal fading is often a problem in wireless networks, which is caused by multipath propagation and shadowing. To deal with these challenges, attractive techniques, such as multiple input and multiple output (MIMO) [2, 3] and cooperative communications [4, 5], have been developed by exploiting spatial diversity [6]. Nonetheless, due to the size, cost and energy limitations of mobile devices, it can be infeasible to deploy multiple antennas in some wireless terminals. In order to meet the needs of future wireless networks, user cooperation [7] is studied as a promising low-cost technique to provide spatial diversity. Taking advantage of the inherent broadcasting nature of the wireless medium, the nodes with good channel conditions can forward the overheard data to facilitate the transmission between source (S) and destination (D).

Originally, most of the research works focus on the physical layer cooperation [4, 5], where the cooperative schemes pay more attention to the various methods of signal processing at the relay node and signal combination at the destination node. With physical layer cooperation, either diversity or multiplexing can be achieved, which improve the quality of communications in the upper layers. Since multiple cooperative nodes are available during packet transmission, it is vital to coordinate these nodes to access the channel in a cooperative fashion. To achieve the cooperation gain at upper layers, considerable research attention has been attracted to the medium access control (MAC) layer [8, 9]. Different from physical layer cooperation, MAC layer cooperation needs to figure out when to cooperate and whom to cooperate with. Although centralized solutions [8, 10, 11] can rely on a central controller to determine the best relays, distributed solutions also attract considerable research attention due to light signaling and good scalability. In the probability-based schemes [12, 13, 14], each relay that successfully overhears the data from the source independently determines a forwarding probability by synthesizing a variety of factors. In the backoff-based schemes [15, 16], each relay makes use of local information to tune a backoff time so that a best relay with a smallest backoff time wins the contention to forward the overheard data. Although cooperative MAC has been widely studied, many practical issues remain to be addressed.

1.1 Research Motivations

1.1.1 Energy Saving

Currently, plenty of schemes have been proposed for MAC layer cooperation. However, most of these works assume that the topology of the network is known *a priori* [14] and focus on the throughput perspective [8]. With rising energy costs and rigid environmental standards, green communications have attracted considerable research attention in recent years, especially for the fast-growing multimedia services in wireless networks [17, 18], since mobile devices are usually energy constrained. In this thesis, we will relax the assumption of deterministic known topology and develop cooperative MAC protocols to reduce energy consumption. Besides, we expect to extend the widely studied scenario with a single source-destination (S-D) pair to a more realistic scenario with multiple S-D pairs.

1.1.2 Incentive Design

As a promising technique, cooperative communications have been shown to have great potential to increase the channel capacity of wireless networks. However, the applications of cooperative communication techniques are rarely seen in reality. A main obstacle that hinders the wide adoption of cooperative communications is the lack of incentives for the wireless devices to serve as relay nodes. As a relay, the wireless device invests its resource, such as energy and network bandwidth, to facilitate packet transmissions for others. To stimulate the participation of wireless devices as relays, the relay nodes can be provided rewards in return. As seen, there exists a trade between the wireless devices requesting relaying services and the relay nodes providing such services.

Auction is a popular trading form that can efficiently distribute resources of sellers to buyers in a market at competitive prices. Auction theory [19] is a well-researched field in economics and has been applied to other domains, e.g., radio resource management in wireless communication systems [20]. An auction mechanism is expected to hold certain desirable properties, such as *individual rationality*, *budget balance*, and *system efficiency* [19]. Besides, *incentive compatibility* or *truthfulness* is another important aspect of auction design. Truthfulness is essential to resist market manipulation and ensure auction fairness. An auction mechanism is incentive compatible or truthful if revealing the private valuation truthfully is always the dominant strategy for each participant to receive an optimal utility, no matter what strategies other participants are taking.

There are many existing auction mechanisms that satisfy some of the above properties but are not directly applicable to cooperative communications. For example, the multi-round auctions studied in [21, 22, 23] are not suitable due to the high communication and computation overhead. We are particularly interested in double auction, in which *buyers* and *sellers* submit their bids and asks, respectively, to an *auctioneer* as an intermediate agent who hosts and directs the auction process, e.g., deciding the auction *commodity* allocation

and the clearing price and payment. Well-known examples of double auction include McAfee double auction [24] and Vickrey-based double auction [25]. Considering only homogeneous commodities, McAfee double auction can achieve three desired properties, i.e., individual rationality, budget balance, and truthfulness. The Vickrey-based auction proposed in [25] can be budget-balanced and efficient but not truthful simultaneously, according to [26]. A truthful double auction mechanism (TASC) is proposed in [27] for cooperative communications with heterogeneous trading commodities, i.e., services of relay nodes. Unfortunately, TASC cannot guarantee the truthfulness of buyers, even though it is still individually rational, budget-balanced, and truthful for sellers. Thus, in this thesis, we will focus on designing a feasible and truthful double auction mechanism to stimulate relay nodes to serve nearby wireless devices.

1.2 Research Contributions

In this thesis, we study two important issues toward the practice of cooperative communications, namely, energy saving and incentive design for cooperative MAC.

In Chapter 3 and Chapter 4, we focus on energy saving for cooperative MAC. In Chapter 3, we first develop an algorithm to estimate the unknown intensity of relay distribution, which is critical to properly engage cooperating nodes. The convergence and accuracy of the estimation algorithm are theoretically justified. Considering a backoff-based distributed relay scheme, we further incorporate an energy saving scheme to minimize energy consumption while maintaining satisfactory transmission success probability. The performance of the proposed cooperative scheme, particularly the collision probability, is analytically evaluated, since it determines the transmission success probability and thus the average energy consumption. The theoretical and simulation results validate our analysis and demonstrate that the proposed cooperative scheme outperforms the uncoordinated reference scheme with respect to transmission performance and energy saving. In Chapter 4, extending the single S-D pair cooperation scenario, we consider a new framework where multiple S-D pairs share a group of relays with energy constraint. To satisfy the quality-of-service (QoS) requirements of multimedia services in a green manner, we propose an energy-aware distributed cooperation scheme based on the backoff timer. Also, its performance is evaluated analytically with respect to the theoretical bounds of the collision probability and the transmission success probability. Extensive simulations are conducted to compare the performance of different distributed schemes and the analytical bounds. The theoretical and simulation results demonstrate that our proposed scheme is preferable for the delay-sensitive multimedia services and achieves significant energy saving.

In Chapter 5, we focus on the incentive design for cooperative MAC. To stimulate wireless devices to serve as relay nodes, we propose an incentive-compatible auction mechanism (ICAM). The ICAM ensures truthfulness for both buyers and sellers. In addition, ICAM is individually rational, budget-balanced, and computationally efficient. We provide rigorous analysis proving that the above desirable properties hold with ICAM. Numerical

results verify that these properties are achieved without substantial degradation to system efficiency, which is another crucial property of auctions.

1.3 Thesis Organization

The remainder of this thesis is structured as follows. We first provide background knowledge in Chapter 2, including cooperative wireless networks, relay selection and medium access control, energy efficient schemes and incentive mechanisms. We then propose two energy efficient schemes in Chapter 3 and Chapter 4 in detail, and give both theoretical and numerical evaluations on them. In Chapter 5, we present a feasible and truthful auction mechanism, as well as the rigorous proof of desirable properties. Finally, in Chapter 6, we conclude our work and point out future directions to explore.

Chapter 2

Background and Related Works

2.1 Cooperative Wireless Networks

2.1.1 Cooperation in Physical Layer

Although the open shared wireless medium poses the interference problem in wireless communications, cooperative diversity can take advantage of the broadcasting nature of wireless transmission. Consider the scenario shown in Fig. 2.1, where there are three nodes, the source node (S), the relay node (R) and the destination node (D).

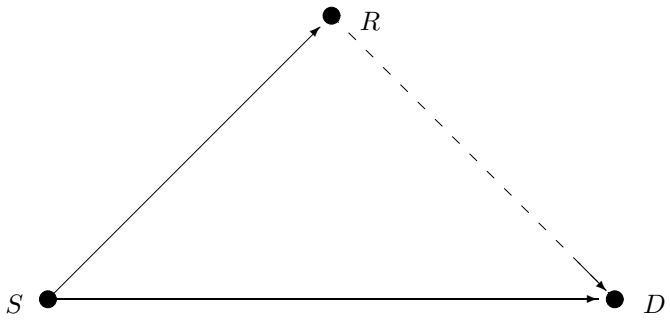

Figure 2.1: An illustration of cooperation in physical layer.

In the first time slot T_o, the source node transmits one packet, then the relay node and destination node will receive one copy of the packet. Let Z_{a_1,a_2} capture the effects of path-loss, shadowing and fading between node a_1 and node a_2, and $N_a[t]$ capture the effects of interference and noise in the receiver side. Then, we have:

$$Y_D[t] = Z_{S,D} \cdot X_S[t] + N_D[t], \quad t \in (0, T_o] \tag{2.1}$$

$$Y_R[t] = Z_{S,R} \cdot X_S[t] + N_R[t], \quad t \in (0, T_o] \tag{2.2}$$

where $X_S[t]$ is the signal transmitted by the source node, $Y_D[t]$ and $Y_R[t]$ are the destination and relay received signals, respectively.

In the second time slot, the relay node forwards the received packet to the destination node, and the desti-

nation node will get the second copy of the packet. Then, we have:

$$Y_D[t] = Z_{R,D} \cdot X_R[t] + N_D[t], \quad t \in (T_o, 2T_o]. \tag{2.3}$$

Here, several relaying schemes can be used by the relay, such as amplify-and-forward (AF), decode-and-forward (DF), and coded-cooperation (CC) [4, 5]. Based on this cooperation model, the destination can retrieve the original signal by combining the two received copies of the packet to improve the decoding reliability.

2.1.2 Cooperation in MAC Layer

Through cooperation in the physical layer, the channel reliability can be improved via spatial diversity. However, when multiple relay nodes are available, they can access the wireless medium at the same time, which leads to packet corruption. Besides, wireless networks may also suffer from some other issues, such as time varying channel, mobility and limited power of the hosts, and hidden terminal problem caused by location-dependent carrier sensing. In order to overcome these problems and achieve good performance in wireless networks, the MAC layer should properly schedule all the cooperative entities to achieve the cooperation gain.

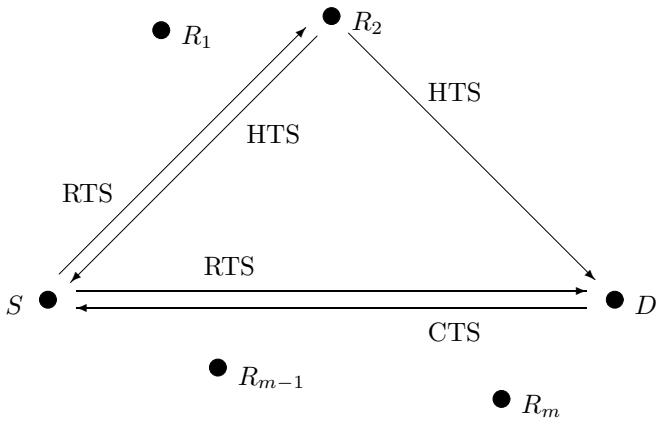

Figure 2.2: An illustration of cooperation in MAC layer.

The cooperative MAC protocol proposed in [8] illustrates the basic idea of cooperation in the MAC layer. Consider the scenario shown in Fig. 2.2, where there are a source node (S), a number of relay nodes ($R_1, ..., R_m$) and a destination node (D). Each node in the network maintains a CoopTable which is used to keep records of potential relay nodes. Besides, an extra control message called HTS (Helper ready To Send) is defined for the relay node to acknowledge its participation in the transmission. The CoopMAC protocol proposed in [8] is briefly described as follows:

Source Node:

(a) Whenever the source node has data to transmit, it will check the CoopTable to search for a relay node candidate (with an average data rate higher than that of direct transmission). If such a relay

node is successfully found, the source node sends the RTS (Request To Send) control message with the indication of the selected relay candidate. If such a relay candidate is not found, the regular IEEE 802.11 MAC procedure will be followed.

(b) If neither an HTS from the relay candidate nor a CTS (Clear To Send) message from the destination node is heard after a time period, or a CTS is lost after an HTS has been received, the source node should perform regular random backoff procedure, assuming a collision has occurred.

(c) If the source node has heard the CTS from the destination node without receiving any HTS from the relay candidate, a direct data transmission will be carried out by the source node. Besides, the CoopTable will be updated.

(d) If both the HTS and the CTS are heard, the source node will send the data packet to the relay candidate, and the CoopTable will be updated as well.

(e) If an acknowledge (ACK) is successfully received, the source node will transmit the next data packet. Otherwise, the source node performs the random backoff procedure, then the packet will be retransmitted.

Relay Node:

(a) If a node receives an RTS message which indicates it as a relay candidate, the node will check whether the conditions are satisfied. If it meets the requirements specified in the RTS, an HTS will be sent out to indicate participation in the data transmission. Otherwise, it just goes back to the initial state.

(b) After the HTS message has been sent out, a CTS from the destination node is expected. If such a CTS message is heard, it will wait for the data packet from the source node. Otherwise, the relay node will go back to the initial state, assuming the data packet transmission has been aborted.

Destination Node:

(a) When an RTS has been heard by the destination node, an HTS is expected from the relay candidate as indicated in the RTS.

(b) If an HTS is heard at a time period after the RTS message, the destination node will send a CTS message to the source node, and a timer corresponding to the expected time of receiving the data packet is set up.

(c) If the expected HTS message has not been heard, the destination node will also send a CTS message to the source node, with a different timer duration being set up.

Through cooperation in the MAC layer, higher throughput and lower transmission delay can be achieved. As the cooperation gain [8, 28] can vary considerably with the relay selection scheme and the medium access

control protocol, it is vital to design an effective and efficient cooperation scheme to identify and coordinate the optimal nodes.

2.2 Relay Selection and Medium Access Control

To achieve the cooperation gain in the MAC layer, various schemes have been proposed. In this section, different types of cooperative MAC schemes will be briefly introduced.

2.2.1 Centralized Cooperative MAC

In the centralized solutions such as [29, 30], a central controller (e.g., the source node) needs to acquire the knowledge of the potential relays via additional handshaking messages, and then chooses the optimal relay. In [29], a dynamic relay selection scheme is proposed, which takes into account the tradeoff between performance improvement and corresponding cost of cooperative communications. To achieve the maximal performance, an optimization model is formulated based on the constrained Markov decision process. In [30], based on the instantaneous channel information and the target user rates, the base station assigns one or more relays to each user to minimize total power in the uplink and satisfy its QoS requirement.

Although centralized schemes can rely on the central controller to determine the best relays, the message exchanging may introduce unacceptable delay for delay-sensitive services (e.g., multimedia service) as well as high energy consumption. Also, a global knowledge of the relays is often infeasible and sometimes unnecessary.

2.2.2 Distributed Cooperative MAC

In the literature, distributed relay selection and medium access control has been widely studied, due to light signalling and good scalability.

For the probability-based schemes in [12, 13], each potential relay independently decides a forwarding probability by considering a variety of factors, such as distance, direction, local signal-to-noise ratio (SNR) [12], or the statistical information of the local environment [13]. As a collision occurs when more than one relay happens to forward the overheard data at the same time, the probabilistic cooperation schemes need to minimize the collision probability and maximize the transmission success probability. However, when the number of relays builds up, it becomes challenging to determine the optimal forwarding probability for each relay. If the forwarding probability is underestimated, the transmission success probability can be low since the relays are overconservative. On the other hand, if the forwarding probability is overvalued, the transmission success probability can be low as well, because of high collisions. As a result, the transmission success probability is

usually upper bounded at a low level, as shown in [13, 31]. Frequent retransmissions not only result in long delay but also cause high energy consumption.

From this point of view, another class of distributed cooperative schemes based on the backoff timer seems more promising, because of their low collision probability and high transmission success probability. In [15], a cross-layer distributed scheme is proposed by extending the conventional ready-to-send/clear-to-send (RTS/CTS) handshaking with a ready-to-help (RTH) message from the optimal relay. The relay selection is based on the composite cooperative transmission rate (CCTR), which involves the broadcast rate from the source and the data rate from the relay to the destination. In order to reduce collisions in relaying, the contention process is divided into inter-group contention and intra-group contention. The relays are grouped according to CCTR and send out indication signals after different backoff time. The optimal relay of the highest CCTR waits for the shortest time and wins the contention. In [16], the authors propose a simple cooperative diversity method based on the local measurements of the instantaneous conditions of the source-to-relay and relay-to-destination channels. Two policies are proposed to map the estimated channel conditions into a backoff timer value. The theoretical analysis of the collision probability also demonstrates the advantage of the two backoff policies.

Because of the low collision probability and high transmission probability, the energy consumption of the backoff-based schemes will be much lower than that of the probability-based schemes. In this thesis, we will focus on the backoff-based scheme.

2.3 Energy Efficient Schemes

2.3.1 Energy Saving

With rising energy costs and rigid environmental standards, green communications have attracted substantial research attention in recent years. Due to the energy constraint of mobile devices, energy efficiency is an important topic for wireless networks [17, 18]. In [32], a distributed energy saving scheme is proposed to coordinate the nodes' sleeping activity, so that a connected backbone network is always present. With the proposed technique, the energy consumption of the multi-hop ad hoc wireless network can be reduced without significantly diminishing the capacity of the network. In [33], the energy consumption is reduced by identifying nodes that are equivalent from a routing point of view and then turning off the unnecessary nodes. As seen, the proposed method not only maintains the application fidelity, but also saves much energy. GeRaF [34] saves energy by using geographic information to put nodes to sleep and wake them up in an uncoordinated manner. Accurate analysis is provided, which is based on a sophisticated semi-Markov model.

These schemes from a routing perspective for ad hoc networks can be too heavy for the two-hop cooperative relay scenario. Further investigation is required to properly integrate effective energy saving into the

cooperative relaying solution.

2.3.2 Energy Balance

Many existing cooperation schemes [8, 12, 13] neglect the energy consumption of relays (i.e., assuming unlimited energy of relays), which may lead to unacceptable performance in the energy constrained scenario [14], especially for the QoS-demanding multimedia services. Besides, many studies focus on a single S-D pair served by a number of dedicated relays. It becomes more complicated to consider multiple S-D pairs that share a group of energy-constrained relays, which is a more realistic scenario in practice.

The energy concern together with the new cooperation scenario pose new challenges in the cooperation scheme design. For example, a relay may run out of energy quickly, which leads to severe performance degradation of some S-D pairs. As seen, it is important to balance the energy consumption among these relays.

2.4 Incentive Mechanisms

Although auction theory has been widely studied in the economics literature, the existing auction mechanisms cannot be directly applied to the cooperative communication scenario for the cooperation incentive design, since they fail to fully satisfy the required properties stated in Chapter 1.1.2. Here, we briefly review three representative double auction mechanisms, i.e., VCG-based double auction, McAfee double auction and TASC double auction.

2.4.1 VCG-based Double Auction

One of the most well-known auction mechanisms is the truthful Vickrey-Clarke-Groves (VCG) auction [35, 36, 37]. In [25], Parkes *et al.* propose a Vickrey-based double auction, which achieves individual rationality and budget balance. The assignment between buyers and sellers is determined to maximize social welfare (system efficiency), while the player's utility equals the incremental contribution to the overall system, i.e., the difference between the social welfare with and without a player's participation. However, the well-known result in [26] reveals that it is impossible to design a truthful, efficient, and budget-balanced double auction, even putting individual rationality aside. Therefore, the Vickrey-based double auction in [25] is only *fairly* efficient and *fairly* truthful.

2.4.2 McAfee Double Auction

In [24], McAfee double auction aims at a scenario with homogeneous commodities, where buyers have no preference over auction items. Each buyer submits only one bid, and each seller submits one ask. Then, according

to the ordered statistics of the bids and asks, the auctioneer determines the winning buyers, winning sellers, and the clearing price and payment. Although McAfee double auction can achieve three desirable economic properties, including individual rationality, budget balance, and truthfulness, the homogeneity of commodities in McAfee double auction limits its application to the cooperative communication scenario, where the S-D pairs as service buyers have preferences over the relays as service sellers.

2.4.3 TASC Double Auction

In [27], Yang *et al.* propose a truthful double auction mechanism (TASC) for cooperative communications with heterogeneous trading commodities, i.e., services of relay nodes. In TASC double auction, there are two stages, namely, *Assignment* and *Winner-Determination & Pricing*. In the assignment stage, the auctioneer applies an assignment algorithm to determine the winning buyer candidates (source nodes), the winning seller candidates (relay nodes), and the mapping between these buyers and sellers. Depending on the design objective, the auctioneer can choose a different assignment algorithm. For example, the optimal relay assignment algorithm [38] can maximize the minimum QoS among all buyers; the maximum weighted matching algorithm [39] can maximize the overall QoS; and the maximum matching algorithm can maximize the number of successful trades (final matchings). In the winner-determination & pricing stage, TASC double auction tightly integrates the winner determination and the pricing operation. Based on the return of the assignment stage, the auctioneer applies McAfee double auction [24] to determine the winning buyers, the winning sellers, and the corresponding clearing price and payment. When TASC double auction is applied, it can satisfy individual rationality, budget balance, and truthfulness for the sellers. However, we illustrate using an example in Chapter 5.2.3 that a buyer can bid untruthfully to improve its utility. Hence, TASC double auction cannot guarantee the truthfulness of buyers.

Chapter 3

Energy-Efficient Cooperative MAC for Single S-D Pair

3.1 Motivation and Overview

Most of the cooperative MAC schemes assume that the number of relays or the relay intensity is known *a priori*. For example, the analytical framework in [14] evaluates the uncoordinated cooperative scheme proposed in [40] for a given and fixed number of relays. An enhancement approach is further developed based on the analytical framework to adapt the forwarding probabilities of participating relays. In [41], different relay selection methods are analyzed using stochastic geometry, given the intensity of relay distribution. As seen, the relay intensity is a critical parameter to guarantee the performance of cooperative schemes. However, such information may not be available in advance and may even dynamically change, e.g., when a network is newly set up or the network topology dynamically changes. Thus, it is vital to estimate the relay intensity accurately and efficiently.

Besides, the energy constraint becomes another primary concern to accommodate green communications with the rising energy cost and rigid environmental standards. Nonetheless, the existing cooperative schemes may suffer a high energy consumption, because of the signalling exchange in the centralized solutions, or excessive packet retransmissions resulting from a bounded transmission success probability of the probability-based schemes. Since only few relays having good channel conditions are important to be ready for packet forwarding, the energy can be wasted unnecessarily to place all relays standby for transmission. Hence, a cooperative relaying scheme needs to be properly integrated with an effective energy saving scheme. Although there are many studies on energy saving, e.g., for ad hoc and sensor networks with sleeping nodes [34], these solutions may not be directly applicable or too heavy for a two-hop cooperative scenario.

In this chapter, we first develop an algorithm to estimate the unknown intensity of relay distribution, which is critical to properly engage cooperating nodes. The convergence and accuracy of the estimation algorithm are theoretically justified. Considering a backoff-based distributed relay scheme, we further incorporate an energy saving scheme to minimize energy consumption while maintaining satisfactory transmission success probability. The performance of the proposed cooperative solution, particularly the collision probability, is analytically evaluated, since it determines the transmission success probability and thus the average energy consumption. The numerical and simulation results validate our analysis and demonstrate that the proposed

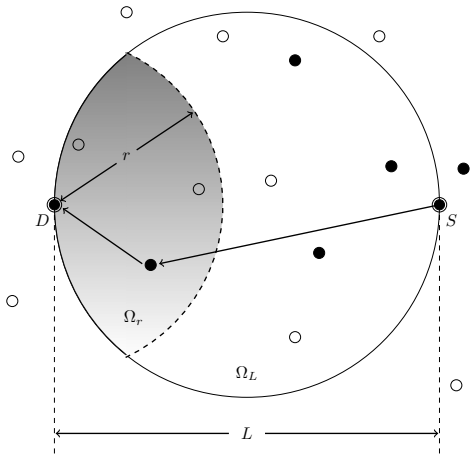

Figure 3.1: An illustration of the system model for cooperative transmission. In addition to S and D, there are potential relays represented by black nodes, while the white nodes indicate other relay nodes.

cooperative solution outperforms the uncoordinated reference scheme with respect to the transmission performance and energy saving.

The remainder of this chapter is structured as follows. Section 3.2 defines the system model and formulates the problem for this study. In Section 3.3, we propose an estimation algorithm for relay intensity. A distributed cooperative solution with an energy saving scheme is introduced and analyzed in Section 3.4. Numerical and simulation results are presented in Section 3.5, followed by conclusions in Section 3.6.

3.2 System Model and Problem Formulation

3.2.1 System Model

Consider a wireless network where nodes are randomly distributed in a given region, following a homogeneous Poisson point process (PPP) with an *unknown* intensity λ. We assume that the node distribution is time-stationary and ergodic, which is generally valid under broad assumptions, e.g., for random direction mobility models [42]. The source (S) is referred to the node that generates data traffic; the destination (D) is the node that receives the data. Relay nodes have no intrinsic traffic demands, and the *potential relays* are referred to those nodes that correctly overhear the packet from the source.

We focus on the cooperative transmission of packets from S to D of a distance L in between, as illustrated in Fig. 3.1. Although the direct transmission from S to D may not definitely fail, the success probability can be very low when L is large. Focusing on this challenging scenario, we aim to improve the forwarding performance via spatially random relays, especially the energy efficiency of the cooperative relaying scheme. Hence, we assume that the source has to communicate with the destination via the relays. In practice, the overall success probability can be even higher further considering the direct transmission.

Fig. 3.2 illustrates how the cooperative relay protocol works. Here, the time is slotted and each time slot is

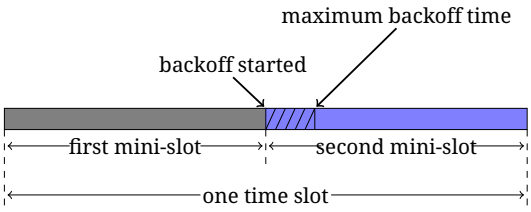

Figure 3.2: Timing structure.

divided into two mini-slots. The source transmits the packet in the first mini-slot. It is assumed that the source always has a packet to transmit, which can be a new packet when the previous packet has been successfully delivered or a retransmitted packet when the previous packet is corrupted. At the beginning of the second mini-slot, the potential relays start the channel access contention with different backoff time. Whenever the backoff timer of a relay expires and no packet relaying is sensed, the relay forwards the overheard packet to the destination immediately. If no relaying happens by the maximum backoff time, the current transmission attempt fails and a retransmission is required in the next time slot.

We assume that each node knows its own location, which can be obtained either from a localization technique based on signal strength, time-of-arrival or angle-of-arrival measurements with nearby nodes [43, 44], or through a GPS receiver which becomes increasingly ubiquitous in mobile devices. Further, the location of D can also be obtained in advance via prior handshaking. By piggybacking the locations within the transmitted packets, the relay nodes can obtain this information from the overheard packets. It should be noted that S does not have the knowledge of the locations of relay nodes, and one relay does not have the location information of other relays either. Besides, we assume that the locations of all nodes in the network do not change significantly during the short cooperative transmission period, which is a typical assumption that generally holds.

For the data transmission between a transmitter located at x and a receiver located at y, the SNR of the received signal can be written as

$$\gamma_{xy} = \frac{P_0}{N_0} h_{xy} g_{xy} \tag{3.1}$$

where P_0 is the transmit power, N_0 is the power of additive white Gaussian noise (AWGN), and h_{xy} denotes the small-scale channel fading which is exponentially distributed with unit mean. The path-loss effect is captured by $g_{xy} = \|x - y\|^{-\nu}$, where $\|x - y\|$ is the Euclidean distance, and ν is the path-loss exponent. The receiver is able to successfully decode the received signal only when the instantaneous SNR is no less than a threshold T_0 [12]. The probability of correctly decoding a packet is given by

$$P_{xy} = \Pr\left[\gamma_{xy} \geq T_0\right] = e^{-K\|x-y\|^{\nu}} \tag{3.2}$$

where $K = T_0 N_0 / P_0$. Thus, the one-hop transmission success probability with $\nu = 2$ is given by

$$P_{SD} = e^{-KL^2}.$$

With the assistance of a relay node, the two-hop transmission success probability is

$$P_{SRD} = e^{-KL_{SR}^2} \cdot e^{-KL_{RD}^2} = e^{-K(L_{SR}^2 + L_{RD}^2)}$$

where L_{SR} is the distance between S and a relay, and L_{RD} is that of the relay and D. To achieve the cooperation gain, we should have

$$\frac{P_{SRD}}{P_{SD}} = e^{-K(L_{SR}^2 + L_{RD}^2 - L^2)} = e^{-2KL_{SR}L_{RD}\cos(\angle SRD)} \geq 1$$

which requires that $\cos(\angle SRD) \leq 0$. Therefore, we only focus on the relays within the region Ω_L, which is the circle with a diameter L, as shown in Fig. 3.1.

Some important notations are summarized in Table 3.1.

3.2.2 Problem Formulation

Cooperative wireless communications have been widely studied and various techniques are proposed for different layers. At the physical layer, a cooperative diversity technique can be used at the relays to forward the received signal from the source in an analog or digital fashion, such as amplify-and-forward (AF) and decode-and-forward (DF) [4]. Then, the destination uses combining techniques such as maximal ratio combining or selective combining to process the contributions from multiple relays. Although such physical-layer techniques can improve the receiving performance, an effective MAC scheme is still needed to coordinate the transmissions from multiple relays. Furthermore, when more relays are engaged, there is a longer delay as well as a higher overall energy consumption to incorporate all relay transmissions (e.g., in orthogonal time slots). In this chapter, we aim to enhance cooperative transmission and minimize the energy consumption from the MAC perspective. The relay selection and channel access mechanisms are the main aspects to be addressed in the cooperative MAC design.

In general, a centralized relay selection protocol aims to identify the best relay(s) by exploiting a global view of the network so as to maximize the transmission success probability and minimize the collision probability. However, because such protocols require additional time to exchange channel state information, the incurred overhead and delay are often large, as well as the energy consumption. On the other hand, due to the high collision probability, the transmission success probability of probability-based uncoordinated protocols is bounded by $1/e \approx 0.368$ [13, 31]. Thus, the energy consumption is also high because of packet retransmission. Besides, it becomes difficult to figure out the optimal forwarding probabilities for the potential relays when

Table 3.1: Important Notations.

Symbol	Definition
S	Source node
D	Destination node
L	Distance between S and D
ν	Path-loss exponent
P_0	Transmit power
N_0	Power of additive white Gaussian noise
T_0	SNR threshold of signal decoding
R_i	Relay node
r_i	Distance of relay R_i to destination D
T_i	Backoff time of relay R_i
L_i	Distance of relay R_i to source S
λ	Relay intensity
$\lambda^{'}$	Potential relay intensity after thinning process
$\widetilde{\lambda}$	Estimated relay intensity
$\Delta\lambda$	Estimation error of relay intensity
Ω_L	The circle region with a diameter L, as shown in Fig. 3.1
Ω_r	The part of the circle centered at D of a radius r within Ω_L
$\mathcal{A}_r$	The area of region Ω_r
Λ_r	Intensity measure of potential relays in Ω_r with respect to λ
$\Lambda_r^{'}$	Intensity measure of potential relays in Ω_r with respect to $\lambda^{'}$
ϱ_i	Sleeping probability of relay R_i
ζ_i	Active probability of relay R_i
$r_{(1)}/r_{(2)}$	Distance of the first/second nearest potential relay to D
$f(r)$	The probability density function (PDF) of $r_{(1)}$
$F(r)$	The cumulative distribution function (CDF) of $r_{(1)}$
$\widetilde{F}(r)$	Estimated CDF of $r_{(1)}$
ΔF	Estimation error of $F(r)$
F_B	The bound of estimation error ΔF
E	Average energy consumption of a successful transmission
E_t	Energy consumption for transmitting a packet
E_r	Energy consumption for listening and receiving a packet
L_0	Threshold that determines the active/sleeping probability
P_{1+}	The probability that at least one potential relay in Ω_{L_0}
P_{2+}	The probability that at least two potential relay in Ω_{L_0}
$g(r_1, r_2)/h(r_1)$	Joint PDF of $r_{(1)}$ and $r_{(2)}$
P_c	Collision probability
P_c^U	Upper bound for P_c
c	Collision window (time interval)
ϖ	Collision window (distance interval)
τ_i	Forwarding probability of R_i in probability-based scheme

the network scales up.

Based on the above observations, we can see that the backoff-based cooperative scheme is more energy-efficient, because of its distributed nature and low collision probability. According to (3.2), we know that the potential relay with a closer distance to the destination has a higher transmission success probability over the relay-to-destination channel. To prioritize such relays closer to the destination, we consider a simple distributed backoff-based cooperative scheme, in which each relay sets the backoff timer to

$$T_i = \frac{r_i}{L} \tag{3.3}$$

where r_i is the distance of the relay R_i to the destination, L is the distance between the source and destination, and the maximum backoff time is taken to be one unit time. As such, the nearest potential relay has the shortest backoff time and forwards the packet to D. If the first two or more relays time out within a certain interval c, a collision will happen [16]. This is generally a valid assumption for MAC-layer study and has been widely considered in the literature [8, 12, 13, 16].

It is worth mentioning that the setting of backoff timer in (3.3) cannot guarantee maximization of the throughput of the source. We see in (3.2) that the distance determines the transmission success probability over the relay-to-destination channel. In other words, the distance actually captures average channel state information in the long term. Hence, the potential relay with the smallest distance to the destination only has the highest transmission success probability on average. It is possible that there exist other potential relays that experience better instantaneous channel conditions than the relay with the smallest distance to the destination. However, more signalling overhead will be incurred to collect instantaneous channel state information, so as to identify the optimal potential relay with the best instantaneous channel quality. This deviates from our primary design goal, which is to improve the energy efficiency of the cooperative solution while maintaining a high throughput for the source.

To reduce the energy consumption, we further propose an energy saving scheme working together with the backoff-based cooperative scheme. At the beginning of each time slot, each relay determines its on/off status according to a sleeping probability. This sleeping probability is independently decided by each relay in a distributed manner based on a variety of factors. Intuitively, when the relays are deployed sparsely with a low intensity, the sleeping probabilities should be relatively small to ensure that a sufficient number of relays are available to achieve the required performance. In contrast, when the relay intensity is high, the relays can be put to sleep at relatively large probabilities to save energy. As seen, the estimation of relay intensity is important to achieve a high energy efficiency. Meanwhile, the local channel condition of the relay should be considered so that the relays having a good relay-destination channel end up with a low sleeping probability in order to balance energy consumption and transmission performance.

3.3 Relay Intensity Estimation

3.3.1 Estimation Algorithm

As discussed in Section 3.2.2, the efficiency of the energy saving scheme depends on appropriate setting of the sleep probability of the relay, which in turn varies with the relay intensity. In practice, the relay intensity is often unknown in advance or dynamically changing. Hence, in this section, we first introduce an algorithm to estimate the relay intensity, which is further used in the energy saving scheme presented in Section 3.4 for cooperative transmission.

Given the system model in Section 3.2.1, the relays are distributed as a homogeneous PPP. Nonetheless, because the receiving success probability of each relay is location-dependent, the distribution of the *potential relays* that correctly overhear the packet from the source is not a homogeneous PPP. To facilitate the relay intensity estimation, we consider a simple node sleeping scheme, which is different from the energy saving scheme used with the cooperative scheme in Section 3.4. According to the backoff scheme in (3.3), the relay closer to the source but farther from the destination sets a longer backoff time, which results in a smaller probability to win the contention and to be selected as the forwarding node. Based on this observation, we initialize the sleeping probability of a relay R_i with a distance L_i towards S to

$$\varrho_i = 1 - \frac{e^{-KL^2}}{e^{-KL_i^2}}. \tag{3.4}$$

Thus, the spatial distribution of the potential relays can be viewed as the result of a $p(x)$-thinning process [45]. The $p(x)$-thinning is a generalized operation that defines a retention probability $p(x)$ for each point of a PPP and yields a thinned point process by deleting the point with a probability $1 - p(x)$. Here, the retention probability for a relay R_i of a distance L_i to S is given by $P_{SR_i} \cdot (1 - \varrho_i) = e^{-KL^2}$. Therefore, the distribution of the potential relays is not only a PPP according to Prekopa's Theorem [45], but also homogeneous with the intensity given by

$$\lambda^{'} = \lambda \cdot e^{-KL^2}. \tag{3.5}$$

Then, we can obtain the intensity measure of the potential relays in the region Ω_r (the gray region in Fig. 3.1), which is part of the circle centered at D of a radius r ($0 \leq r \leq L$) within Ω_L:

$$\Lambda_r^{'} = \lambda^{'} \cdot \mathcal{A}_r \tag{3.6}$$

where $\mathcal{A}_r$ is the area of region Ω_r, given by

$$\mathcal{A}_r = r^2 \arccos\left(\frac{r}{L}\right) + \frac{L^2}{2} \arcsin\left(\frac{r}{L}\right) - \frac{L \cdot r}{2}\sqrt{1 - \left(\frac{r}{L}\right)^2}. \tag{3.7}$$

Let $r_{(1)}$ and $r_{(2)}$ be the distance of the nearest and second nearest potential relays to D, receptively. If only

the nearest potential relay lies within a distance $[r, r+\Delta r]$ to D, we have the occurrence probability

$$\Pr[r \le r_{(1)} \le r+\Delta r] = \frac{1}{1-e^{-\Lambda_L^{'}}} \cdot e^{-\Lambda_r^{'}} \cdot \Lambda_{\Delta r}^{'} e^{-\Lambda_{\Delta r}^{'}} \tag{3.8}$$

where $1-e^{-\Lambda_L^{'}}$ is the probability that there is at least one potential relay within Ω_L, and $\Lambda_{\Delta r}^{'}$ is given by

$$\Lambda_{\Delta r}^{'} = \lambda^{'} \cdot (\mathcal{A}_{r+\Delta r} - \mathcal{A}_r).$$

Similarly, the probability that the nearest two potential relays both fall into $[r, r+\Delta r]$ is given by

$$\begin{aligned} &\Pr[r \le r_{(1)} \le r+\Delta r, r \le r_{(2)} \le r+\Delta r] \\ &= \frac{1}{1-e^{-\Lambda_L^{'}} - \Lambda_L^{'} e^{-\Lambda_L^{'}}} e^{-\Lambda_r^{'}} \frac{\left(\Lambda_{\Delta r}^{'}\right)^2}{2} e^{-\Lambda_{\Delta r}^{'}} = o(\Delta r). \end{aligned} \tag{3.9}$$

Here, a function $\mathcal{Y}(\Delta r)$ is said to be $o(\Delta r)$ if $\lim_{\Delta r \to 0} \frac{\mathcal{Y}(\Delta r)}{\Delta r} = 0$. Similarly, the probability that there are more than two potential relays within $[r, r+\Delta r]$ is also $o(\Delta r)$. Therefore, we can obtain the probability density function (PDF) of $r_{(1)}$ as

$$\begin{aligned} f(r) &= \lim_{\Delta r \to 0} \frac{\Pr[r \le r_{(1)} \le r+\Delta r] + o(\Delta r)}{\Delta r} \\ &= \lambda^{'} \frac{e^{-\Lambda_r^{'}}}{1-e^{-\Lambda_L^{'}}} 2r \arccos\left(\frac{r}{L}\right). \end{aligned} \tag{3.10}$$

The corresponding cumulative distribution function (CDF) is given by

$$F(r) = \frac{1-e^{-\Lambda_r^{'}}}{1-e^{-\Lambda_L^{'}}}. \tag{3.11}$$

When $e^{-\Lambda_L^{'}} \to 0$, we can approximate the CDF as follows:

$$F(r) \approx 1 - e^{-\Lambda_r^{'}} = 1 - e^{-\lambda \mathcal{A}_r e^{-K L^2}}. \tag{3.12}$$

In (3.12), the relay intensity λ is directly related to $F(r)$, which can be easily observed from the packets forwarded by the relays. Table 3.2 presents the details of our estimation algorithm for λ. As seen in Line 1 to Line 10, each relay initializes its sleeping probability according to (3.4) and an awake relay R_i that overhears a packet from S sets its backoff time based on (3.3). To collect statistics for $F(r)$, the relay piggybacks its location when forwarding the packet to D. Thus, the destination can obtain the estimated CDF of the distance of the nearest potential relay to D, denoted by $\widetilde{F}(r)$.

Table 3.2: Intensity Estimation Algorithm.

for $i = 1 : N_o$ **do** ▷ N_o packets are transmitted to estimate λ
  The source node transmits a packet;
  for all the relays **do**
    Set the sleeping probability according to (3.4);
    if a relay is awake and correctly receives the packet **then**
      Set its backoff time according to (3.3);
    end if
  end for
  The destination node records the distance of the first potential relay that forwards the packet;
end for
Initialize r_1 and calculate $\mathcal{A}_{r_1}$ according to (3.7);
for $i = 1 : I_o$ **do** ▷ I_o iterations are run to estimate λ
  The destination node estimates $\widetilde{F}(r_i)$ according to the record obtained above;
  Calculate $\widetilde{\lambda}_i$ from $\widetilde{F}(r_i)$ according to (3.12);
  Calculate $\mathcal{A}_{r_{i+1}}$ according to (3.17) by using $\widetilde{\lambda}_i$;
  Calculate r_{i+1} from $\mathcal{A}_{r_{i+1}}$ according to (3.7);
end for
Return $\widetilde{\lambda}$;

Supposing that the estimated $\widetilde{F}(r)$ involves an error ΔF, we have

$$\widetilde{F}(r) = F(r) + \Delta F = 1 - e^{-\lambda \mathcal{A}_r e^{-KL^2}} + \Delta F. \tag{3.13}$$

Denoting the intensity estimated from $\widetilde{F}(r)$ by $\widetilde{\lambda}$, we define $\widetilde{\lambda} = \lambda + \Delta\lambda$, where $\Delta\lambda$ indicates the estimation error of the intensity. Then, we rewrite $\widetilde{F}(r)$ as

$$\widetilde{F}(r) = 1 - e^{-\widetilde{\lambda} \mathcal{A}_r e^{-KL^2}} = 1 - e^{-\lambda \mathcal{A}_r e^{-KL^2}} \cdot e^{-\Delta\lambda \mathcal{A}_r e^{-KL^2}}. \tag{3.14}$$

Combining (3.13) and (3.14), we obtain

$$\Delta\lambda = \frac{-1}{\mathcal{A}_r e^{-KL^2}} \ln\left(1 - \Delta F \cdot e^{\lambda \mathcal{A}_r e^{-KL^2}}\right) \approx \frac{e^{\lambda \mathcal{A}_r e^{-KL^2}}}{\mathcal{A}_r e^{-KL^2}} \cdot \Delta F. \tag{3.15}$$

Since $\Delta\lambda$ is a function of $\mathcal{A}_r$ (as well as r), we have

$$\frac{\mathrm{d}\Delta\lambda}{\mathrm{d}\mathcal{A}_r} = \frac{\Delta F}{e^{-KL^2}} \cdot \frac{e^{\lambda \mathcal{A}_r e^{-KL^2}} \cdot \left(\lambda \mathcal{A}_r e^{-KL^2} - 1\right)}{{\mathcal{A}_r}^2}. \tag{3.16}$$

If the estimation error ΔF is bounded, $\Delta\lambda$ is minimized when

$$\mathcal{A}_r = \frac{1}{\lambda e^{-KL^2}}. \tag{3.17}$$

Since the $\mathcal{A}_r$ and the corresponding r that satisfies (3.17) are unknown, we use the iterative algorithm in Ta-

ble 3.2 to approach the exact intensity λ so as to minimize the estimation error. As seen in Line 11 to Line 17, an intensity estimate $\widetilde{\lambda}_i$ is obtained from the observed $\widetilde{F}(r_i)$ in the i^{th} round. Then, $\mathcal{A}_{r_{i+1}}$ and r_{i+1} are updated for the $(i+1)^{th}$ round by applying $\widetilde{\lambda}_i$ to (3.17).

3.3.2 Convergence

The following lemma proves that the iterative algorithm approaches to the optimal r that satisfies (3.17) and minimizes the estimation error $\Delta\lambda$.

Lemma 3.1. *For any $\epsilon > 0$, there exists an I_o so that, when the number of iterations $I > I_o$, we have $|r_i - r_o| < \epsilon$, where r_o is the achievable distance that approaches the minimum estimation error $\Delta\lambda$, given that the estimation error of $F(r)$ is bounded by F_B, i.e., $0 \leq |\Delta F| \leq F_B \ll F(r_o)$.*

Proof. According to (3.17), we need to show that $\mathcal{A}_{r_i}e^{-KL^2}$ converges to $\mathcal{A}_{r_o}e^{-KL^2} \triangleq x_o$, so as to prove that r_i is updated with the iterative algorithm in a manner so that it converges to r_o. Letting λ_o denote the optimal estimation of λ, we have $x_o = \frac{1}{\lambda_o}$. For the i^{th} iteration, we define the iterative term $x_i = \mathcal{A}_{r_i}e^{-KL^2}$. Given $-F_B \leq \Delta F \leq F_B$, if $\Delta F > 0$, we would have $x_i < x_o = \frac{1}{\lambda_o} < \frac{1}{\lambda}$ after very few iterations. Then, we define the estimation errors of any two adjacent rounds as follows:

$$\Delta x_i = x_o - x_i > 0$$

$$\Delta x_{i+1} = x_o - x_{i+1} = x_o - \frac{1}{\widetilde{\lambda}_i} > 0.$$

From (3.13) and (3.14), we have

$$F(r_i) + \Delta F = 1 - e^{-\widetilde{\lambda}_i \mathcal{A}_{r_i} e^{-KL^2}} = 1 - e^{-\widetilde{\lambda}_i x_i}. \tag{3.18}$$

Therefore, we have

$$\begin{aligned}
\Delta x_{i+1} - \Delta x_i = x_i - \frac{1}{\widetilde{\lambda}_i} &= \frac{-1}{\widetilde{\lambda}_i} \cdot \ln\Big[1 - F(r_i) - \Delta F\Big] - \frac{1}{\widetilde{\lambda}_i} \\
&\approx \frac{-1}{\widetilde{\lambda}} \cdot \Big[\ln\big(1 - F(r_i)\big) + 1\Big] = \frac{-1}{\widetilde{\lambda}_i} \cdot \Big[\ln\big(e^{-\lambda \cdot x_i}\big) + 1\Big] \\
&= \frac{-1}{\widetilde{\lambda}_i} \cdot \big(-\lambda \cdot x_i + 1\big) = \frac{\lambda}{\widetilde{\lambda}_i} \cdot \Big(x_i - \frac{1}{\lambda}\Big) < 0.
\end{aligned}$$

For other cases of ΔF, it can be shown similarly that x_i converges to x_o. Thus, r_i can converge to r_o to approach the minimum estimation error $\Delta\lambda$. □

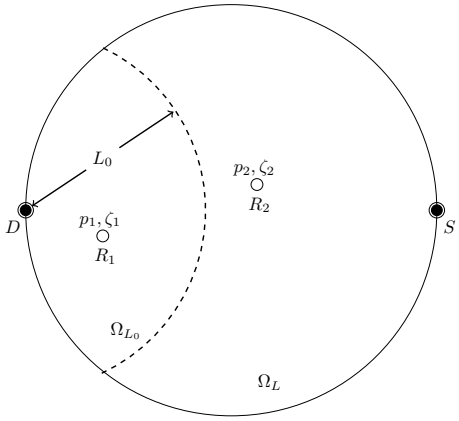

Figure 3.3: An illustration of sleeping scheduling for relays.

3.4 Energy-Efficient Cooperative Scheme

The estimation algorithm in Section 3.3 can be used to obtain the relay intensity. In this section, we further propose an energy-efficient cooperative scheme, which exploits such information so as to satisfy the required transmission performance while reducing the energy consumption. The performance of the proposed scheme is also analytically evaluated.

3.4.1 An Energy-Efficient Cooperative Scheme

For the backoff-based cooperative schemes, each individual relay determines its backoff time, so that a good relay ends up with a short backoff time, while there is a small probability that more than one relay times out within an indistinguishable interval and results in a collision. There are many studies on the determination of the backoff time such as [16]. In this chapter, we focus more on the energy efficiency of the cooperative scheme and consider the simple design in (3.3), where each relay sets the backoff time based on its distance to D. To reduce the energy consumption, each relay R_i independently decides its on/off status at the beginning of a slot according to a sleeping probability ϱ_i. Intuitively, a relay closer to D should choose a lower sleeping probability, since such relays have a smaller backoff time according to (3.3) and their forwarding transmission can succeed with a higher probability. Thus, there will be fewer retransmissions and lower energy consumption.

Lemma 3.2. *Assume perfect relaying over the relay-to-destination channel. To minimize energy consumption, the active probability $\zeta_i = 1 - \varrho_i$ of a relay R_i in the region Ω_L should be either 0 or 1.*

Proof. The extended proof for the general case with m relays is given in Appendix A.1. In the following, we present the proof for a special case with two relay nodes for easy comprehension. Consider two arbitrary relay nodes R_1 and R_2 in the region Ω_L, as illustrated in Fig. 3.3, where p_1 and p_2 are their corresponding successful receiving probabilities from S. Let ζ_1 and ζ_2 be the active probabilities of R_1 and R_2, respectively. Assume that

the energy consumption for transmitting a packet, and that for listening to and receiving a packet are both constants, denoted by E_t and E_r, respectively. Obviously, the overall transmission success probability depends on the available relay candidates. Generally, the more relay candidates, the greater total energy consumption, and the higher transmission success probability. Intuitively, more collisions are involved with more relays and degrade the transmission success probability. On the other hand, the opportunity of locating a good relay also increases with the number of relays, which reduces packet loss caused by poor channel conditions. Moreover, the collision probability of the backoff-based cooperative scheme is very low and increases slowly with the number of relays, as illustrated in Section 3.5.3. Hence, the transmission success probability is not lowered with more relays. The trade-off between the energy consumption and the transmission success probability will be discussed in depth in Section 3.5.2. Here, we first focus on the energy consumption and assume perfect forwarding from the relays. The average energy consumption of a packet transmission is then given by

$$\begin{aligned} E = {} & \zeta_1\zeta_2\Big[2E_r + p_1E_t + (1-p_1)p_2E_t + (1-p_1)(1-p_2)E\Big] \\ & + \zeta_1(1-\zeta_2)\Big[E_r + p_1E_t + (1-p_1)E\Big] \\ & + (1-\zeta_1)\zeta_2\Big[E_r + p_2E_t + (1-p_2)E\Big] \\ & + (1-\zeta_1)(1-\zeta_2)E. \end{aligned} \tag{3.19}$$

In (3.19), the first term gives the total energy consumption if both R_1 and R_2 are active during the packet transmission, which includes the listening and receiving energy consumption of the two nodes, the transmission energy consumption with a forwarding priority to R_1, and the retransmission energy consumption if both nodes fail to successfully receive the packet. The other three terms define the energy consumption when only one node or none correctly overhears the packet. We can simplify (3.19) to

$$E = E_t + \frac{\zeta_1 + \zeta_2}{1-(1-p_1\zeta_1)(1-p_2\zeta_2)} \cdot E_r. \tag{3.20}$$

Eq. (3.20) provides a physical interpretation of the average energy consumption, which is the transmission energy consumption plus the normalized average energy consumption for listening and receiving. Here, the normalization factor is the probability that at least one active relay among R_1 and R_2 correctly overhears the packet from the source.

Assuming that p_1, p_2 and ζ_1 are known, we next determine ζ_2 so as to minimize the energy consumption. Thus, we consider

$$\frac{\mathrm{d}E}{\mathrm{d}\zeta_2} = \frac{p_1\zeta_1 - (1-p_1\zeta_1)p_2\zeta_1}{\Big[1-(1-p_1\zeta_1)(1-p_2\zeta_2)\Big]^2} \cdot E_r \tag{3.21}$$

and obtain the active probability ζ_2 of R_2 according to p_1, p_2 and ζ_1 as

$$\zeta_2 = \begin{cases} 0, & \text{if} \quad p_2 \leq P_\zeta \\ 1, & \text{if} \quad p_2 > P_\zeta \end{cases} \tag{3.22}$$

where P_ζ is derived by setting $\frac{\mathrm{d}E}{\mathrm{d}\zeta_2} = 0$ and given by

$$P_\zeta = \frac{1}{\zeta_1} \cdot \Big(\frac{1}{1 - p_1 \zeta_1} - 1 \Big). \tag{3.23}$$

As seen, to minimize the energy consumption, the active probability of the relay R_2 is either 0 or 1, depending on its successful receiving probability p_2 and the status of other relays captured by P_ζ. □

Based on the conclusion of Lemma 3.2, we assume that there exists a distance L_0 such that any relay R_i in the region Ω_L and with a distance less than L_0 to D has an active probability $\zeta_i = 1$, and all the other relays have $\zeta_i = 0$. Extending (3.20), we write the average energy consumption for the above energy saving scheme as

$$E = E_t + \frac{\iint_{\Omega_{L_0}} 1 \cdot \lambda r \mathrm{d}\theta \mathrm{d}r}{1 - e^{-\Lambda_{L_0}}} \cdot E_r \tag{3.24}$$

where Ω_{L_0} denotes the region within Ω_L and with a distance less than L_0 to D, and Λ_{L_0} is the intensity measure of the potential relays in Ω_{L_0}, given by

$$\Lambda_{L_0} = \iint_{\Omega_{L_0}} e^{-K(L^2 + r^2 - 2Lr\cos\theta)} \lambda r \mathrm{d}\theta \mathrm{d}r.$$

Hence, the probability that at least one relay in Ω_{L_0} correctly overhears the packet is given by

$$P_{1^+} = 1 - e^{-\Lambda_{L_0}} \tag{3.25}$$

which is actually the upper bound of the transmission success probability. Following an approach similar to (3.21)-(3.23), we can take the first-order derivative of E with respect to L_0 and determine L_0 that minimizes the energy consumption by setting $\frac{\mathrm{d}E}{\mathrm{d}L_0} = 0$. The threshold L_0 should satisfy

$$\bar{P}_{L_0} = P_\zeta \tag{3.26}$$

where $\bar{P}_{L_0}$ is the average successful receiving probability of the relays on the separating arc of Ω_{L_0} as illustrated in Fig. 3.3, given by

$$\bar{P}_{L_0} = \frac{\int_0^{\arccos(\frac{L_0}{L})} e^{-K(L^2 + L_0^2 - 2LL_0\cos\theta)} \mathrm{d}\theta}{\arccos(\frac{L_0}{L})} \tag{3.27}$$

and P_ζ captures the status of the relays in Ω_{L_0}, given by

$$P_\zeta = \frac{1}{\iint_{\Omega_{L_0}} 1 \cdot \lambda r \mathrm{d}\theta \mathrm{d}r} \cdot \left(\frac{1}{e^{-\Lambda_{L_0}}} - 1\right) = \frac{1}{\lambda \mathcal{A}_{L_0}} \cdot \left(\frac{1}{e^{-\Lambda_{L_0}}} - 1\right). \tag{3.28}$$

As seen, the proposed energy saving scheme is distributed, since the active probability is determined individually by each relay according to its distance to D and the relay intensity λ. The relay intensity can be estimated by the destination with the algorithm in Table 3.2 and obtained by each relay via prior handshaking. Intuitively, if the relay intensity is overvalued, the threshold L_0 will be underestimated, and P_{1^+} will be too small. Consequently, the energy consumption will be high due to retransmissions, since the transmission success probability is bounded by P_{1^+} at a low level. If the relay intensity is underestimated, the threshold L_0 will be overvalued and more relays will be involved unnecessarily in the cooperative transmission. As a result, the energy consumption will also be high. Thus, the accuracy of the estimated relay intensity λ becomes important to properly determine L_0. In Section 3.5.2, we will provide a numerical example to further discuss the impact of L_0 on the tradeoff between the transmission success probability and the energy consumption.

It is worth mentioning that the proposed scheme is not optimal since we set bias for the relays close to D due to their high transmission success probability. In fact, it is very difficult to find the optimal ζ_i for all the relays in Ω_L, because the global information of the relays will be required. We leave that to future work. Although the proposed scheme is not optimal, it is highly efficient due to the distributed nature, which is validated by the results in Section 3.5.3.

3.4.2 Analysis of Collision Probability

Since collisions are a main concern with distributed cooperative solutions, we evaluate the collision probability of the backoff-based cooperative scheme with energy saving in this section. A collision happens when the first two or more potential relays time out within an indistinguishable time interval c. As discussed in [16], this uncertainty interval depends on factors such as radio switch time between the receive and transmit modes, and different signal propagation time in the wireless medium. Although an explicit time synchronization protocol among the relays is usually not required for the backoff-based schemes, the packet reception from the source can initiate a "crude" timing process at each relay. To account for the asynchronization among contending relays, we can consider a sufficiently large value for the interval c. Then, the performance is assessed in a worst-case scenario since the higher the uncertainty interval, the higher the collision probability. For analysis purposes, we further map the time interval c to a distance interval ϖ, which means that two potential relays nearest to the destination are spaced less than ϖ apart. According to (3.3), the backoff time of a potential relay is linearly related to its distance to the destination. As a result, the time interval c is linearly mapped to the distance interval ϖ, which also captures the relay differences as well as the synchronization margin.

Provided that at least two potential relays lie in Ω_{L_0} with a probability

$$P_{2+} = 1 - e^{-\Lambda_{L_0}} - \Lambda_{L_0} \cdot e^{-\Lambda_{L_0}} \tag{3.29}$$

we next obtain the joint distribution of the distance of the first and second nearest potential relays to D. Let $r_{(1)}$ and $r_{(2)}$ denote the distance of the two nearest potential relays to D, where $r_{(1)} \leq r_{(2)}$. We consider two cases depending on whether the two potential relays fall into the same sufficiently small area. In the first case, the first nearest potential relay is located in the region $[r_1, r_1 + \Delta r]$, while the second nearest potential relay falls into the region $[r_2, r_2 + \Delta r]$, where $r_1 < r_2 \leq L_0$. The corresponding occurrence probability is given by

$$\begin{aligned} &\Pr[r_1 \leq r_{(1)} \leq r_1 + \Delta r, r_2 \leq r_{(2)} \leq r_2 + \Delta r] \\ &= \frac{e^{-\Lambda_{r_1}} \cdot \Lambda_{\Delta r_1} e^{-\Lambda_{\Delta r_1}} \cdot e^{-(\Lambda_{r_2} - \Lambda_{r_1 + \Delta r_1})} \cdot \Lambda_{\Delta r_2} e^{-\Lambda_{\Delta r_2}}}{P_{2+}} \\ &= \frac{\Lambda_{\Delta r_1} \cdot \Lambda_{\Delta r_2} \cdot e^{-\Lambda_{\Delta r_2}} \cdot e^{-\Lambda_{r_2}}}{P_{2+}} \end{aligned} \tag{3.30}$$

where

$$\begin{aligned} \Lambda_{\Delta r_1} &= 2 \int_{r_1}^{r_1 + \Delta r} \int_0^{\arccos(\frac{r}{L})} e^{-K(L^2 + r^2 - 2Lr\cos\theta)} \lambda r \mathrm{d}\theta \mathrm{d}r \\ \Lambda_{\Delta r_2} &= 2 \int_{r_2}^{r_2 + \Delta r} \int_0^{\arccos(\frac{r}{L})} e^{-K(L^2 + r^2 - 2Lr\cos\theta)} \lambda r \mathrm{d}\theta \mathrm{d}r \\ \Lambda_{r_2} &= 2 \int_0^{r_2} \int_0^{\arccos(\frac{r}{L})} e^{-K(L^2 + r^2 - 2Lr\cos\theta)} \lambda r \mathrm{d}\theta \mathrm{d}r. \end{aligned}$$

Therefore, we obtain the joint PDF as

$$\begin{aligned} g(r_1, r_2) &= \lim_{\Delta r \to 0} \frac{\Pr[r_1 \leq r_{(1)} \leq r_1 + \Delta r, r_2 \leq r_{(2)} \leq r_2 + \Delta r]}{(\Delta r)^2} \\ &= \frac{e^{-\Lambda_{r_2}}}{P_{2+}} \cdot \left[2\lambda r_1 e^{-K(L^2 + r_1^2)} \int_0^{\arccos(\frac{r_1}{L})} e^{2KLr_1\cos\theta} \mathrm{d}\theta \right] \\ &\quad \left[2\lambda r_2 e^{-K(L^2 + r_2^2)} \int_0^{\arccos(\frac{r_2}{L})} e^{2KLr_2\cos\theta} \mathrm{d}\theta \right]. \end{aligned} \tag{3.31}$$

In the second case, the two potential relays lie in the same sufficiently small region $[r_1, r_1 + \Delta r]$, which occurs with a probability

$$\begin{aligned} &\Pr[r_1 \leq r_{(1)} \leq r_1 + \Delta r, r_1 \leq r_{(2)} \leq r_1 + \Delta r] \\ &= \frac{1}{P_{2+}} \cdot e^{-\Lambda_{r_1}} \cdot \frac{(\Lambda_{\Delta r_1})^2}{2} e^{-\Lambda_{\Delta r_1}}. \end{aligned} \tag{3.32}$$

The PDF for the second case is then

$$\begin{aligned} h(r_1) &= \lim_{\Delta r \to 0} \frac{\Pr[r_1 \le r_{(1)} \le r_1 + \Delta r, r_1 \le r_{(2)} \le r_1 + \Delta r]}{\Delta r} \\ &= \lim_{\Delta r \to 0} \frac{o(\Delta r)}{\Delta r} = 0. \end{aligned} \tag{3.33}$$

According to the distributions of the distance of the two nearest potential relays to D, we obtain the conditional collision probability given that at least two potential relays lie in Ω_{L_0} as follows:

$$P_c = 1 + \frac{\Lambda_{L_0-\varpi} \cdot e^{-\Lambda_{L_0}}}{P_{2^+}} - \frac{1}{P_{2^+}} \int_0^{L_0-\varpi} e^{-\Lambda_{r_1}} \cdot e^{-\Lambda_{\Delta\varpi}} \mathrm{d}\Lambda_{r_1} \tag{3.34}$$

where

$$\begin{aligned} \Lambda_{\Delta\varpi} &= 2 \int_{r_1}^{r_1+\varpi} \int_0^{\arccos(\frac{r}{L})} e^{-K(L^2+r^2-2Lr\cos\theta)} \lambda r \mathrm{d}\theta \mathrm{d}r \\ \Lambda_{L_0-\varpi} &= 2 \int_0^{L_0-\varpi} \int_0^{\arccos(\frac{r}{L})} e^{-K(L^2+r^2-2Lr\cos\theta)} \lambda r \mathrm{d}\theta \mathrm{d}r. \end{aligned}$$

The derivation of (3.34) is given in Appendix A.2. An upper bound is also obtained for P_c in Appendix A.2, given by

$$P_c \le 1 + \frac{\Lambda_{L_0-\varpi} \cdot e^{-\Lambda_{L_0}}}{P_{2^+}} - \frac{e^{-\Gamma}}{P_{2^+}} \cdot \left(1 - e^{-\Lambda_{L_0-\varpi}}\right) \triangleq P_c^U \tag{3.35}$$

where

$$\Gamma = \max\{\Lambda_{\Delta\varpi}\} = 2 \int_{L_0-\varpi}^{L_0} \int_0^{\arccos(\frac{r}{L})} e^{-K(L^2+r^2-2Lr\cos\theta)} \lambda r \mathrm{d}\theta \mathrm{d}r.$$

3.5 Numerical Results

In this section, numerical and simulation results are first presented to demonstrate the accuracy of the estimation algorithm for relay intensity introduced in Section 3.3. Then, we validate our theoretical analysis in Section 3.4.2 for the cooperative scheme with energy saving. The proposed scheme is also compared with an uncoordinated probability-based scheme. Table 3.3 lists the default system parameters.

Table 3.3: System Parameters.

Symbol	Value	Definition
P_0/N_0	40 dB	SNR of the transmitter
T_0	5	SNR threshold of signal decoding
ν	2	Path-loss exponent
L	70 m	Distance between source and destination
λ	$10^{-2} \sim 10^{-1}$	Relay distribution intensity
ϖ	0.5 m	Collision window (distance interval)

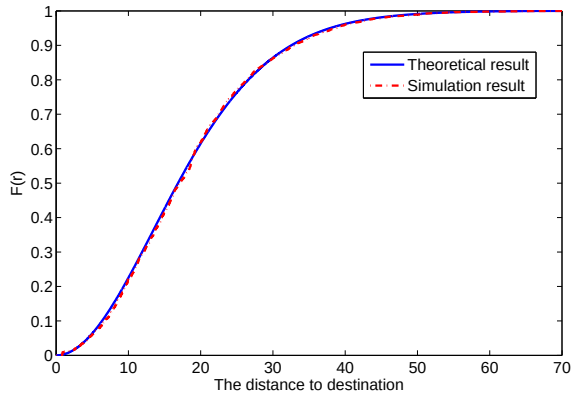

Figure 3.4: CDF of the distance of the nearest potential relay to the destination.

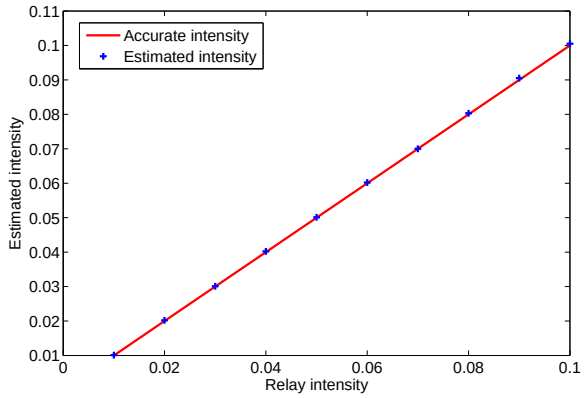

Figure 3.5: Estimated relay intensity $\widetilde{\lambda}$ vs. exact relay intensity λ.

3.5.1 Relay Intensity Estimation

Because the relay intensity estimation depends on the collected statistics of $F(r)$, we first validate the analysis of $F(r)$. As seen in Fig. 3.4, the simulation results and theoretical results match well, which confirms the analysis accuracy for $F(r)$.

The simulation results of the estimated intensity $\widetilde{\lambda}$ are shown in Fig. 3.5. As seen, the estimated $\widetilde{\lambda}$ is of high accuracy, which demonstrates the effectiveness of our proposed estimation algorithm. To further investigate the efficiency of our estimation, we illustrate its convergence speed in Fig. 3.6. It is observed that the estimated $\widetilde{\lambda}$ converges very quickly to the optimal solution with the minimum achievable estimation error. The maximum error bound for $F(r)$ (i.e., F_B) is always less than 0.02, as seen in Fig. 3.4. Also, it can be found that when the error bound F_B is 0.005, the relative estimation error of λ is around 1% after convergence, while it is around 5.5% when the estimation error of $F(r)$ is 0.02. Note that if the proposed iterative algorithm is not applied, the relative estimation error of λ can be very large even when F_B is small. For example, if we choose an improper distance r to collect the statistics of $F(r)$ without using the iterative algorithm, the estimation error for λ can be as high as 30%. Hence, we see that the proposed intensity estimation algorithm is effective and efficient.

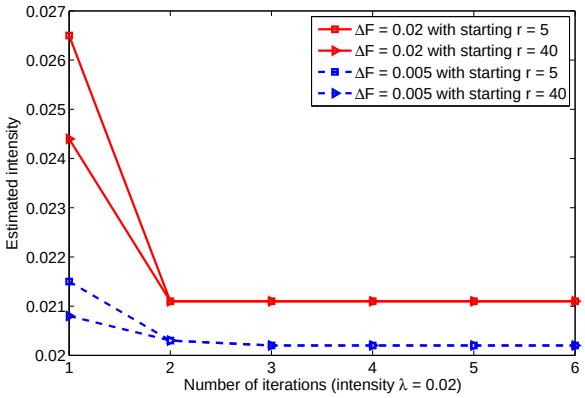

Figure 3.6: Estimated relay intensity $\widetilde{\lambda}$ vs. number of iterations.

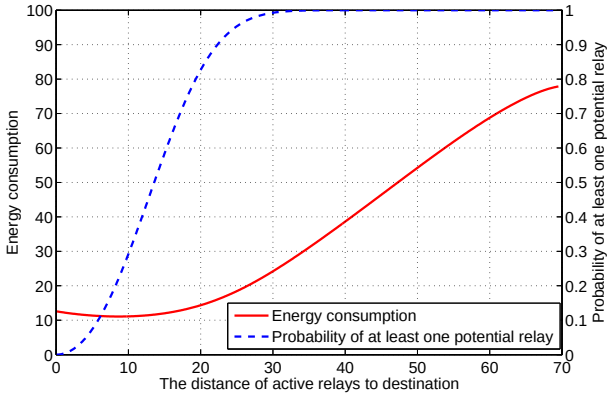

Figure 3.7: Energy consumption and the probability of at least one potential relay vs. distance to the destination.

3.5.2 Energy Saving Scheme

Fig. 3.7 shows the analytical results of energy consumption (E) against the distance r, where all the relays of a distance to D less than r are active and others are sleeping during the packet transmission. Here, the energy for transmission and that for listening/receiving are taken to be a constant [46], and the energy consumption in Fig. 3.7 is in the unit of this constant. Besides, Fig. 3.7 also shows the probability that at least one potential relay lies in the region Ω_r (P_{1+}), which is the upper bound of the transmission success probability. As seen, the energy consumption slightly goes down at the beginning. When r further increases, the energy consumption goes up. This is because the benefit of involving more relays with a greater P_{1+} cannot offset the side effect of higher incurred energy consumption.

Since the transmission success probability is bounded by P_{1+}, there is a trade-off between the transmission success probability and the energy consumption. As seen in Fig. 3.7, the minimum energy consumption is achieved with $L_0 \approx 12$, which can be obtained from (3.26)-(3.28). However, the corresponding transmission success probability with such L_0 may be too low to be acceptable for certain loss-sensitive applications. Therefore, a better threshold can be chosen for L_0 so as to satisfy certain required transmission success prob-

ability and ensure reasonable energy consumption. For example, by choosing $L_0 = 30$, we have P_{1+} almost 1 and achieve about 70% energy saving compared to $L_0 = L$. If P_{1+} can be relaxed to 0.8, $L_0 = 20$ will be a good choice and almost minimizes the energy consumption. As such, we can achieve a balance between the transmission performance and energy consumption by properly adapting the parameter L_0 based on our preceding analysis in Section 3.4.1. For the experiments in Section 3.5.3, we use the values in Table 3.4 for L_0, which ensures a P_{1+} around 0.8.

Table 3.4: L_0 for Numerical Analysis and Simulations.

λ	0.01	0.02	0.03	0.04	0.05
L_0	25.5	20	16.5	14.5	13.5
λ	0.06	0.07	0.08	0.09	0.10
L_0	12.5	11.5	11	10.5	10

3.5.3 Performance Evaluation

For comparison purposes, we consider an uncoordinated probability-based solution for reference. Similar to the local SNR based scheme proposed in [12], a potential relay R_i forwards an overheard packet with a probability τ_i, given by

$$\tau_i = e^{-\Lambda_{r_i}} \tag{3.36}$$

where r_i is the distance of R_i to D. Thus, τ_i gives the probability that no potential relay in Ω_{r_i} has an average SNR greater than that of R_i.

Fig. 3.8 shows the numerical results and simulation results of the collision probability against the threshold L_0 of the energy saving scheme. As seen, the simulation results match closely the analytical results, which validates the accuracy of our analysis. As expected, the collision probability increases with L_0 and λ due to a greater number of potential relays. Also, it is observed that the collision probability is tightly bounded by the upper bound when L_0 is small, and it is much smaller than the bound when L_0 gets larger. As shown in Fig. 3.8, the upper bound increases almost linearly with L_0. In contrast, the collision probability of the proposed cooperative scheme increases much slower than the linear growth. This is an attractive feature since it means that the collision probability increases slowly when there are more active relays.

Fig. 3.9 compares the collision probability of the cooperative scheme proposed in Section 3.4.1 to that of the probability-based scheme defined in (3.36). It can be seen that our scheme achieves a much lower collision probability. The proposed energy saving scheme can reduce the collision probability of both schemes, since the number of contending relays is smaller by turning off relays outside the region Ω_{L_0}.

Fig. 3.10 shows the transmission success probability of the two cooperative solutions with respect to the relay distribution intensity. We can see that the transmission success probability of the probability-based scheme is bounded by $1/e \approx 0.368$, which matches the observations in [13, 31]. In contrast, the backoff-based solution can achieve a transmission success probability higher than 0.65, because of the low collision probability shown

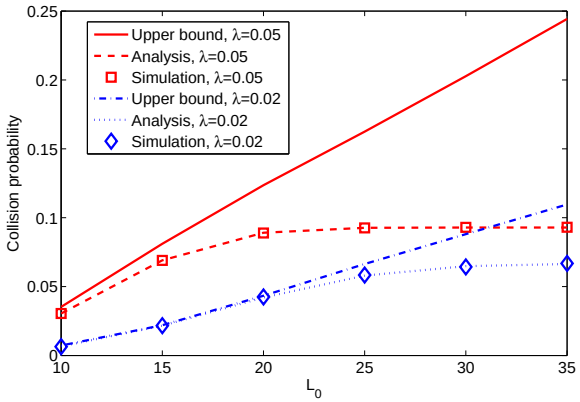

Figure 3.8: Collision probability P_c vs. L_0.

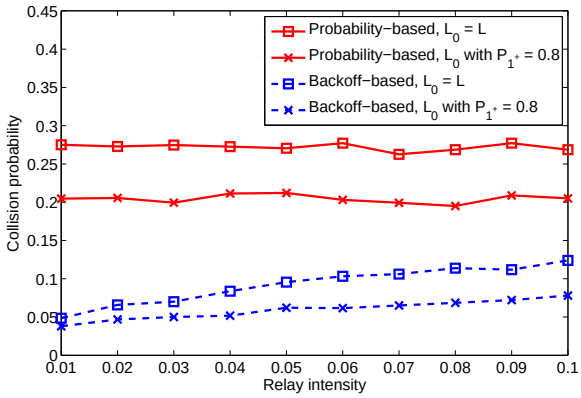

Figure 3.9: Collision probability P_c vs. relay intensity λ.

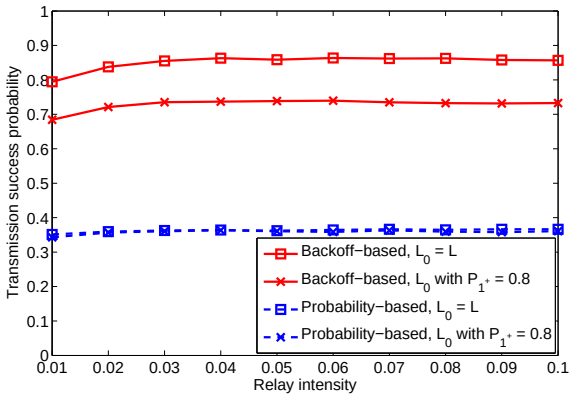

Figure 3.10: Transmission success probability vs. relay intensity λ.

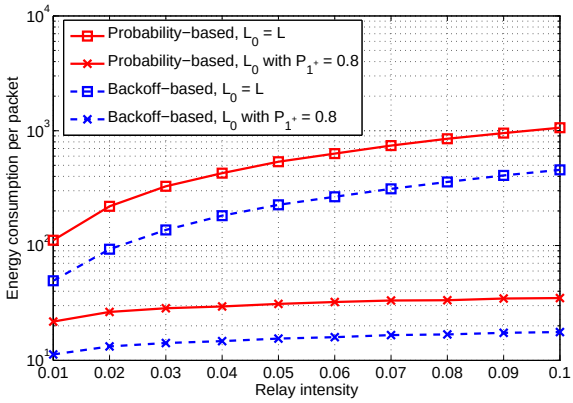

Figure 3.11: Energy consumption vs. relay intensity λ.

in Fig. 3.9. Moreover, we can find that the transmission success probability of the backoff-based scheme is slightly degraded by considering the energy saving threshold L_0 in Table 3.4, although the threshold L_0 reduces the collision probability, as shown in Fig. 3.9. This is because the transmission success probability is upper bounded by P_{1+}, and we select L_0 here to ensure a P_{1+} around 0.8. It is also observed in Fig. 3.10 that the transmission success probability only varies slightly with the relay intensity. This seems counter-intuitive since there will be more collisions when the relay intensity increases. This is because more potential relays also result in a higher chance of finding good relays, which mitigates packet loss caused by poor channel conditions and offsets the impact of increased packet collisions.

To investigate the energy consumption of the two cooperative schemes, we evaluate the average energy consumption of the relays for a packet against the relay intensity, as shown in Fig. 3.11. Compared to the probability-based scheme, the backoff-based scheme can save around 50% of energy on average, when the energy saving thresholds L_0 in Table 3.4 are applied. This is achieved by taking advantage of the low collision probability and high transmission success probability of the backoff-based scheme. Besides, we find that both schemes can achieve substantial energy saving as opposed to that with $L_0 = L$. For example, the backoff-based scheme can save more than 75% of energy, although the transmission success probability is slightly reduced. Therefore, our proposed cooperative scheme is highly energy-efficient.

3.6 Chapter Summary

In this chapter, we study distributed cooperative communications between a source-destination pair, where the relays are deployed as a PPP with an *unknown* intensity. Particularly, we focus on a backoff-based cooperative scheme, where the potential relay closest to the destination has the smallest backoff time and wins the contention. To estimate the relay distribution intensity, the PDF and CDF of the distance of the nearest potential relay to the destination are derived, and an iterative estimation algorithm is proposed with the proof of convergence. Although the backoff-based scheme can save considerable energy consumption when compared

to the centralized schemes and probability-based schemes, we find that many relays may be active unnecessarily. Hence, we also propose a distributed energy saving strategy, which selectively turns off low-quality relays in certain regions. To evaluate the performance of the proposed scheme with energy saving, we analyze the collision probability and derive an upper bound.

Extensive numerical and simulation results validate our analysis on the probability distribution of the distance of the nearest potential relay to the destination. The proposed estimation algorithm for the relay intensity also shows a high accuracy and a fast convergence speed. In addition, we properly characterize the tradeoff between the energy consumption and the transmission success probability. An energy saving threshold can be derived accordingly to guarantee a required transmission success probability and effectively reduce the energy consumption at the same time. The simulation results show that the proposed energy saving strategy can significantly reduce the energy consumption for both the backoff-based and probability-based schemes. Although the transmission success probability of the backoff-based scheme is slightly degraded by the energy saving strategy, it is still much higher than that of the probability-based scheme. Moreover, the backoff-based scheme can save around 50% of energy on average when compared to the probability-based scheme.

Chapter 4

Energy-Efficient Cooperative MAC for Multiple S-D Pairs

4.1 Motivation and Overview

Most of the cooperative MAC schemes focus on the scenario, where a single source-destination (S-D) pair is served by a number of dedicated relays [8, 14, 41]. Extending the simple cooperation scenario, we consider a new framework where multiple S-D pairs share a group of relays with energy constraint, which is a more realistic scenario in practice. The energy concern together with the new cooperation scenario pose new challenges in the cooperative scheme design, e.g., a relay may run out of energy. In addition, the scalability of the cooperative schemes is another key issue that requires further investigation.

In this chapter, considering the new framework with multiple S-D pairs sharing a number of energy-constrained relays, to satisfy the QoS requirements of multimedia services in a green manner, we propose an energy-aware uncoordinated cooperation scheme based on the backoff timer. Also, its performance is evaluated analytically with respect to the theoretical bounds of the collision probability and the transmission success probability. Extensive simulations are conducted to compare the performance of different uncoordinated schemes and the analytical bounds. The numerical and simulation results demonstrate that our proposed scheme is preferable for the delay-sensitive multimedia services and achieves significant energy saving.

The remainder of this chapter is structured as follows. Section 4.2 gives the system model and the problem formulation. In Section 4.3, we propose a novel uncoordinated cooperation scheme and then analyze its performance bounds in Section 4.4. Numerical and simulation results are presented in Section 4.5, followed by conclusions in Section 4.6.

4.2 System Model and Problem Formulation

4.2.1 System Model

Consider a wireless network with n S-D pairs and m relay nodes as illustrated in Fig. 4.1. We assume that the relays are uniformly distributed in a given region and the relay distribution is time-stationary. This assumption is generally valid for a variety of scenarios, e.g., under random direction mobility [42, 47]. The sources refer

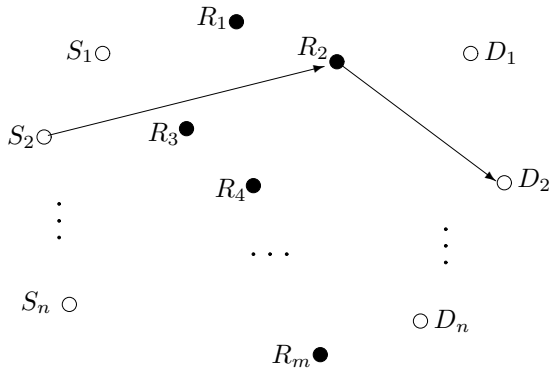

Figure 4.1: An illustration of the system model for cooperative transmission.

to the nodes that generate data traffic, while the destinations refer to the nodes that receive data traffic. Relay nodes have no intrinsic traffic demands. Since the relays are shared by multiple S-D pairs, we consider that the relays are energy constrained. When a relay runs out of energy, it is not eligible for future relaying. The sources can communicate with their destinations only through these shared relays using a two-hop decode-and-forward (DF) [4] protocol; other cooperative communication protocols can also be considered in a similar way.

Similar to the system model in Section 3.2.1, we assume that each node knows its own location, which can be obtained either from a positioning technique or through a GPS receiver. Further, the relay nodes can obtain the locations of the sources and destinations from the piggybacked information within the overheard packets. It should be noted that the sources do not have the knowledge of the locations of the relays, and one relay does not have the location information of other relays either. Besides, we assume that the locations of all the nodes in the network do not change significantly during the short cooperative transmission period, which is a typical assumption that generally holds.

For the data transmission between a transmitter located at x and a receiver located at y, the SNR of the received signal can be characterized by (3.1). For reference convenience, we rewrite (3.1) here:

$$\gamma_{xy} = \frac{P_0}{N_0} h_{xy} g_{xy} \tag{4.1}$$

where P_0 is the transmit power, N_0 is the power of additive white Gaussian noise (AWGN), and h_{xy} denotes the small-scale channel fading which is exponentially distributed with unit mean. The path-loss effect is captured by $g_{xy} = \|x - y\|^{-\nu}$, where $\|x - y\|$ is the Euclidean distance, and ν is the path-loss exponent. We assume that the receiver is able to correctly decode the received signal only when the instantaneous SNR is no less than a threshold T_0 [12]. Therefore, the probability that a packet is successfully received is the same as (3.2), given by

$$P_{xy} = \Pr[\gamma_{xy} \geq T_0] = \exp\Big(- \frac{T_0}{P_0/N_0} \|x - y\|^{\nu} \Big). \tag{4.2}$$

Since the location information of the sources and destinations is available to the relays, the distances between them can be calculated. Thus, we can estimate the transmission success probabilities from the n sources to the relay R_i by

$$P_{S,R_i} = \left[P_{S_1R_i}, P_{S_2R_i}, \ldots, P_{S_nR_i}\right], \qquad i = 1, 2, \ldots, m.$$

Similarly, the transmission success probabilities from the relay R_i to the n destinations are given by

$$P_{R_i,D} = \left[P_{R_iD_1}, P_{R_iD_2}, \ldots, P_{R_iD_n}\right], \qquad i = 1, 2, \ldots, m.$$

Some important notations are summarized in Table 4.1.

4.2.2 Problem Formulation

As discussed in Section 3.2.2, a centralized relay selection scheme is subject to large overhead and long delay incurred with exchange of channel state information. On the other hand, the distributed solutions often require an effective approach to mitigate collisions among multiple potential relays. While the probability-based uncoordinated schemes suffer from high collisions, the backoff-based schemes can handle collisions more effectively and present better performance in terms of the transmission success probability and delay. Hence, in this chapter, we also focus on the backoff-based cooperation similar to Chapter 3.

Specifically, we propose a novel backoff-based uncoordinated cooperation scheme, in which each potential relay sets a backoff timer based on a variety of factors. Considering the group cooperation model in Section 4.2.1, we need to effectively address the energy constraint of the relays, which are shared by multiple S-D pairs. The proposed cooperation scheme should not only provide QoS guarantee to the delay-sensitive multimedia services but also perform well in a large-scale network. It is known that the real-time multimedia services are sensitive to delay and delay jitter. In view of the time-varying nature of wireless networks, we consider a statistical QoS guarantee for the delay. That is, the delay outage probability defined in (4.3) is ensured bounded within an acceptable range:

$$P_{out} = \Pr[\mathcal{D} \geq \mathcal{D}_{max}] < \varepsilon \tag{4.3}$$

where $\mathcal{D}$ is the packet delay, $\mathcal{D}_{max}$ is the acceptable upper bound, and ε is a small probability that is allowed for QoS violation.

Table 4.1: Important Notations.

Symbol	Definition
S_j / D_j	Source node / destination node
R_i	Relay node
n	Total number of S-D pairs
m	Total number of relay nodes
ν	Path-loss exponent
P_0	Transmit power
N_0	Power of additive white Gaussian noise
T_0	SNR threshold of signal decoding
$P_{S_j R_i}$	Transmission success probability of packets from S_j to R_i
$P_{R_i D_j}$	Transmission success probability of packets from R_i to D_j
$\mathcal{D}$ / $\overline{\mathcal{D}}$	Packet delay / average packet delay
$\mathcal{D}_{max}$	Acceptable upper bound of packet delay
P_{out}	Delay outage probability
ε	A small probability that is allowed for QoS violation
d_{ij}	Distance between relay R_i and destination D_j
l	Maximum distance of potential relays to a destination
W_{ij}^d	Cooperation capability of R_i for D_j with respect to d_{ij}
E_i	Energy level of R_i
E_c	Energy upper limit
W_{ij}^e	Cooperation capability of R_i for D_j with respect to E_i
$U(0,\ 1)$	Uniform distribution between 0 and 1
W_{ij}	Overall cooperation capability of R_i for D_j
ρ	Trade-off parameter between energy status and distance metric
χ_j	Set of relays that correctly overhear packet from S_j
$\mathbf{1}_{\chi_j}(\cdot)$	Indicator function
T_{ij}	Backoff time of R_i for the S_j-D_j pair
κ	Update step length
$f(d)$	The probability density function (PDF) of distance d_{ij}
$f_w(w)$	The PDF of the overall cooperation capacity
$f_T(t)$	The PDF of the backoff time
$F_T(t)$	The cumulative distribution function (CDF) of the backoff time
c	Collision window (time interval)
P_c	Collision probability
P_c^U	Upper bound for P_c
P_{suc}	Transmission success probability
P_{ij}	The probability that W_{ij} is the largest for D_j
Q_j	The probability that at least one potential relay forwards packet for S_j
$\overline{P_{ij}}$	The probability that R_i transmits packets for S_j in the long term
P_{suc}^L	Lower bound for P_{suc}
P_{suc}^U	Upper bound for P_{suc}
$\widetilde{P_{suc}^U}$	Relaxed upper bound for P_{suc}
$P_\tau^{(i)}$	Normalized relaying probability of R_i in probability-based scheme

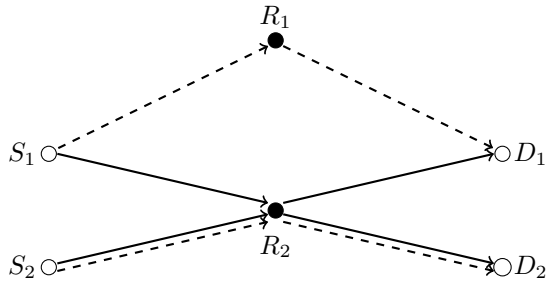

Figure 4.2: An illustration showing how the energy constraint of the relays affects relay selection. The solid lines indicate the cooperative transmissions without considering the energy status; and the dashed lines indicate the cooperative transmissions with the energy status taken into account.

4.3 Energy-Aware Cooperative Scheme

4.3.1 Cooperation Criteria

For a backoff-based cooperation scheme, the determination of the backoff timer is critical to reduce collisions, because a collision may occur when the backoff timers of the first two or more relays expire within an indistinguishable small interval. To improve the achievable performance, the backoff timer is often based on the cooperation capability of the relay. Hence, we need to properly choose the metrics that characterize the cooperation capability, so that the backoff timers of the group of relays can be appropriately scattered to decrease the collision probability.

First, we consider the distance between a relay and a destination, which can be estimated from the location information without incurring extra cost. This distance can capture the transmission success probability of the relay-to-destination channel according to (4.2). This is because we are interested in the potential relays that have correctly overheard the packet from the source and thus only focus on the relay-to-destination channel condition. Denoting the distance between the relay R_i and the destination D_j by d_{ij}, we define the cooperation capability of R_i for D_j with respect to the distance as

$$W_{ij}^{d} = \begin{cases} 1 - \left(\frac{d_{ij}}{l}\right)^2, & \text{if} \quad d_{ij} \leq l \\ 0, & \text{if} \quad d_{ij} > l \end{cases} \tag{4.4}$$

where l is the largest distance to the destination for a node to be considered as a potential relay. As such, a relay with a smaller distance to the destination is characterized with a greater cooperation capability, because of a higher transmission success probability over the relay-to-destination channel.

Second, the energy status of the relay is also accounted into the estimation of the cooperation capability, since the shared relays are energy constrained. The example in Fig. 4.2 illustrates the importance of incorporating the energy status into the characterization of the cooperation capability. As seen, the relay R_2 is the best relay for both S_1-D_1 and S_2-D_2 pairs, if only the distance to the destination is concerned. Consequently, R_2 will

run out of energy quickly. The S_1-D_1 and S_2-D_2 pairs will need to switch to the relay R_1. The performance of the S_1-D_1 pair will remain almost the same, whereas the S_2-D_2 pair will suffer from a performance degradation since R_1 is far from S_2 and D_2. On the other hand, if both the distance and the energy status are taken into account, R_1 and R_2 should serve S_1-D_1 and S_2-D_2, respectively. Thus, the relaying capacities are utilized in a more balanced manner. Therefore, we further consider the energy status of R_i to characterize its cooperation capability by

$$W_i^e = E_i/E_c \tag{4.5}$$

where E_i is the energy level of R_i with an energy upper limit of E_c. Here, we assume that all the relays have the same energy upper limit and their energy levels are uniformly distributed. Therefore, W^e follows a uniform distribution between 0 and 1, denoted by $U(0,\ 1)$. As seen, a relay of a higher energy level thus has a greater cooperation capability.

Based on the two metrics in (4.4) and (4.5), the overall cooperation capability of the relay R_i for the destination D_j is defined as

$$W_{ij} = \rho \cdot W_i^e + (1-\rho) \cdot W_{ij}^d \tag{4.6}$$

where $\rho \in [0, 1]$ is a weighting parameter to trade-off between the importance of the energy status and that of the distance metric. As seen, $W_{ij} \in [0,\ 1]$.

4.3.2 Distributed Cooperative Scheme

Table 4.2 presents the proposed energy-aware cooperation scheme in detail. Based on the cooperation capabilities of the relays, the optimal relay for the S_j-D_j pair is defined as

$$R_i \ = \ \arg \max_{i \in \{1,\ldots,K\}} \{\mathbf{1}_{\chi_j}(i) \cdot W_{ij}\}$$

where χ_j is the set of relays that correctly overhear the data packet from S_j, and

$$\mathbf{1}_{\chi_j}(i) = \begin{cases} 1, & \text{if} \quad R_i \in \chi_j \\ 0, & \text{if} \quad R_i \notin \chi_j. \end{cases}$$

To ensure that the optimal relay has the fastest access to the channel, the relay R_i sets an initial backoff time inversely proportional to its cooperation capability for the S_j-D_j pair as

$$T_{ij} = 1 - W_{ij} \tag{4.7}$$

in which the maximum backoff time is taken to be one unit time. As such, the optimal relay of the highest cooperation capability sets the smallest backoff time. If the first two or more relays time out within an indistinguishable small interval c, a collision happens [16].

Table 4.2: Energy-Aware Cooperative Scheme.

Initialize cooperation capabilities W of relays according to (4.6)
while a new transmission occurs between any S_j-D_j pair **do**
    for all the relays **do**
        if relay R_i overhears the packet correctly **then**
            Set the backoff timer of R_i to $1 - W_{ij}$
        end if
    end for
    for all the relays correctly received the packet **do**
        if backoff timer expires and no relaying sensed **then**
            Forward the packet to D_j
        end if
    end for
    if only one relay R_i transmits within time interval c **then**
        if D_j decodes the packet correctly **then**
            Transmission succeeds
        else
            Transmission fails
        end if
        // Update W concerning energy consumption
        $W_{iq} \leftarrow W_{iq} - \rho \cdot \kappa$, for $q = 1, 2, \ldots, n$
    else
        Collision happens and transmission fails
        for every relay R_c that transmitted **do**
            // Update W concerning energy consumption
            $W_{cq} \leftarrow W_{cq} - \rho \cdot \kappa$, for $q = 1, 2, \ldots, n$
            // Update W concerning collision
            $W_{cj} \leftarrow W_{cj} - (1 - \rho) \cdot W_{cj}^{d} \cdot \kappa$
        end for
    end if
end while

To account for the energy consumption of packet forwarding of R_i for any S-D pair, we update the cooperation capability of R_i for all S-D pairs as follows

$$W_{iq} = W_{iq} - \rho \cdot \kappa, \qquad q = 1, 2, \ldots, n \tag{4.8}$$

where κ is the update step length. This is to yield the forwarding opportunities to other relays and thus balance the energy consumption.

Here comes a problem when a collision happens among the relays. If all the relays involved in the collision update their cooperation capabilities according to (4.8), a collision will happen again in the next transmission. Therefore, we need to penalize these relays by updating their cooperation capabilities to

$$W_{ij} = W_{ij} - (1 - \rho) \cdot W_{ij}^{d} \cdot \kappa, \qquad i = c_1, c_2, \ldots, c_z \tag{4.9}$$

where $c_1, c_2, \ldots, c_z$ are the indices of the relays $R_{c_1}, \ldots, R_{c_z}$ that collide when forwarding the packet for the S_j-D_j pair. As a higher W_{ij}^{d} implies a lower energy level when a collision happens, the corresponding relay is punished more to achieve the energy balance and avoid further collisions.

4.4 Performance Analysis

To satisfy the delay requirements of multimedia services, it is essential to minimize the collision probability so as to maximize the transmission success probability. In this section, we analyze the performance bounds of the proposed cooperation scheme in terms of the collision probability and the transmission success probability. Here, we focus on one S-D pair, since the achievable performance of all S-D pairs is the same, given the homogeneous setting of S-D pairs in the system model.

4.4.1 Upper Bound of Collision Probability

Lemma 4.1. *If the relays are uniformly distributed, the probability density function (PDF) of their distance d to the destination D within l is given by*

$$f(d) = \begin{cases} \dfrac{2d}{l^2}, & \textit{if} \quad d \leq l \\ 0, & \textit{otherwise}. \end{cases} \tag{4.10}$$

Proof. Consider the polar coordinate system where D is the origin and an arbitrary relay is located at $(d,\ \theta)$. The corresponding location of the relay in the Cartesian coordinate system is then $(x,\ y)$, where $x = d \cdot \cos(\theta)$, and $y = d \cdot \sin(\theta)$. For the relays uniformly distributed within the circle of a radius l and centered at D, the

joint PDF of their locations $(x,\ y)$ is given by

$$f_{X,Y}(x,y) = \begin{cases} \frac{1}{\pi l^2}, & \text{if} \quad \sqrt{x^2+y^2} \le l \\ 0, & \text{otherwise.} \end{cases}$$

Since $d = \sqrt{x^2+y^2}$, according to the Jacobian matrix, we can obtain the PDF of d as shown in (4.10). □

Lemma 4.2. *If the PDF of the distance of a relay to the destination follows (4.10), the general cooperation capability concerning the distance, W^d defined in (4.4), follows a uniform distribution between 0 and 1.*

Proof. The cumulative distribution function (CDF) of W^d is given by

$$\begin{aligned} \Pr[W^d \le w] &\overset{\text{Eq. (4.4)}}{=} \Pr[1-(d/l)^2 \le w] &= 1 - \Pr[d \le l\sqrt{1-w}] \\ &\overset{\text{Lemma 4.1}}{=} 1 - \int_0^{l\sqrt{1-w}} f(x)\mathrm{d}x &= 1 - \frac{d^2}{l^2}\Big|_0^{l\sqrt{1-w}} = w. \end{aligned}$$

Therefore, $W^d \sim U(0,\ 1)$. □

Theorem 4.1. *Since $W^e \sim U(0,\ 1)$ and $W^d \sim U(0,\ 1)$, the overall cooperation capability defined in (4.6) with $\rho \in (0, 0.2]$ concerning both the distance and the energy status follows a distribution with a PDF*

$$f_W(w) = \begin{cases} \frac{w}{\rho(1-\rho)}, & \textit{if} \quad 0 \le w \le \rho \\ \frac{1}{1-\rho}, & \textit{if} \quad \rho < w \le 1-\rho \\ \frac{1-w}{\rho(1-\rho)}, & \textit{if} \quad 1-\rho < w \le 1 \\ 0, & \textit{otherwise.} \end{cases} \tag{4.11}$$

Proof. Given two continuous random variables V_1 and V_2, if $V_2 = aV_1$, the PDFs of V_1 and V_2 are related according to

$$f_{V_2}(x) = \Big(\frac{1}{a}\Big) f_{V_1}\Big(\frac{x}{a}\Big).$$

where $f_{V_1}(\cdot)$ and $f_{V_2}(\cdot)$ are the PDFs of V_1 and V_2, respectively. Since $W^e \sim U(0,\ 1)$ and $W^d \sim U(0,\ 1)$ (Lemma 4.2), we have

$$X = \rho \cdot W^e \sim U(0,\ \rho)\ ,\ Y = (1-\rho)\cdot W^d \sim U(0,\ 1-\rho)\ .$$

Then, for $W = \rho \cdot W^e + (1-\rho)\cdot W^d = X + Y$, we have

$$\begin{aligned} f_W(w) &= \int_{-\infty}^{\infty} f_X(w-y) f_Y(y)\mathrm{d}y \\ &= \frac{1}{1-\rho}\int_0^{1-\rho} f_X(w-y)\mathrm{d}y \end{aligned}$$

Only when $0 \le w - y \le \rho$, i.e., $w - \rho \le y \le w$, $f_X(w-y) = 1/\rho$ and the above integral is not zero. Therefore, we

have

$$f_W(w) = \frac{1}{1-\rho}\int_0^w \frac{1}{\rho}\,\mathrm{d}y = \frac{w}{\rho(1-\rho)}, \quad \text{if } 0 \le w \le \rho$$
$$f_W(w) = \frac{1}{1-\rho}\int_{w-\rho}^w \frac{1}{\rho}\,\mathrm{d}y = \frac{1}{1-\rho}, \quad \text{if } \rho < w \le 1-\rho$$
$$f_W(w) = \frac{1}{1-\rho}\int_{w-\rho}^{1-\rho} \frac{1}{\rho}\,\mathrm{d}y = \frac{1-w}{\rho(1-\rho)}, \text{ if } 1-\rho < w \le 1$$

which conclude the proof. □

According to Theorem 4.1 for $\rho \in (0,\ 0.2]$, it can be easily shown that the backoff time as defined by (4.7) follows a distribution with a PDF, given by

$$f_T(t) = \begin{cases} \dfrac{t}{\rho(1-\rho)}, & \text{if} \quad 0 \le t \le \rho \\ \dfrac{1}{1-\rho}, & \text{if} \quad \rho < t \le 1-\rho \\ \dfrac{1-t}{\rho(1-\rho)}, & \text{if} \quad 1-\rho < t \le 1 \\ 0, & \text{otherwise.} \end{cases} \tag{4.12}$$

Assume that N relays ($R_{i_1}, \ldots, R_{i_N}$) correctly overhear the transmitted packet from one particular source. Let $T_1 < T_2 < \cdots < T_N$ denote the order statistics of the backoff time of the N relays. According to [16], the collision probability P_c is given by

$$P_c \ = \ \Pr[T_2 < T_1 + c] \ = \ 1 - I_c \tag{4.13}$$
$$I_c \ = \ N(N-1)\int_c^1 f_T(t)\Big[1 - F_T(t)\Big]^{N-2} F_T(t-c)\mathrm{d}t \tag{4.14}$$

where $f_T(t)$ is the PDF of the backoff time and $F_T(t)$ is the corresponding CDF. Here, c is an indistinguishable small interval and a collision happens when the backoff timers of the first two or more relays time out within c. As one example, the distributed coordination function (DCF) of IEEE 802.11 can choose a maximum backoff time of 1024 time slots [48]. Then, the interval c can be considered as one time slot. Provided that the maximum backoff time is taken to be one unit time, the interval c can be in the order of 10^{-3}.

When $\rho = 0$, we have $W = W^d$ according to (4.6). Based on Lemma 4.2, this means that the cooperation capability W follows a uniform distribution between 0 and 1. Thus, the backoff time defined in (4.7) is also uniformly distributed with $f_T(t) = 1$ and $F_T(t) = t$ for $0 \le t \le 1$. From (4.14), we can easily obtain

$$I_c \ = \ (1-c)^N. \tag{4.15}$$

For $0 < \rho \leq c$, we have

$$\begin{aligned} I_c \;=\; & \frac{N(N-1)}{(1-\rho)^N}\Bigg\{\Big(1-\frac{3}{2}\rho\Big)^{N-1}\Big(\frac{1-\rho-c}{N-1}-\frac{1-3\rho/2}{N}\Big) \\ & +\Big(\frac{\rho}{2}\Big)^{N-1}\Big(\frac{2c-c^2/\rho}{2N-2}-\frac{2c}{2N-1}\Big)\Bigg\}. \end{aligned} \tag{4.16}$$

For $\rho > c$, because a closed-form I_c is not tractable, we derive the following lower bound in Appendix B.1

$$\begin{aligned} I_c \;>\; & \frac{N(N-1)}{(1-\rho)^N}\Bigg\{\Big(1-\frac{3}{2}\rho\Big)^{N-2}\Big(\rho-c\Big)^3\Big(\frac{1}{8\rho}+\frac{c}{24\rho^2}\Big) \\ & +\Big(1-\frac{3}{2}\rho\Big)^{N-1}\Big(\frac{1-\rho-c}{N-1}-\frac{1-3\rho/2}{N}\Big) \\ & +\Big(\frac{\rho}{2}\Big)^{N-1}\Big(\frac{2c-c^2/\rho}{2N-2}-\frac{2c}{2N-1}\Big)\Bigg\}. \end{aligned} \tag{4.17}$$

Defining the righthand-side terms in (4.15)-(4.17) as I_c^L, we have $I_c \geq I_c^L$ and

$$P_c \;=\; 1-I_c \;\leq\; 1-I_c^L \;\triangleq\; P_c^U \tag{4.18}$$

where P_c^U denotes an upper bound of the collision probability.

4.4.2 Lower Bound of Transmission Success Probability

When the traffic load is high, most of the relays will run out of energy quickly, and the distribution of their cooperation capabilities will no longer follow (4.11). Thus, it is hard to theoretically derive a lower or upper bound for the transmission success probability. Therefore, we focus on a normal traffic load when analyzing the lower bound of the transmission success probability in this section and its upper bound in the next section. In this circumstance, the energy constraint can be relaxed by setting $\rho = 0$. Then, the cooperation capability is only determined by the distance metric and follows a uniform distribution between 0 and 1.

A relay R_i participates in the cooperative relaying for the S_j-D_j pair only if R_i correctly receives the packet from S_j and its cooperation capability W_{ij} is the maximum among the N relays ($R_i, R_{i_1}, \ldots, R_{i_{N-1}}$) that overhear this packet successfully. With the largest W_{ij}, R_i sets the shortest backoff time and becomes the first to forward the packet. We have the corresponding occurrence probability

$$\begin{aligned} P_{ij} \;&=\; P_{S_jR_i}\cdot\prod_{q=1}^{N-1}\Pr[W_{ij}>W_{i_qj}] \\ &=\; P_{S_jR_i}\cdot(W_{ij})^{N-1}. \end{aligned} \tag{4.19}$$

Besides, the probability that at least one relay successfully overhears and forwards the packet for S_j is given

by

$$Q_j = 1 - \prod_{q=1}^{m} (1 - P_{S_j R_q}). \tag{4.20}$$

Hence, the probability that R_i transmits the packet for S_j in the long term is given by

$$\overline{P_{ij}} = Q_j \cdot \frac{P_{ij}}{\sum_{q=1}^{m} P_{qj}}. \tag{4.21}$$

Finally, we have the transmission success probability for the S_j-D_j pair

$$\begin{aligned} P_{suc}^{(j)} &= \sum_{r=1}^{m} \overline{P_{qj}} \cdot P_{R_q D_j} \cdot (1 - P_c) \\ &\geq (1 - P_c^U) \cdot \sum_{q=1}^{K} \overline{P_{qj}} \cdot P_{R_q D_j} \triangleq P_{suc}^L \end{aligned} \tag{4.22}$$

where P_{suc}^L denotes the lower bound of the transmission success probability.

4.4.3 Upper Bound of Transmission Success Probability

In Section 4.4.2, the energy constraint is relaxed to derive the lower bound of the transmission success probability. To obtain the upper bound, we assume no collisions among the relays in data forwarding. The upper bound of the transmission success probability for an arbitrary S_j-D_j pair is then given by

$$\begin{aligned} P_{suc}^U = P_{S_j R_{(1)}} \cdot P_{R_{(1)} D_j} + (1 - P_{S_j R_{(1)}}) \cdot P_{S_j R_{(2)}} \cdot P_{R_{(2)} D_j} \\ + \cdots + \prod_{q=1}^{m-1} (1 - P_{S_j R_{(q)}}) \cdot P_{S_j R_{(m)}} \cdot P_{R_{(m)} D_j} \end{aligned} \tag{4.23}$$

where $P_{R_{(1)} D_j} > P_{R_{(2)} D_j} > \cdots > P_{R_{(m)} D_j}$. The first term in (4.23) represents the case that the best relay $R_{(1)}$ has correctly received the packet from S_j with a probability $P_{S_j R_{(1)}}$, and its forwarding over the relay-to-destination channel to D_j succeeds with a probability $P_{R_{(1)} D_j}$. The second term in (4.23) indicates that the best relay $R_{(1)}$ fails to receive the packet from S_j with a probability $(1 - P_{S_j R_{(1)}})$, while the second best relay $R_{(2)}$ successfully receives and forwards the packet to D_j with a probability $P_{S_j R_{(2)}} \cdot P_{R_{(2)} D_j}$. The other terms in (4.23) can be interpreted in a similar way.

In addition, a relaxed upper bound of the transmission success probability can be obtained as

$$\widetilde{P_{suc}^U} = Q_j \cdot \max_{q \in \{1,2,\ldots,m\}} \{P_{R_q D_j}\} > P_{suc}^U \tag{4.24}$$

where Q_j is given by (4.20). Here, $\widetilde{P_{suc}^U}$ is derived by considering the maximum success probability over the relay-to-destination channel when at least one relay forwards the packet.

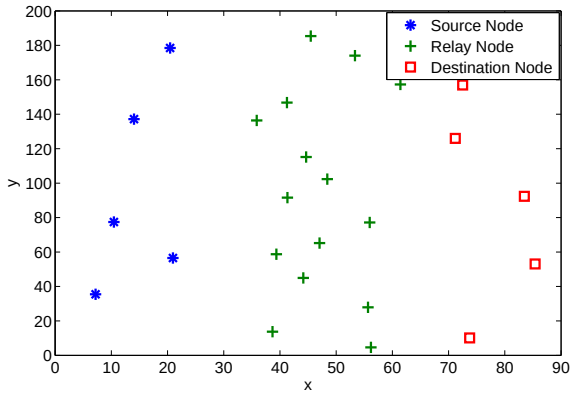

Figure 4.3: Nodes topology for analysis and simulation.

4.5 Numerical Results

In this section, numerical and simulation results are presented to demonstrate the effectiveness of our proposed cooperation scheme and the analytical bounds. For comparison purposes, we consider an uncoordinated probability-based algorithm, in which each potential relay R_i chooses its forwarding probability according to

$$P_{\tau_i} = \left[1 + \frac{P_0}{N_0 T_0 l^2} \cdot \ln\left(P_{R_i D}\right)\right]^{N-1} \tag{4.25}$$

where N is the number of relays that correctly overhear the packet from the source. Here, P_{τ_i} is actually the probability that R_i is the relay with the maximum transmission success probability over the relay-to-destination channel (with $\nu = 2$). The derivation of (4.25) is given in Appendix B.2. In the simulation, we further minimize collisions by normalizing P_{τ_i} to

$$P_{\tau}^{(i)} = \frac{P_{\tau_i}}{\sum_{q=1}^{N} P_{\tau_q}}. \tag{4.26}$$

In practice, it is not appropriate for a distributed approach to allow a relay to obtain the forwarding probabilities of other relays. Thus, the real performance of the probability-based algorithm can be worse.

In the following experiments, we assume that the nodes are uniformly distributed in a 40m $\times$ 200m area, as illustrated by the example in Fig. 4.3. The maximum distance of potential relays to a destination is $l = 55$ m, since the transmission success probability over the relay-to-destination channel is lower than 0.25 when $l > 55$ m. Assume that all the relays are fully charged at the beginning, and each relay can transmit up to 10^4 packets. More system parameters are given in Table 4.3.

4.5.1 Collision Probability

Fig. 4.4 shows the analytical bounds and simulation results of the collision probability. As seen, when the collision interval c increases, the collision probability increases accordingly. Further, when the number of relays

Table 4.3: System Parameters.

Symbol	Value	Definition
P_0/N_0	40 dB	Transmit SNR
T_0	5	SNR threshold of signal decoding
ν	2	Path-loss exponent
l	55 m	Maximum distance of potential relays to a destination
ρ	$0 \sim 0.2$	Weighting parameter for distance and energy
κ	0.0001	Update step length
c	$0.001 \sim 0.01$	Indistinguishable backoff time interval for collision

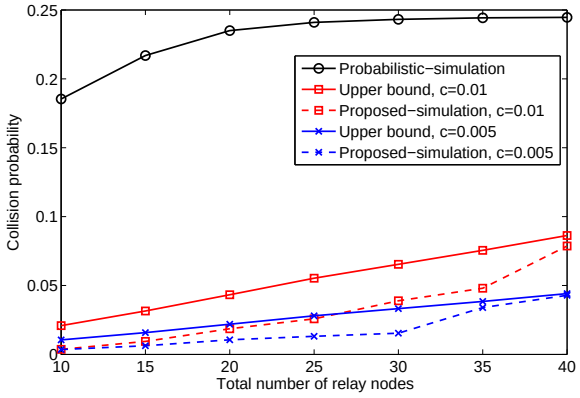

Figure 4.4: Collision probability P_c vs. total number of relay nodes.

m increases, the collision probability increases as well. We also find that the analytical upper bound of the collision probability works well for the proposed scheme. Besides, it is observed that the collision probability of the proposed scheme is smaller than 10%, even when the collision interval and the number of relays are large. In contrast, the probability-based algorithm has a collision probability greater than 18%, which is much higher than that of the proposed scheme. It should be noted that the collision probability of the probability-based algorithm has been minimized by normalizing the forwarding probability of each relay, which makes the approach not purely distributed.

4.5.2 Transmission Success Probability

Fig. 4.5 compares the transmission success probability of different schemes with the analytical bounds. We can see that the transmission success probability of the probability-based algorithm is bounded by $1/e \approx 0.368$, which verifies the conclusions in [13, 31]. In contrast, our proposed backoff-based scheme can easily achieve a transmission success probability higher than 0.6, because of the reduced collision probability. Moreover, we find that the upper bound and the lower bound of the transmission success probability both work well. The proposed scheme approaches the upper bound in a normal traffic load.

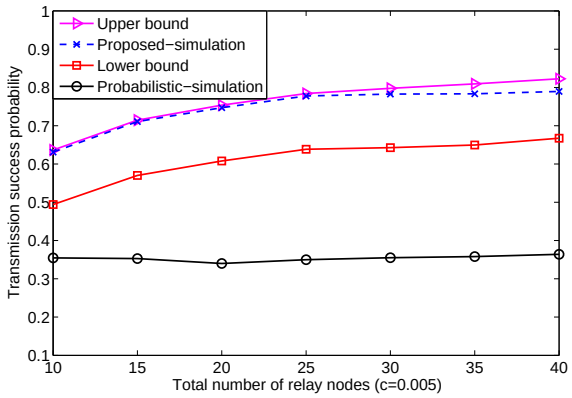

Figure 4.5: Transmission success probability vs. total number of relay nodes.

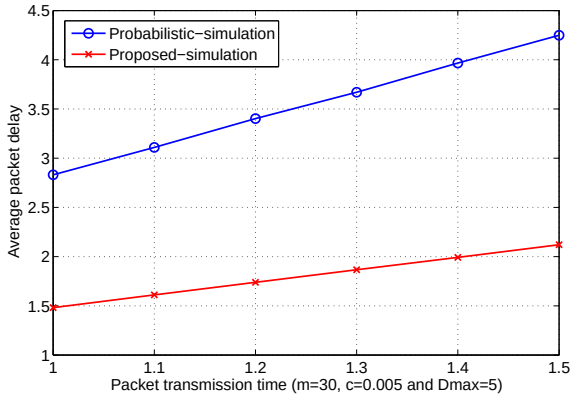

Figure 4.6: Average packet delay $\overline{\mathcal{D}}$ vs. packet transmission time.

Furthermore, it is seen in Fig. 4.5 that the transmission success probability of the proposed scheme increases with a greater number of relays, whereas that of the probability-based algorithm remains almost the same. This seems counter-intuitive since Fig. 4.4 shows the collision probability of both algorithms increases with the number of relays. This is because the opportunity of finding a good relay increases with more potential relays. Thus, packet loss caused by poor channel conditions can be reduced.

4.5.3 Average Delay and Delay Outage Probability

Fig. 4.6 shows the average packet transfer delay of the two algorithms against the packet transmission time. The packet transfer delay represents the time duration from a packet generation to successful transmission, while the packet transmission time is given by the packet length over the transmission rate. Here, the maximum backoff time is taken to be one unit time. As seen, the average packet delay of the proposed algorithm is much smaller than that of the probability-based algorithm, even though the proposed algorithm requires extra backoff time. This is because the collision probability of the proposed backoff-based algorithm is much lower than that of the probability-based algorithm, as shown in Fig. 4.4. As a result, the transmission success

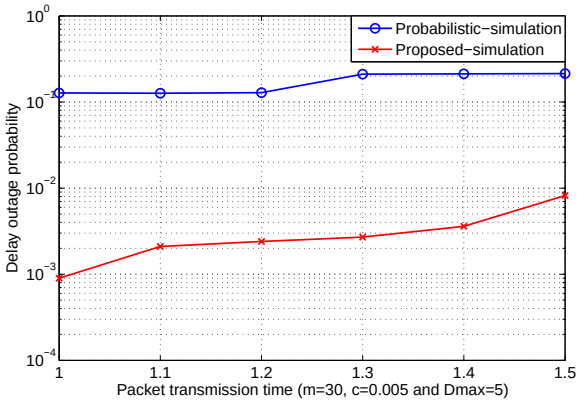

Figure 4.7: Delay outage probability P_{out} vs. packet transmission time.

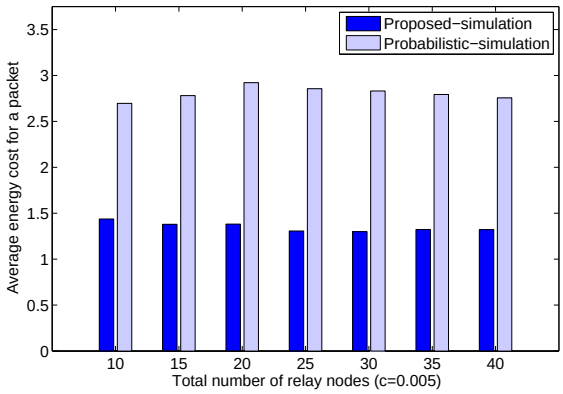

Figure 4.8: Average energy cost for a packet vs. total number of relay nodes.

probability is improved significantly, as seen in Fig. 4.5. Thus, the average packet transfer delay is reduced accordingly. In addition, we find that the average packet delay of the backoff-based algorithm increases slower than that of the probability-based algorithm, which implies that our proposed algorithm can achieve more gain for a larger packet length.

Fig. 4.7 compares the delay outage probability (in log scale) of the two algorithms with respect to the packet transmission time. It can be seen that the backoff-based algorithm has a delay outage probability smaller than 0.01. On the other hand, the delay outage probability of the probability-based algorithm increases faster from 0.12 to 0.21, when the packet transmission time increases from 1 to 1.5. Therefore, our proposed algorithm is preferable for the real-time delay-sensitive services.

4.5.4 Energy Saving and Energy Balance

To further investigate the energy consumption of the two algorithms, Fig. 4.8 shows the average energy cost of the relays for a packet with respect to the total number of relays. Here, the unit of energy cost is the energy consumption of one transmission attempt for a packet with a transmission time of one time unit. As seen in

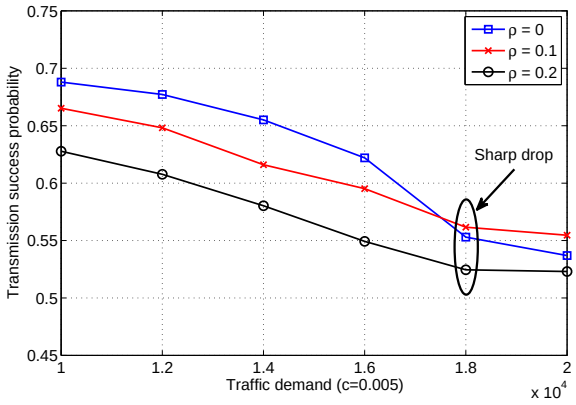

Figure 4.9: Transmission success probability P_{suc} vs. traffic demand.

Fig. 4.8, our proposed backoff-based algorithm can save around 50% of energy on average, compared to the probability-based algorithm. This energy saving is due to the low collision probability and high transmission success probability of the backoff-based algorithm.

In Fig. 4.9, we show the variations of the transmission success probability with the traffic demand of an S-D pair. Here, the traffic demand is the number of packets transmitted for an S-D pair, excluding the retransmitted packets. It is assumed in the simulation that all n S-D pairs have the same traffic demand. As seen, when the traffic demand is low, the highest transmission success probability is achieved at $\rho = 0$. Given a low traffic demand, no relay runs out of energy to satisfy the demand and the relays with the best channel conditions are always available to forward the packets. Hence, the energy constraint does not take effect and it is not necessary to consider energy balance in relay selection.

On the other hand, the situation becomes different with a high traffic demand. As seen in Fig. 4.9, when the traffic demand is greater than 1.8×10^4, the transmission success probability with $\rho = 0$ is no longer higher than that of $\rho = 0.1$. This is because the energy constraint is not addressed with $\rho = 0$ and consequently the best relay candidates may run out of energy very quickly. In contrast, we can take advantage of energy balance by setting $\rho = 0.1$ for relay selection and thus extend the survival time of the relays. As a result, the average transmission success probability can be improved. Moreover, it is observed in Fig. 4.9 that the transmission success probability with $\rho = 0.2$ is always worse than that of $\rho = 0$ and $\rho = 0.1$. This implies that the weight $\rho = 0.2$ overvalues the importance of energy status but underestimates that of the relay's distance to the destination. Consequently, the relay selection becomes kind of "blind" to the transmission success probability over the relay-to-destination channel. Therefore, it is usually assumed that $\rho \leq 0.2$.

4.5.5 Scalability

To study the scalability of the proposed scheme, we vary the total number of relays m and the total number of S-D pairs n in the simulation. Given a fixed number of S-D pairs, $n = 5$, Fig. 4.10(a) shows that the trans-

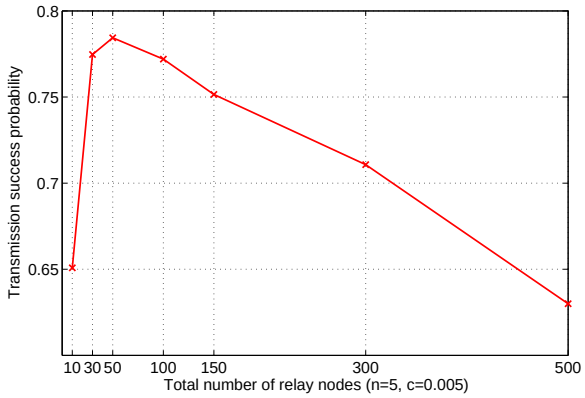

(a) P_{suc} vs. m

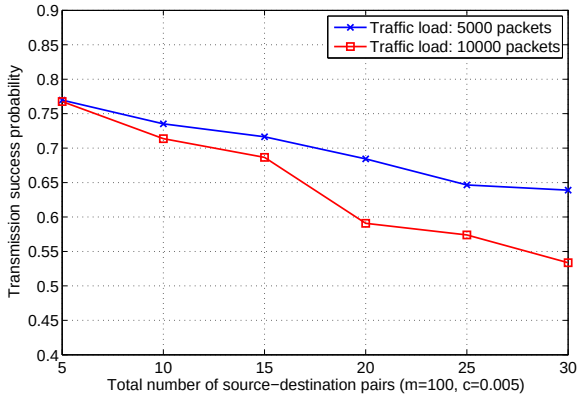

(b) P_{suc} vs. n

Figure 4.10: Scalability of the proposed cooperation scheme.

mission success probability first increases with the number of relays and then decreases when $m \geq 50$. On one hand, more good relays become available for an S-D pair when the total number of relays is larger. On the other hand, the collision probability also increases correspondingly. At the beginning, the advantage of having more good relays dominates the side effect of collisions. On the contrary, when the number of relays further grows, the collision probability becomes very high and the transmission success probability decreases. For example, the collision probability with $m = 300$ is 20.86%, which is much higher than 10.34% with $m = 100$. For the relaying area considered in the simulation, $m = 500$ is an extremely high and rare density in practice. Even so, we still find that the transmission success probability is above 60% and much larger than that of the probability-based scheme.

Fig. 4.10(b) shows the transmission success probability vs. the number of S-D pairs n given a fixed number of relays $m = 100$. The two scenarios in comparison have different traffic loads, which are the total number of packets transmitted for each S-D pair, including the retransmitted packets. It is observed that the transmission success probability is above 50% with a reasonable number of S-D pairs ($n \leq 30$) when the traffic load is

normal. This verifies that our proposed scheme can be deployed in a large-scale network. Moreover, it is seen that the transmission success probability decreases with a larger number of S-D pairs. When more S-D pairs share a group of common relays, the relays with better channel conditions to the destinations will run out of energy quickly. As a result, the transmission success probability goes down, but decreases more slowly with a lower traffic load. Hence, in order to guarantee the QoS requirements, the amount of traffic that enters the network should be regulated by controlling the number of S-D pairs and/or their admissible traffic loads. In addition, we find that the Jain's fairness index of the transmission success probability among the n S-D pairs is almost 1, which implies that the group of relays are evenly shared by all S-D pairs with the proposed scheme.

4.6 Chapter Summary

In this chapter, we study the uncoordinated cooperative communications between multiple S-D pairs that share a group of energy-constrained relays. A novel cooperation scheme is proposed based on backoff timers. It makes use of the cooperative capability, which is characterized by the distance information and the energy status of the relay. Thus, the relay of a higher cooperative capability ends up with a shorter backoff time. The best relay times out first and wins the contention. However, a collision still happens if the backoff timers of the first two or more relays expire within an indistinguishable time interval. Hence, we also derive the theoretical performance bounds for the proposed scheme with respect to the collision probability and the transmission success probability.

As shown in the numerical results, our proposed scheme can achieve a much lower collision probability and thus a higher transmission success probability, compared to a probability-based reference scheme. We find that the transmission success probability can approach the upper bound in a normal traffic load, which verifies that our algorithm can effectively and efficiently identify the optimal relay in an uncoordinated manner. Besides, our algorithm also outperforms the probability-based scheme in terms of average packet delay, delay outage probability, as well as the energy consumption. By adjusting the weighting parameter ρ, we can achieve good performance in the high traffic load condition through energy balance. Therefore, it is safe to conclude that our proposed algorithm can serve as an energy-efficient cooperation scheme for delay-sensitive multimedia services and it is a scalable solution for a large-scale network.

Chapter 5

Auction-Based Incentive Mechanism

5.1 Motivation and Overview

As a promising technique, cooperative communications exploit the broadcasting nature of wireless media to facilitate data transmission, and have shown to have great potential to increase the channel capacity of wireless networks. In contrast to 3G/4G wireless networks, cooperative communications do not require extra infrastructure and offer more flexibility. However, the applications of cooperative communication techniques are rarely seen in reality, even in some scenarios where the demands for bandwidth-intensive applications have pushed the researchers to design innovative network solutions. A main obstacle that hinders the wide adoption of cooperative communications is the lack of incentives for the wireless devices to serve as relay nodes. As shown in Chapter 3 and Chapter 4, even though we can reduce the overall energy consumption in cooperative communications, the involved relays still need to cost their own resources, such as energy, and network bandwidth.

In this chapter, we focus on designing an incentive-compatible auction mechanism (ICAM) to stimulate relays to serve nearby source-destination (S-D) pairs. With the property of incentive-compatibility (or truthfulness), ICAM is free of market manipulation, and ensures auction fairness. Besides, ICAM satisfies three other desirable properties, namely, *individual rationality*, *budget balance*, and *computational efficiency*, which together guarantee the feasibility of ICAM. We provide rigorous analysis proving that the above desirable properties hold with ICAM. Numerical results verify that these properties are achieved without substantial degradation to system efficiency, which is another crucial property of auctions.

The remainder of this chapter is structured as follows. First, Section 5.2 provides the problem formulation as a double auction and an example demonstrating the challenges to achieve the desired properties. After that, we give the design details of the proposed ICAM in Section 5.3 and analyze its properties in Section 5.4. Numerical results are presented in Section 5.5, followed by conclusions in Section 5.6.

5.2 Problem Formulation

5.2.1 Auction Model

Focusing on the multiple S-D pairs scenario, we aim to design an incentive-compatible mechanism to stimulate the m relays to serve nearby n S-D pairs. Similar to the single-round multi-item double auction model in [27], the S-D pairs are *buyers* in this auction, while relays are *sellers*. A base station can serve as the *auctioneer*. The work in [49] shows that it is sufficient for a source node to choose the best relay node even when multiple are available to achieve full diversity. Thus, we assume that each buyer wants at most one relay to facilitate the cooperative communication. Besides, we assume that each relay node can be shared by at most one S-D pair, as it would provide different capacity from what the buyer expects otherwise. Considering a sealed-bid auction, each buyer (resp. seller) can submit its bid (resp. ask) privately to the auctioneer so that everyone has no information of other bids or asks.

- For each buyer $b_i \in \mathcal{B}$, $\mathcal{B} = \{b_1, b_2, \ldots, b_n\}$, its bid vector is denoted by $\mathbf{D}_i = (D_i^1, D_i^2, \ldots, D_i^m)$, where D_i^j is the bid for seller $s_j \in \mathcal{S}$, $\mathcal{S} = \{s_1, s_2, \ldots, s_m\}$. The bid matrix consisting of the bid vectors of all buyers is defined as $\mathbf{D} = (\mathbf{D}_1; \mathbf{D}_2; \ldots; \mathbf{D}_n)$.
- For all sellers in $\mathcal{S}$, the ask vector is denoted by $\mathbf{A} = (A_1, A_2, \ldots, A_m)$, where A_j is the ask of seller $s_j \in \mathcal{S}$.

As seen, the asks of sellers do not differentiate among buyers since the sellers only aim at collecting payments for using their resources, such as energy and network bandwidth. On the other hand, the bids of buyers differ with respect to sellers as S-D pairs have preferences over the relays, which can offer different capabilities.

Given $\mathcal{B}, \mathcal{S}, \mathbf{D}$ and $\mathbf{A}$, the auctioneer decides the winning buyer set $\mathcal{B}_w \subseteq \mathcal{B}$, the winning seller set $\mathcal{S}_w \subseteq \mathcal{S}$, the mapping between $\mathcal{B}_w$ and $\mathcal{S}_w$, i.e., $\sigma : \{j : s_j \in \mathcal{S}_w\} \rightarrow \{i : b_i \in \mathcal{B}_w\}$, the price P_i^{b} that the winning buyer $b_i \in \mathcal{B}_w$ is charged, and the payment P_j^{s} that the winning seller $s_j \in \mathcal{S}_w$ is rewarded[1]. To highlight the utilities for the particular matching between b_i and s_j, we also use P_{ij}^{b} and P_{ij}^{s} in certain cases to denote the price and payment, respectively.

In addition to the price and payment, the utilities of the buyers and sellers further depend on the valuations of the buyers toward the acquired relaying services and the costs for providing such services by the sellers. Let V_i^j be the valuation to buyer b_i for having the relaying service from seller s_j, and C_j be the cost to seller s_j for providing the service. Here, $V_i^j > 0$ means that b_i can benefit from the relaying service of s_j, while there is no benefit with $V_i^j = 0$. The valuation vector of buyer b_i is denoted by $\mathbf{V}_i = (V_i^1, V_i^2, \ldots, V_i^m)$. Given a buyer-seller

[1]To distinguish the price charged to *buyers* and the payment rewarded to *sellers*, we use b and s in the normal form as the superscript, respectively. The same naming routine is also applied to the utilities of buyers and sellers.

mapping, $i = \sigma(j)$, the *utility* of buyer b_i and that of seller s_j are respectively defined as follows:

$$U_i^{\mathrm{b}} = \begin{cases} V_i^j - P_i^{\mathrm{b}}, & \text{if} \quad b_i \in \mathcal{B}_w \\ 0, & \text{otherwise} \end{cases}$$

$$U_j^{\mathrm{s}} = \begin{cases} P_j^{\mathrm{s}} - C_j, & \text{if} \quad s_j \in \mathcal{S}_w \\ 0, & \text{otherwise}. \end{cases}$$

We use U_{ij}^{b} and U_{ij}^{s} when necessary to capture that the utilities are with respect to the matching between b_i and s_j.

Some important notations are summarized in Table 5.1.

5.2.2 Desirable Properties and Design Objective

The auction model in Section 5.2.1 is represented by $\Psi = (\mathcal{B}, \mathcal{S}, \mathbf{D}, \mathbf{A})$. Accordingly, the auctioneer should follow an auction mechanism to determine the set of winning buyers $\mathcal{B}_w$, the set of winning sellers $\mathcal{S}_w$, the mapping σ between $\mathcal{B}_w$ and $\mathcal{S}_w$, the set of clearing price $\mathcal{P}_w^{\mathrm{b}}$ charged to the winning buyers, and the set of clearing payment $\mathcal{P}_w^{\mathrm{s}}$ rewarded to the winning sellers. An effective auction mechanism should satisfy four desirable properties in the following.

- *Individual Rationality*: No winning buyer is charged more than its bid and no winning seller is rewarded less than its ask. With respect to the auction model Ψ, this means that for every winning matching between $b_i \in \mathcal{B}_w$ and $s_j \in \mathcal{S}_w$, we have $P_i^{\mathrm{b}} \leq D_i^j$ and $P_j^{\mathrm{s}} \geq A_j$.
- *Budget Balance*: The total price that the auctioneer charges all winning buyers is no less than the total payment that the auctioneer rewards all winning sellers, so that there is no deficit for the auctioneer. That is, $\sum_{b_i \in \mathcal{B}_w} P_i^{\mathrm{b}} \geq \sum_{s_j \in \mathcal{S}_w} P_j^{\mathrm{s}}$.
- *Truthfulness or Incentive-Compatibility*: We need to first give the definition of a *weakly dominant* strategy in the following. Based on this definition, we can further express the property of truthfulness or incentive-compatibility.

  Definition 1. *For player i, strategy a_i weakly dominates strategy a_i' if the utilities satisfy $u_i(a_i, a_{-i}) \geq u_i(a_i', a_{-i})$ for all partial action profiles a_{-i} of the other players except i. Further, for player i, strategy a_i is weakly dominant if it weakly dominates all other strategies of player i.*

  Then, an auction mechanism is truthful or incentive-compatible if playing (bidding or asking) truthfully is a weakly dominant strategy for each player (buyer or seller). In other words, no buyer can improve its utility by submitting a bid different from its true valuation, and no seller can improve its utility by submitting an ask different from its true cost. Specifically, it implies the following for our auction model:

Table 5.1: Important Notations.

Symbol	Definition
b_i	Buyer (S-D pair)
s_j	Seller (relay)
n	Total number of buyers
m	Total number of sellers
$\mathcal{B}$	Set of buyers (S-D pairs)
b_{ij}	Buyer b_i with positive valuation toward seller s_j
$\mathcal{B}'$	Extended set of buyers with positive valuations
$\mathcal{S}$	Set of sellers (relays)
$\mathbb{B}$	Sorted buyer list of $\mathcal{B}'$ in a descending order of positive valuations
$\mathbb{S}$	Sorted seller list of $\mathcal{S}$ in an ascending order of asks
$\mathcal{B}_c$	Set of winning buyer candidates ($\mathcal{B}_c \subseteq \mathcal{B}$)
$\mathcal{S}_c$	Set of winning seller candidates ($\mathcal{S}_c \subseteq \mathcal{S}$)
$\mathcal{B}_a$	Set of winning buyers before elimination ($\mathcal{B}_a \subseteq \mathcal{B}_c$)
$\mathcal{S}_a$	Set of winning sellers before elimination ($\mathcal{S}_a = \mathcal{S}_c$)
$\mathcal{B}_w$	Set of winning buyers ($\mathcal{B}_w = \mathcal{B}_a$)
$\mathcal{S}_w$	Set of winning sellers ($\mathcal{S}_w \subseteq \mathcal{S}_a$)
$\hat{\sigma}(\cdot)$	Mapping function from the indices of $\mathcal{S}_a$ to $\mathcal{B}_a$
$\sigma(\cdot)$	Mapping function from the indices of $\mathcal{S}_w$ to $\mathcal{B}_w$
D_i^j	Bid of buyer b_i on seller s_j
$\mathbf{D}_i$	Bid vector of buyer b_i
$\mathbf{D}$	Bid matrix of all buyers
A_j	Ask of seller s_j
$\mathbf{A}$	Ask vector of all sellers
$\mathbf{A}_{-j}$	Ask vector of all sellers except s_j
V_i^j	Valuation of buyer b_i on relaying service from seller s_j
$\mathbf{V}_i$	Valuation vector of buyer b_i
C_j	Cost of seller s_j for providing relaying service
ϕ / φ	Parameters that determine the winning candidates
P_i^{b}	Price charged to buyer b_i
P_j^{s}	Payment rewarded to seller s_j
P_{ij}^{b}	Price charged to buyer b_i for relaying service of seller s_j
P_{ij}^{s}	Payment rewarded to seller s_j with assigned buyer b_i
U_i^{b}	Utility of buyer b_i
U_j^{s}	Utility of seller s_j
U_{ij}^{b}	Utility of buyer b_i with assigned seller s_j
U_{ij}^{s}	Utility of seller s_j with assigned buyer b_i

Table 5.2: An Illustrative Example.

(a) Bid matrix of 5 buyers.

	s_1	s_2	s_3	s_4	s_5	s_6	s_7
b_1	6	0	0	0	5	10	0
b_2	4	0	0	3	0	0	8
b_3	0	0	6	0	0	9	0
b_4	0	10	0	0	0	0	7
b_5	0	2	7	9	0	0	0

(b) Ask vector of 7 sellers.

Seller	s_1	s_2	s_3	s_4	s_5	s_6	s_7
Ask	3	2	5	6	4	1	7

$\forall b_i \in \mathcal{B}$, U_i^{b} is maximized when the bidding $\mathbf{D}_i = \mathbf{V}_i$; and $\forall s_j \in \mathcal{S}$, U_j^{s} is maximized when the asking $A_j = C_j$.

- *Computational Efficiency*: The auction outcome, which includes the winning sets of buyers and sellers, their mapping, and the clearing price and payment, is tractable with a polynomial time complexity.

5.2.3 Technical Challenges

As discussed in Chapter 2.4, the existing auction mechanisms cannot satisfy the preceding desirable properties when directly applied to the cooperative communication scenario with heterogeneous relays as auction commodities. The pioneer work in [27] provides a promising solution. Unfortunately, the following example shows that TASC double auction (i.e., the enhanced version in [27]) cannot guarantee truthfulness of buyers, although there is no problem with individual rationality, budget balance, and truthfulness of sellers.

To illustrate that buyers can gain higher utilities by bidding untruthfully, we consider a bid matrix of 5 buyers with true valuations in Table 5.2(a), and the ask vector of 7 sellers with true costs in Table 5.2(b). Suppose that the auctioneer uses the maximum weighted matching algorithm in the assignment stage to maximize the total capacity. According to the assignment algorithm, the winning buyer candidates, the winning seller candidates and the mapping between them are shown in Fig. 5.1. Then, following the TASC strategy for winner-determination & pricing, we have the set of wining buyers $\mathcal{B}_w = \{b_1, b_4\}$, the set of winning sellers $\mathcal{S}_w = \{s_6, s_2\}$, the clearing price $\mathcal{P}_w^{\mathrm{b}} = \{8\}$, and the clearing payment $\mathcal{P}_w^{\mathrm{s}} = \{6\}$. The utility of b_3 is 0 since it is not within the winner set $\mathcal{B}_w$.

If buyer b_3 bids untruthfully by increasing its bid D_3^6 from its true valuation 9 to $9 + \delta$ ($\delta > 1$), the new assignment result is shown in Fig. 5.2. The set of winning buyers becomes $\mathcal{B}_w = \{b_3, b_4\}$, while the set of winning sellers is still $\mathcal{S}_w = \{s_6, s_2\}$. The clearing price and payment remain unchanged according to TASC, i.e., $\mathcal{P}_w^{\mathrm{b}} = \{8\}$ and $\mathcal{P}_w^{\mathrm{s}} = \{6\}$. The new utility of b_3 becomes $9 - 8 = 1$. As seen, b_3 can improve its utility from 0 to 1 by bidding untruthfully. Hence, TASC double auction cannot guarantee truthfulness of buyers. In Section 5.3, we propose a new double auction mechanism, ICAM, which can guarantee truthfulness of both sellers and buyers, while holding the other desirable properties.

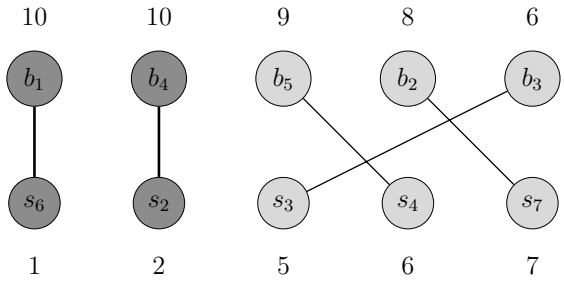

Figure 5.1: Assignment result with truthful bidding and asking: A bipartite graph of winning buyer candidates and winning seller candidates and their mapping.

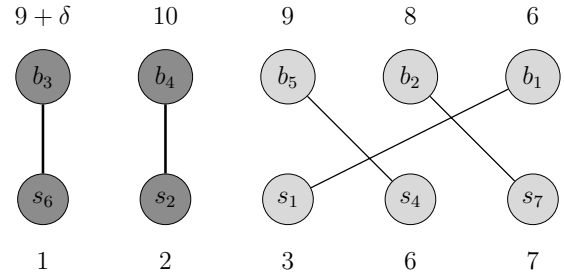

Figure 5.2: Different assignment result with untruthful bidding of buyer b_3, which increases its bid D_3^6 from its true valuation 9 to $9+\delta$ ($\delta > 1$).

5.3 Proposed Auction Mechanism

As discussed in Chapter 2.4, the well-known Vickrey-based double auction [25] cannot simultaneously achieve truthfulness in addition to individual rationality and budget balance, while McAfee double auction [24] cannot be directly applied to the scenario with heterogeneous commodities. TASC double auction overcomes the limitation of McAfee double auction and accommodates heterogeneity, however, we have seen from the example in Section 5.2.3 that TASC is subject to the manipulation of untruthful buyers in the assignment stage.

In this section, we propose ICAM to resolve this problem. First of all, we change the sequence of the assignment stage and the winner-determination & pricing stage in TASC. In ICAM, the auctioneer first identifies the winning candidates. Then, each winning seller candidate is assigned to one winning buyer candidate. Also, the clearing price charged to each buyer candidate and the clearing payment rewarded to the seller candidate are determined accordingly. More importantly, ICAM can keep potentially multiple sellers for a single buyer until a new last stage. In the end, the new stage of winner elimination can guarantee that a winning buyer is assigned to only one winning seller.

Next, we give the detailed algorithms of ICAM, followed by a walk-through example. The properties of ICAM are analyzed in Section 5.4.

5.3.1 Details of ICAM

Following the above design rationale, we propose ICAM in Algorithm 5.1, which includes three stages, namely, *winning candidate determination*, *assignment & pricing*, and *winner elimination*.

Algorithm 5.1 ICAM($\mathcal{B}$, $\mathcal{S}$, $\mathbf{D}$, $\mathbf{A}$).

Input: $\mathcal{B}$, $\mathcal{S}$, $\mathbf{D}$, $\mathbf{A}$
Output: $\mathcal{B}_w, \mathcal{S}_w, \sigma, \mathcal{P}^{\mathrm{b}}_w, \mathcal{P}^{\mathrm{s}}_w$
1: $(\mathcal{B}_c, \mathcal{S}_c, D^{q_\varphi}_{p_\varphi}, A_{j_\phi})$ ← ICAM-WCD($\mathcal{B}, \mathcal{S}, \mathbf{D}, \mathbf{A}$);
2: $(\mathcal{B}_a, \mathcal{S}_a, \hat{\sigma}, \mathcal{P}^{\mathrm{b}}_a, \mathcal{P}^{\mathrm{s}}_a)$ ← ICAM-A&P($\mathcal{B}_c, \mathcal{S}_c, D^{q_\varphi}_{p_\varphi}, A_{j_\phi}, \mathbf{D}$);
3: $(\mathcal{B}_w, \mathcal{S}_w, \sigma, \mathcal{P}^{\mathrm{b}}_w, \mathcal{P}^{\mathrm{s}}_w)$ ← ICAM-WE($\mathcal{B}_a, \mathcal{S}_a, \hat{\sigma}, \mathcal{P}^{\mathrm{b}}_a, \mathcal{P}^{\mathrm{s}}_a, \mathbf{D}$);
4: **return** $(\mathcal{B}_w, \mathcal{S}_w, \sigma, \mathcal{P}^{\mathrm{b}}_w, \mathcal{P}^{\mathrm{s}}_w)$;

In the stage of winning candidate determination, Algorithm 5.2 is used by the auctioneer to shortlist the buyer and seller candidates. Algorithm 5.2 first constructs a new buyer set $\mathcal{B}'$ from the original buyer set $\mathcal{B}$. Specifically, buyer $b_i \in \mathcal{B}$ becomes b_{ij} in $\mathcal{B}'$ if $V_i^j > 0$. That is, a buyer can appear for a number of times with respect to the sellers for which the buyer has positive valuations. Then, $\mathcal{B}'$ is ranked to $\mathbb{B}$ in an ascending order of all positive bids (valuations), denoted by $\mathbb{D}' = \langle D^{q_1}_{p1}, \ldots, D^{q_x}_{p_x} \rangle$, where $x = |\mathcal{B}'|$. Seller set $\mathcal{S}$ is sorted to $\mathbb{S}$ in a descending order of $\mathbf{A}$, where the ordered list of $\mathbf{A}$ is denoted by $\mathbb{A} = \langle A_{j_1}, \ldots, A_{j_m} \rangle$. The ask of the median seller in $\mathbb{S}$, denoted by A_{j_ϕ}, where $\phi = \lceil \frac{m+1}{2} \rceil$, is used to find the smallest φ such that $D^{q_{\varphi+1}}_{p_{\varphi+1}} < A_{j_\phi}$. The two selected thresholds, $D^{q_\varphi}_{p_\varphi}$ and A_{j_ϕ}, are used to select winning candidates. Buyer b_{pq} is a winning buyer candidate if $D^q_p \geq D^{q_\varphi}_{p_\varphi}$ and $A_q < A_{j_\phi}$. Seller s_q is a winning seller candidate if $A_q < A_{j_\phi}$ and at least one winning buyer candidate bids for s_q with a positive bid.

Algorithm 5.2 ICAM-WCD($\mathcal{B}, \mathcal{S}, \mathbf{D}, \mathbf{A}$).

Input: $\mathcal{B}$, $\mathcal{S}$, $\mathbf{D}$, $\mathbf{A}$
Output: $\mathcal{B}_c, \mathcal{S}_c, D^{q_\varphi}_{p_\varphi}, A_{j_\phi}$
1: $\mathcal{B}_c \leftarrow \emptyset$, $\mathcal{S}_c \leftarrow \emptyset$;
2: Construct a set $\mathcal{B}' = \{b_{pq} : D^q_p > 0, b_p \in \mathcal{B}\}$ according to $\mathbf{D}$;
3: Sort all buyers in $\mathcal{B}'$ to obtain an ordered list $\mathbb{B} = \langle b_{p_1q_1}, b_{p_2q_2}, \ldots, b_{p_xq_x} \rangle$ such that $D^{q_1}_{p_1} \geq D^{q_2}_{p_2} \geq \cdots \geq D^{q_x}_{p_x}$;
4: Sort all sellers in $\mathcal{S}$ to obtain an ordered list $\mathbb{S} = \langle s_{j_1}, s_{j_2}, \ldots, s_{j_m} \rangle$ such that $A_{j_1} \leq A_{j_2} \leq \cdots \leq A_{j_m}$;
5: Find the median ask A_{j_ϕ} of $\mathbb{S}$, where $\phi = \lceil \frac{m+1}{2} \rceil$;
6: Find the smallest φ, such that $D^{q_{\varphi+1}}_{p_{\varphi+1}} < A_{j_\phi}$;
7: $\mathcal{B}_c \leftarrow \mathbb{B}_\varphi$, where $\mathbb{B}_\varphi$ is the sublist with first φ buyers in $\mathbb{B}$;
8: **for** $b_{pq} \in \mathcal{B}_c$ **do**
9: **if** $A_q \geq A_{j_\phi}$ **then**
10: $\mathcal{B}_c \leftarrow \mathcal{B}_c \setminus \{b_{pq}\}$;
11: **else**
12: **if** $s_q \notin \mathcal{S}_c$ **then**
13: $\mathcal{S}_c \leftarrow \mathcal{S}_c \cup \{s_q\}$;
14: **end if**
15: **end if**
16: **end for**
17: **return** $(\mathcal{B}_c, \mathcal{S}_c, D^{q_\varphi}_{p_\varphi}, A_{j_\phi})$;

In the assignment & pricing stage, we tightly couple winner determination and pricing to prevent possible

Algorithm 5.3 ICAM-A&P($\mathcal{B}_c, \mathcal{S}_c, D^{q_\varphi}_{p_\varphi}, A_{j_\phi}, \mathbf{D}$).

Input: $\mathcal{B}_c, \mathcal{S}_c, D^{q_\varphi}_{p_\varphi}, A_{j_\phi}, \mathbf{D}$
Output: $\mathcal{B}_a, \mathcal{S}_a, \hat{\sigma}, \mathcal{P}^{\mathrm{b}}_a, \mathcal{P}^{\mathrm{s}}_a$

$\mathcal{B}_a \leftarrow \emptyset$, $\mathcal{S}_a \leftarrow \mathcal{S}_c$, $\mathcal{P}^{\mathrm{b}}_a \leftarrow \emptyset$, $\mathcal{P}^{\mathrm{s}}_a \leftarrow \emptyset$;
for $s_j \in \mathcal{S}_a$ **do**
  $P^{\mathrm{s}}_j = A_{j_\phi}, \mathcal{P}^{\mathrm{s}}_a \leftarrow \mathcal{P}^{\mathrm{s}}_a \cup \{P^{\mathrm{s}}_j\}$;
  $\mathcal{B}^j = \{b_{ij} : b_{ij} \in \mathcal{B}_c\}$;
  if $|\mathcal{B}^j| = 1$ **then**
    $\mathcal{B}_a \leftarrow \mathcal{B}_a \cup \{b_{ij}\}, \hat{\sigma}(j) = i$;
    $P^{\mathrm{b}}_{ij} = D^{q_\varphi}_{p_\varphi}, \mathcal{P}^{\mathrm{b}}_a \leftarrow \mathcal{P}^{\mathrm{b}}_a \cup \{P^{\mathrm{b}}_{ij}\}$;
  else
    Sort $\mathcal{B}^j$ to an ordered list $\mathbb{B}^j$ such that $D^j_{i_{(1)}} \geq D^j_{i_{(2)}} \geq \cdots \geq D^{q_\varphi}_{p_\varphi}$;
    if the first τ ($\tau \geq 2$) bids of $\mathbb{B}^j$ are the same **then**
      Randomly select a b_{ij} from the first τ buyers of $\mathbb{B}^j$;
    else
      Select the first buyer b_{ij} of $\mathbb{B}^j$ with the highest bid;
    end if
    $\mathcal{B}_a \leftarrow \mathcal{B}_a \cup \{b_{ij}\}, \hat{\sigma}(j) = i$;
    $P^{\mathrm{b}}_{ij} = D^j_{i_{(2)}}, \mathcal{P}^{\mathrm{b}}_a \leftarrow \mathcal{P}^{\mathrm{b}}_a \cup \{P^{\mathrm{b}}_{ij}\}$;
  end if
end for
return $(\mathcal{B}_a, \mathcal{S}_a, \hat{\sigma}, \mathcal{P}^{\mathrm{b}}_a, \mathcal{P}^{\mathrm{s}}_a)$;

untruthful manipulation. As given in Algorithm 5.3, the auctioneer first determines the winning buyer for each winning seller candidate s_j. If only one buyer candidate b_{ij} bids for s_j, then b_{ij} is added into the winning buyer set $\mathcal{B}_a$ and charged a clearing price $D^{q_\varphi}_{p_\varphi}$. If more than one buyer candidate bids for s_j, the buyer candidate with the highest bid is added into the winning buyer set and charged a price of the second highest bid. Seller s_j is paid the median ask, A_{j_ϕ}. When there is a tie among the highest bids of buyer candidates, the auctioneer randomly selects a winning buyer from the candidates. For example, supposing $D^{q_\varphi}_{p_\varphi} = 3$ and $D^j_\alpha = D^j_\beta = 10$, the winning buyer for s_j can be either $b_{\alpha j}$ or $b_{\beta j}$, each with a 50% chance. If the next lower bid for s_j by $b_{\gamma j}$ is $D^j_\gamma = 5$, the winning buyer is charged 10 instead of 5, because the first two highest bids in the sorted list are both 10, i.e., $D^j_{i_{(1)}} = D^j_{i_{(2)}} = 10$. This is essential to avoid untruthful actions of buyers.

Algorithm 5.4 ICAM-WE($\mathcal{B}_a, \mathcal{S}_a, \hat{\sigma}, \mathcal{P}^{\mathrm{b}}_a, \mathcal{P}^{\mathrm{s}}_a, \mathbf{D}$).

Input: $\mathcal{B}_a, \mathcal{S}_a, \hat{\sigma}, \mathcal{P}^{\mathrm{b}}_a, \mathcal{P}^{\mathrm{s}}_a, \mathbf{D}$
Output: $\mathcal{B}_w, \mathcal{S}_w, \sigma, \mathcal{P}^{\mathrm{b}}_w, \mathcal{P}^{\mathrm{s}}_w$

$\mathcal{B}_w \leftarrow \mathcal{B}_a$, $\mathcal{S}_w \leftarrow \mathcal{S}_a$, $\sigma \leftarrow \hat{\sigma}$, $\mathcal{P}^{\mathrm{b}}_w \leftarrow \mathcal{P}^{\mathrm{b}}_a$, $\mathcal{P}^{\mathrm{s}}_w \leftarrow \mathcal{P}^{\mathrm{s}}_a$;
for any two buyers $b_{\sigma(\alpha)\alpha}, b_{\sigma(\beta)\beta} \in \mathcal{B}_w, \alpha \neq \beta$ **do**
  if $\sigma(\alpha) = \sigma(\beta)$ **then**
    $U^{\mathrm{b}}_{\sigma(j)j} = D^j_{\sigma(j)} - P^{\mathrm{b}}_{\sigma(j)j}, j = \{\alpha, \beta\}$;
    if $U^{\mathrm{b}}_{\sigma(\alpha)\alpha} = U^{\mathrm{b}}_{\sigma(\beta)\beta}$ **then**
      $j' \leftarrow$ randomly selected from $\{\alpha, \beta\}$;
    else
      $j' \leftarrow \arg\min_{j \in \{\alpha,\beta\}} \{U^{\mathrm{b}}_{\sigma(j)j}\}$;
    end if
    $\mathcal{B}_w \leftarrow \mathcal{B}_w \setminus \{b_{\sigma(j')j'}\}, \mathcal{S}_w \leftarrow \mathcal{S}_w \setminus \{s_{j'}\}$;
    $\mathcal{P}^{\mathrm{b}}_w \leftarrow \mathcal{P}^{\mathrm{b}}_w \setminus \{P^{\mathrm{b}}_{\sigma(j')j'}\}, \mathcal{P}^{\mathrm{s}}_w \leftarrow \mathcal{P}^{\mathrm{s}}_w \setminus \{P^{\mathrm{s}}_{j'}\}, \sigma(j') = \emptyset$;
  end if
end for
return $(\mathcal{B}_w, \mathcal{S}_w, \sigma, \mathcal{P}^{\mathrm{b}}_w, \mathcal{P}^{\mathrm{s}}_w)$;

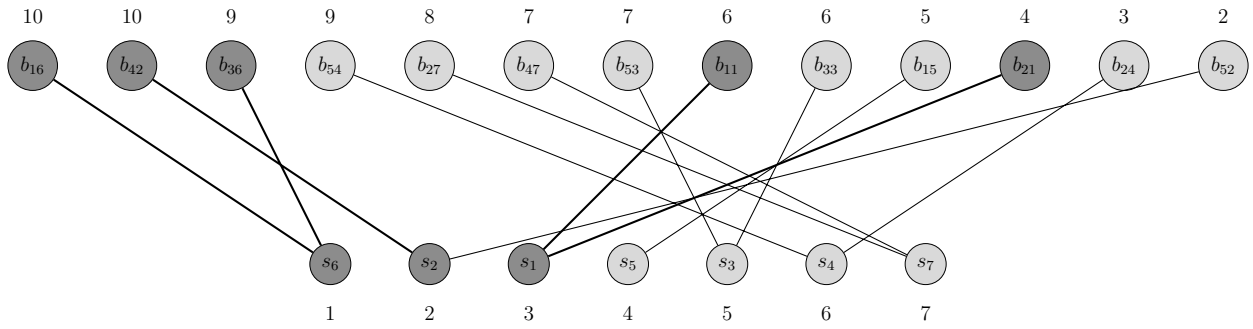

Figure 5.3: Initial bipartite graph showing the ordered lists of the new buyer set and the seller set.

In the last stage, if a buyer in the original buyer set $\mathcal{B}$ wins two or more sellers in $\mathcal{S}_a$, the auctioneer, depending on system requirements, can choose only one seller for such a buyer using Algorithm 5.4. For example, if both $b_{i\alpha}$ and $b_{i\beta}$ belong to $\mathcal{B}_a$, it means that b_i in the original buyer set $\mathcal{B}$ wins two sellers, s_α and s_β. The auctioneer can select only one seller so that the corresponding buyer achieves the highest utility. Likewise, when there is a tie in terms of the achievable utilities, one seller is randomly selected. At the end of the winner elimination stage, every buyer $b_{\sigma(j)j} \in \mathcal{B}_w$ has a one-to-one mapping with only one winning seller $s_j \in \mathcal{S}_w$.

For the auction model in [27], each seller can be assigned to at most one buyer, while one buyer needs at most one seller. It is worth noting that our proposed auction mechanism can be easily modified to retain multiple winning sellers for one buyer by skipping the above elimination stage. Then, one buyer (an S-D pair) is allowed to acquire relaying services from multiple sellers (relays).

5.3.2 A Walk-Through Example

Considering the bid matrix in Table 5.2(a) and the ask vector in Table 5.2(b), the following shows how ICAM works for the auctioneer to derive the auction outcome.

Winning candidate determination according to Algorithm 5.2:

- Construct the new buyer set from original set $\mathcal{B}$: $\mathcal{B}' = \{b_{11}, b_{15}, b_{16}, b_{21}, b_{24}, b_{27}, b_{33}, b_{36}, b_{42}, b_{47}, b_{52}, b_{53}, b_{54}\}$;
- Sort buyers in $\mathcal{B}'$ in a descending order to obtain: $\mathbb{B} = \{b_{16}, b_{42}, b_{36}, b_{54}, b_{27}, b_{47}, b_{53}, b_{11}, b_{33}, b_{15}, b_{21}, b_{24}, b_{52}\}$;
- Sort sellers in $\mathcal{S}$ in an ascending order to obtain: $\mathbb{S} = \{s_6, s_2, s_1, s_5, s_3, s_4, s_7\}$;
- Based on $\mathbb{B}$ and $\mathbb{S}$, construct an initial bipartite graph between $\mathcal{B}'$ and $\mathcal{S}$ as shown in Fig. 5.3;
- Decide two thresholds: $A_{j_\phi} = A_5 = 4$, $D_{p_\varphi}^{q_\varphi} = D_2^1 = 4$;
- Determine the set of winning buyer candidates: $\mathcal{B}_c = \{b_{16}, b_{42}, b_{36}, b_{11}, b_{21}\}$;
- Determine the set of winning seller candidates: $\mathcal{S}_c = \{s_6, s_2, s_1\}$.

According to the output of Algorithm 5.2, a bipartite graph between $\mathcal{B}_c$ and $\mathcal{S}_c$ is constructed as shown in Fig. 5.4. Then, Algorithm 5.3 is run to identify the winning buyers and sellers.

Assignment & pricing according to Algorithm 5.3:

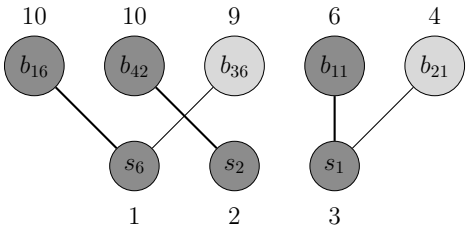

Figure 5.4: Bipartite graph between winning candidates $\mathcal{B}_c$ and $\mathcal{S}_c$.

- The set of winning buyers: $\mathcal{B}_a = \{b_{16}, b_{42}, b_{11}\}$;
- The set of winning sellers: $\mathcal{S}_a = \{s_6, s_2, s_1\}$;
- The assignment (mapping) between winning buyers and sellers ($\mathcal{B}_a$ and $\mathcal{S}_a$): $\hat{\sigma}(\cdot) = \{\hat{\sigma}(6) = 1, \hat{\sigma}(2) = 4, \hat{\sigma}(1) = 1\}$;
- The clearing price charged to winning buyers: $\mathcal{P}_a^{\mathrm{b}} = \{P_{16}^{\mathrm{b}} = D_3^6 = 9, P_{42}^{\mathrm{b}} = D_{p_\varphi}^{q_\varphi} = 4, P_{11}^{\mathrm{b}} = D_2^1 = 4\}$;
- The clearing payment rewarded to winning sellers: $\mathcal{P}_a^{\mathrm{s}} = \{P_6^{\mathrm{s}} = P_2^{\mathrm{s}} = P_1^{\mathrm{s}} = A_{j_\phi} = 4\}$.

Algorithm 5.3 returns the mapping between $\mathcal{B}_a$ and $\mathcal{S}_a$, $\hat{\sigma}(\cdot) = \{\hat{\sigma}(6) = \hat{\sigma}(1) = 1, \hat{\sigma}(2) = 4\}$, which means that $b_1 \in \mathcal{B}$ wins two sellers (s_6 and s_1). If the auctioneer requires to keep only one winning seller for buyer b_1, Algorithm 5.4 is run to remove redundant sellers.

Winner elimination according to Algorithm 5.4:

- Compute the utilities of buyer b_1 with respect to seller s_6 and s_1, respectively: $U_{16}^{\mathrm{b}} = D_1^6 - P_{16}^{\mathrm{b}} = 10 - 9 = 1$, $U_{11}^{\mathrm{b}} = D_1^1 - P_{11}^{\mathrm{b}} = 6 - 4 = 2$;
- Since $U_{16}^{\mathrm{b}} < U_{11}^{\mathrm{b}}$, seller s_6 is eliminated so that a higher utility is provided to buyer b_1 by seller s_1. Then, the set of winning buyers is obtained as: $\mathcal{B}_w = \{b_{16}, b_{42}, b_{11}\} \setminus \{b_{16}\} = \{b_{42}, b_{11}\} = \{b_4, b_1\}$;
- Update the set of winning sellers: $\mathcal{S}_w = \{s_6, s_2, s_1\} \setminus \{s_6\} = \{s_2, s_1\}$;
- Update the clearing price charged to winning buyers: $\mathcal{P}_w^{\mathrm{b}} = \{P_{16}^{\mathrm{b}}, P_{42}^{\mathrm{b}}, P_{11}^{\mathrm{b}}\} \setminus \{P_{16}^{\mathrm{b}}\} = \{P_{16}^{\mathrm{b}} = 9, P_{42}^{\mathrm{b}} = 4\} = \{P_1^{\mathrm{b}} = 9, P_4^{\mathrm{b}} = 4\}$;
- Update the clearing payment rewarded to winning sellers: $\mathcal{P}_w^{\mathrm{s}} = \{P_6^{\mathrm{s}}, P_2^{\mathrm{s}}, P_1^{\mathrm{s}}\} \setminus \{P_6^{\mathrm{s}}\} = \{P_2^{\mathrm{s}} = 4, P_1^{\mathrm{s}} = 4\}$;
- Update the final one-to-one mapping between winning buyers and sellers ($\mathcal{B}_w$ and $\mathcal{S}_w$): $\sigma(\cdot) = \{\sigma(2) = 4, \sigma(1) = 1\}$.

Recall that one motivation for the proposed ICAM is to solve the problem illustrated by the example in Section 5.2.3. Next, we briefly show how ICAM prevents such an untruthful buyer bidding, and leave the formal proof of truthfulness and other properties in Section 5.4. Suppose similarly that buyer b_3 increases its bid D_3^6 from its truthful valuation 9 to $9 + \delta$, where $\delta > 1$. The winning candidates obtained from Algorithm 5.2 will change to the bipartite graph in Fig. 5.5. As a result, b_3 needs to pay a price 10 to win seller s_6, and its utility is $9 - 10 = -1 < 0$. Therefore, biding truthfully should be the dominant strategy of b_3.

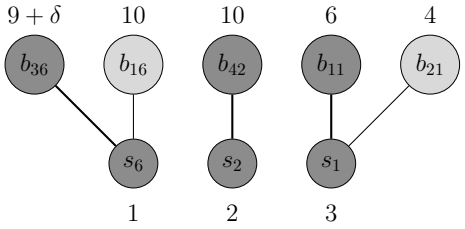

Figure 5.5: Bipartite graph between winning candidates $\mathcal{B}_c$ and $\mathcal{S}_c$, when b_3 deviates its bid D_3^6 from its true valudation 9 to $9+\delta$ ($\delta > 1$).

5.4 Analysis of Desirable Properties

In this section, we analyze the proposed auction mechanism ICAM with respect to the four desirable properties discussed in Section 5.2.2. The following theorems prove that all four properties hold with ICAM. We leave the proof for truthfulness in the end, which requires complex and rigorous reasoning.

Theorem 5.1. *ICAM is computationally efficient.*

Proof. In the winning candidate determination stage, Algorithm 5.2 involves at most nm buyers in the new buyer set $\mathcal{B}'$. Sorting the buyers in $\mathcal{B}'$ takes $O(nm \log (nm))$ time, while sorting the sellers in $\mathcal{S}$ takes $O(m \log m)$ time. In Line 7, there are at most $n\lceil\frac{m+1}{2}\rceil$ buyers in the winning candidate set $\mathcal{B}_c$. Hence, the for-loop (Line 8 – Line 16) has a time complexity $O(n\lceil\frac{m+1}{2}\rceil \cdot \lceil\frac{m+1}{2}\rceil) = O(nm^2)$. Thus, Algorithm 5.2 takes $O(nm \cdot (m + \log n))$ time.

In the assignment & pricing stage, Algorithm 5.3 processes at most $n\lceil\frac{m+1}{2}\rceil$ buyers in $\mathcal{B}_c$ and $\lceil\frac{m+1}{2}\rceil$ sellers in $\mathcal{S}_c$. Line 4 determines subset $\mathcal{B}^j \subseteq \mathcal{B}_c$ for the buyers with positive valuations toward seller $s_j \in \mathcal{S}_a$, which takes $O(n\lceil\frac{m+1}{2}\rceil) = O(nm)$ time. Taking advantage of the ordered list $\mathbb{B}$, we can sort $\mathcal{B}^j$ without cost to obtain $\mathbb{B}^j$. Since there are at most $n\lceil\frac{m+1}{2}\rceil$ buyers in $\mathbb{B}^j$, it takes $O(n\lceil\frac{m+1}{2}\rceil) = O(nm)$ time to determine the winning buyer for s_j. Hence, the for-loop (Line 2 – Line 18) costs $O(\lceil\frac{m+1}{2}\rceil \cdot (nm)) = O(nm^2)$. Thus, Algorithm 5.3 takes $O(nm^2)$ time.

In the winner elimination stage, we know that set $\mathcal{B}_a$ before elimination has a size $|\mathcal{B}_a| = |\mathcal{S}_a| \leq \lceil\frac{m+1}{2}\rceil$. Thus, the for-loop (Line 2 – Line 13) takes $O(\frac{|\mathcal{B}_a|(|\mathcal{B}_a|-1)}{2}) = O(m^2)$ time. Thus, Algorithm 5.4 takes $O(m^2)$ time.

Therefore, the overall time complexity of ICAM in Algorithm 5.1 is $O(nm \cdot (m + \log n))$. □

Theorem 5.2. *ICAM is individually rational.*

Proof. For each winning seller $s_j \in \mathcal{S}_w \subseteq \mathcal{S}_c$, the payment rewarded to seller s_j is $P_j^{\mathrm{s}} = A_{j_\phi} > A_j$ according to ICAM. Thus, the winning sellers satisfy individual rationality.

Next, consider the winning buyer set $\mathcal{B}_a$ produced by Algorithm 5.3. For each winning buyer $b_{ij} \in \mathcal{B}_a \subseteq \mathcal{B}_c$, there are two cases.

- In the first case, buyer b_{ij} wins s_j without competition, which means that b_{ij} is the only buyer in $\mathcal{B}_c$ that bids for s_j. In this situation, we know that $P_{ij}^{\mathrm{b}} = D_{p_\varphi}^{q_\varphi} \leq D_i^j$.

- In the second case, buyer b_{ij} wins s_j with competition, which means that more than one buyer in $\mathcal{B}_c$ bids for s_j, and D_i^j is the highest. In this situation, b_{ij} is charged the second highest bid in $\mathbb{B}^j$. Obviously, $P_{ij}^{\mathrm{b}} \leq D_i^j$.

Therefore, individual rationality also holds for the winning buyer set $\mathcal{B}_a$ determined by Algorithm 5.3.

If a winning buyer, $b_i \in \mathcal{B}$, wins multiple sellers, e.g., $b_{i\alpha} \in \mathcal{B}_a$ and $b_{i\beta} \in \mathcal{B}_a$, running Algorithm 5.4 can eliminate redundant sellers and keep only one best seller for each winning buyer. Among all the sellers that buyer b_i wins, Algorithm 5.4 simply keeps the seller, s_j (e.g., s_α or s_β), which gives b_i the highest utility. It is evident that this procedure does not change the charging price P_{ij}^{b} to the winning buyers. Thus, the buyers in $\mathcal{B}_w$ after the winner elimination still satisfy individual rationality.

In summary, ICAM is individually rational. □

Theorem 5.3. *ICAM is budget-balanced.*

Proof. After the winner elimination stage, every winning buyer $b_i \in \mathcal{B}_w$ has only one winning seller $s_j \in \mathcal{S}_w$. Considering this one-to-one mapping between $\mathcal{B}_w$ and $\mathcal{S}_w$, we have $|\mathcal{B}_w| = |\mathcal{S}_w|$. For each matching $\sigma(j) = i$ between winning buyer b_i and assigned winning seller s_j, it is true that

$$P_{\sigma(j)}^{\mathrm{b}} \geq D_{p_\varphi}^{q_\varphi} \geq A_{j_\phi} = P_j^{\mathrm{s}}.$$

Then, it can be easily shown that

$$\sum_{b_i \in \mathcal{B}_w} P_i^{\mathrm{b}} - \sum_{s_j \in \mathcal{S}_w} P_j^{\mathrm{s}} = \sum_{s_j \in \mathcal{S}_w} \left(P_{\sigma(j)}^{\mathrm{b}} - P_j^{\mathrm{s}}\right) \geq 0$$

which completes the proof. □

Before drawing a conclusion on truthfulness of ICAM, we first derive Lemma 5.1 and Lemma 5.2 in the following.

Lemma 5.1. *ICAM is truthful for sellers.*

Proof. Lemma 5.1 can be proved by Proportions C.1-C.3, which are presented and proved in Appendix C.1. Let $k = \phi = \lceil \frac{m+1}{2} \rceil$, $\mathcal{S}_{l_1} = \mathcal{S}_{<k} \setminus \mathcal{S}_c$ and $\mathcal{S}_{l_2} = \mathcal{S}_a \setminus \mathcal{S}_w$. Then, according to Proportions C.1-C.3, telling truth $(A_j = C_j)$ is a weakly dominant strategy for each seller $s_j \in \mathcal{S}$ in ICAM, which completes the proof of Lemma 5.1. □

Lemma 5.2. *ICAM is truthful for buyers.*

Proof. Similar to the proof of Lemma 5.1, we provide Proportions C.4-C.7 in Appendix C.2, which lay the basis for Lemma 5.2. Following the notations therein and letting $D_\varphi = A_\varphi = A_{j_\phi}$, $B_{l_1} = \mathcal{B}_\varphi \setminus \mathcal{B}_c$ and $B_{l_2} = \mathcal{B}_c \setminus \mathcal{B}_a$, we can draw a logical conclusion that telling truth is a weakly dominant strategy for each buyer $b_i \in \mathcal{B}$ in ICAM. This proves Lemma 5.2. □

Theorem 5.4. *ICAM is truthful (incentive-compatible).*

Proof. Lemma 5.1 and Lemma 5.2 together prove that ICAM is truthful (incentive-compatible). □

According to Theorems 5.1-5.4, we can draw the final conclusion in Theorem 5.5.

Theorem 5.5. *ICAM is computationally efficient, individually rational, budget-balanced and truthful (incentive-compatible).*

As discussed in Section 5.3, ICAM also works when the elimination stage is skipped so that an S-D pair (buyer) can acquire services from more than one relay (seller). The four desired properties in Theorem 5.5 still hold.

5.5 Numerical Results

In this section, we present numerical results to validate the properties of ICAM analyzed in Section 5.4. In addition, we evaluate the performance of ICAM in terms of system efficiency. Because there are no existing statistics on relaying demands of S-D pairs or resource costs of relays, for generality, the experimental data for the asks of sellers are randomly generated according to a uniform distribution within $(0, 1]$. The bids of buyers are uniformly distributed within $(0, V_{max}]$. Intuitively, V_{max} will affect the auction outcome, and even the parameter ϕ that is used to determine the auction thresholds and winning candidates. In the following, we first illustrate the impact of ϕ and its variation with V_{max}, so that the numerical results thereafter will be only based on fixed ϕ and V_{max}.

5.5.1 Impact of Parameter ϕ

In the winning candidate determination stage of ICAM, buyer and seller candidates are selected based on the ϕ-th ask of the ascending ordered list of all sellers' asks, A_{j_ϕ}. The candidate sets, $\mathcal{B}_c$ and $\mathcal{S}_c$, are determined in Algorithm 5.2. Intuitively, a larger value of ϕ results in a smaller set for $\mathcal{B}_c$. On the other hand, $\mathcal{S}_c$ can be too small if ϕ is too small. The candidate sets directly affect the auction outcome. Fig. 5.6 shows the impact of ϕ on the performance of ICAM with different values of V_{max}, with 100 buyers and 100 sellers.

Fig. 5.6(a) shows the number of successful trades (N_{ST}) versus ϕ. The variation therein is due to the opposite effects of ϕ on the sizes of $\mathcal{B}_c$ and $\mathcal{S}_c$. When ϕ is too small or too large, the size of $\mathcal{S}_c$ or $\mathcal{B}_c$ is too small, respectively. As a result, the number of successful trades (i.e., matchings between winning buyers and sellers) is small. In addition, examining the peak points of the curves with different V_{max}, we find out that the optimal value of ϕ that attains the highest N_{ST} increases with a larger V_{max}. The highest N_{ST} also increases accordingly. This is because a larger ϕ can be selected when V_{max} increases so as to enlarge $\mathcal{B}_c$ and $\mathcal{S}_c$. Thus, the highest N_{ST} increases with a larger V_{max}.

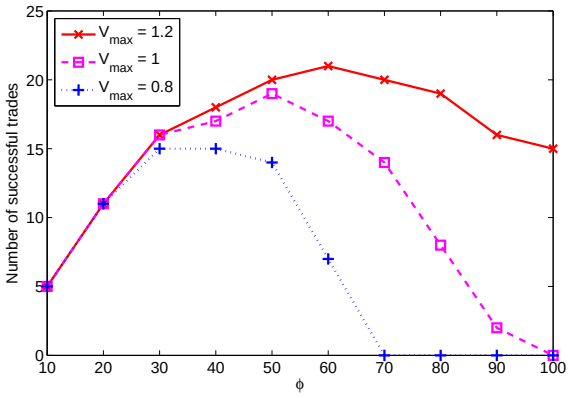

(a) Number of successful trades vs. ϕ.

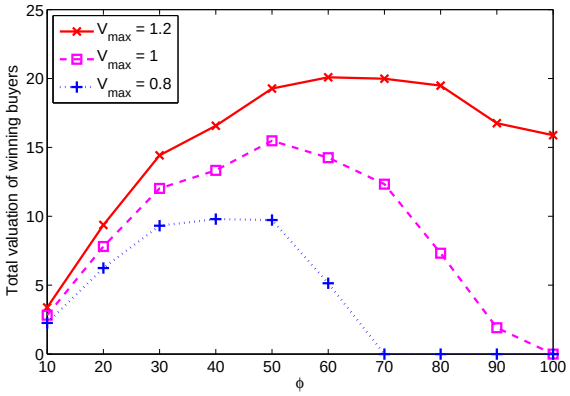

(b) Total valuation of winning buyers vs. ϕ.

Figure 5.6: Impact of ϕ on the performance of ICAM.

Fig. 5.6(b) shows the impact of ϕ on the total valuation of winning buyers, with different V_{max}. It is clear that Fig. 5.6(b) exhibits a similar trend as Fig. 5.6(a). The reason is that the total valuation is proportional to the number of successful trades.

Given the observations in Fig. 5.6, we can see that ϕ should be adapted to V_{max} for the best performance. In the following experiments, we fix $V_{max} = 1$ and set $\phi = \lceil \frac{m+1}{2} \rceil$ based on the observations in Fig. 5.6. The relative difference between the number of buyers (n) and the number of sellers (m) may also affect the selection of ϕ. In fact, the performance of ICAM can be improved when the optimal ϕ is selected according to different values of n and m.

5.5.2 Computational Efficiency

To confirm our analysis on time complexity in Theorem 5.1, we obtain the computation time of ICAM with different settings in Table 5.3. For each setting, we randomly generate 1000 instances and average the results. All the tests are run on a Windows PC with 3.16 GHz Intel® Core™2 Duo processor and 4 GB memory. As seen,

Table 5.3: Computation Time.

$n = 100$	m	50	100	150	200	250	300
	Time (ms)	0.4	0.7	1.0	1.2	1.5	1.8
$m = 100$	n	50	100	150	200	250	300
	Time (ms)	0.4	0.7	0.9	1.1	1.2	1.5

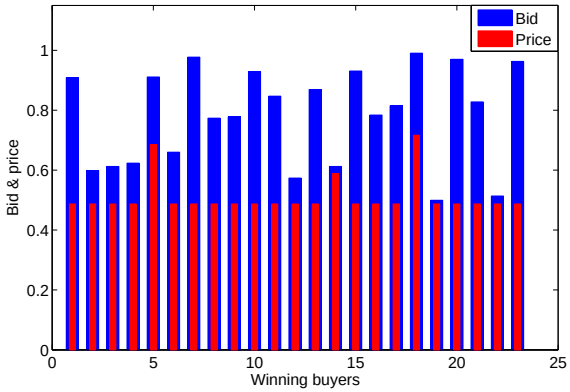

(a) Bids & prices of winning buyers.

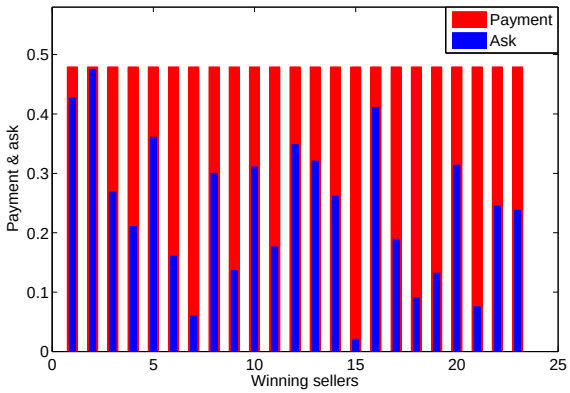

(b) Payments & asks of winning sellers.

Figure 5.7: Individual rationality of ICAM.

ICAM is subject to a polynomial computation time with respect to n and m, which are the numbers of buyers and sellers, respectively.

5.5.3 Individual Rationality

To validate Theorem 5.2 regarding individual rationality of ICAM, we present the bids and prices of winning buyers in Fig. 5.7(a), and the payments and asks of winning sellers in Fig. 5.7(b). Clearly, each winning buyer is charged a price no higher than its bid, while each winning seller receives a payment no less than its ask from the auctioneer. Therefore, ICAM is individually rational.

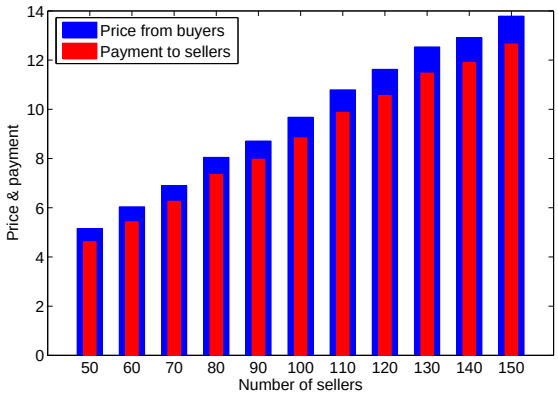

Figure 5.8: Budget balance of ICAM.

5.5.4 Budget Balance

Theorem 5.3 proves that ICAM is budget-balanced, which means that the total price charged to the winning buyers is no less than the total payment rewarded to the winning sellers. Fig. 5.8 shows the total price and the total payment with different settings. Here, we fix the number of buyers to 100, and vary the number of sellers from 50 to 150 with an increment of 10. As seen, the total price from the winning buyers is always greater than the total payment to the winning sellers. Therefore, the auctioneer can conduct the auction without a deficit.

5.5.5 Truthfulness

To verify truthfulness of ICAM, we randomly pick two buyers and two sellers to examine how their utilities change when they bid or ask different values. The results are depicted in Fig. 5.9.

Fig. 5.9(a) shows a case that buyer b_i wins the seller s_j and gains utility $U_i^{\mathrm{b}} = 0.2131$ when it bids truthfully with $D_i^j = V_i^j = 0.7444$. It can be seen that buyer b_i cannot improve its utility no matter what other bids it takes. Fig. 5.9(b) shows a different scenario that buyer b_i does not win the seller s_j when it bids truthfully with $D_i^j = V_i^j = 0.6841$. Thus, b_i achieves zero utility $(U_i^{\mathrm{b}} = 0)$ without having the service. Fig. 5.9(b) shows the utility cannot be greater than zero even when b_i bids untruthfully.

Fig. 5.9(c) shows an example with winning seller s_j that asks truthfully with $A_j = C_j = 0.1706$ and achieves utility $U_j^{\mathrm{s}} = 0.3546$. As seen, the utility with a truthful ask is the highest among all possible asks. Fig. 5.9(d) shows that seller s_j loses when asking truthfully with $A_j = C_j = 0.8564$ and thus obtains zero utility $(U_j^{\mathrm{s}} = 0)$. For all other asks, the achievable utility is either zero or negative, but cannot be more than zero.

In summary, ICAM guarantees truthfulness for both buyers and sellers since the utility cannot be improved by bidding or asking untruthfully.

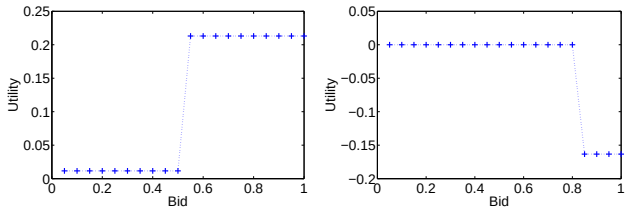

(a) Buyer $b_i \in \mathcal{B}_w$. (b) Buyer $b_i \notin \mathcal{B}_w$.

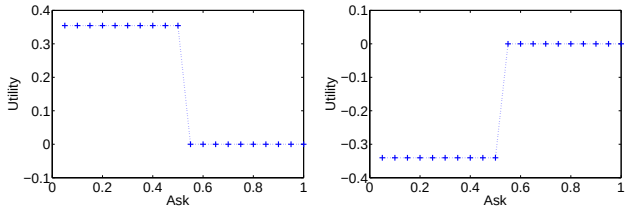

(c) Seller $s_j \in \mathcal{S}_w$. (d) Seller $s_j \notin \mathcal{S}_w$.

Figure 5.9: Truthfulness of buyers and sellers with ICAM.

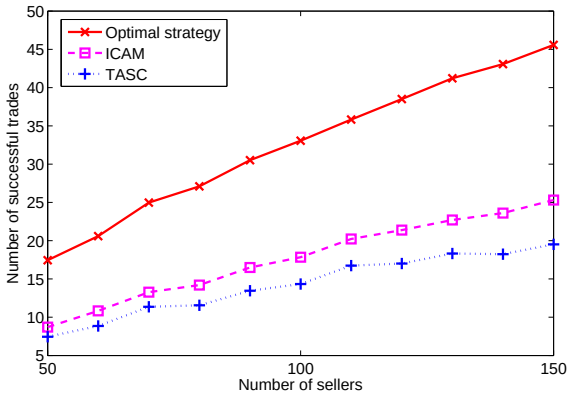

Figure 5.10: System efficiency.

5.5.6 System Efficiency

Both the theoretical proof in Section 5.4 and the numerical results show that ICAM is computationally efficient, individually rational, budget-balanced and truthful. System efficiency is another important metric for an auction mechanism. Unfortunately, it has been shown in [26] that a double auction is impossible to achieve truthfulness, budget balance, and system efficiency simultaneously. Depending on the system requirement, we can evaluate system efficiency in terms of the number of successful trades or the total valuation of winning buyers. Usually, the total valuation is proportional to the number of successful trades, which has been observed in Fig. 5.6. Hence, we focus on the number of successful trades (N_{ST}) in the following to evaluate system efficiency.

Fig. 5.10 compares the number of successful trades among three different auction mechanisms. The optimal strategy refers to the strategy that the auctioneer applies to maximize N_{ST} with complete information. As

seen, ICAM achieves around 50% of the system efficiency of the optimal strategy, where the loss is mainly due to the cost of truthfulness with ICAM. On the other hand, the performance of ICAM is better than that of TASC. This improvement is attributed to the fact that ICAM involves much more winning buyer candidates in the assignment & pricing stage, and removes very few winning players in the winner elimination stage. Therefore, ICAM can achieve all the desirable properties while maintaining a reasonable system efficiency.

5.6 Chapter Summary

In this chapter, we focus on designing a truthful auction mechanism to stimulate wireless devices to serve as relay nodes. Due to spatial distributions of relays and their distinct capabilities, the relays offer heterogeneous valuations toward nearby S-D pairs. Considering the unique features of the application scenario, we propose a double action mechanism ICAM, which coordinates the trading between S-D pairs as service users (buyers) and relays as service providers (sellers). It is proved that ICAM has the desirable properties, including computational efficiency, individual rationality, budget balance, and truthfulness for both buyers and sellers. With the property of truthfulness, ICAM is free of market manipulation, and ensures auction fairness. Besides, the other three properties together guarantee the feasibility of ICAM. Simulation results validate our theoretical analysis and demonstrate that ICAM can achieve a reasonable system efficiency.

Chapter 6

Concluding Remarks

6.1 Conclusions

With rising energy costs and rigid environmental standards, green communications have attracted considerable research attention. As a promising technique, cooperative communications are expected to accommodate green wireless networks. Due to the lack of incentives for wireless devices to serve as relay nodes, cooperative communication techniques are not yet widely used in practice. In this thesis, we studied the two important issues in cooperative MAC to expedite practice of cooperative communications, i.e., energy saving and incentive design. The main research results are summarized as follows:

- We first developed an algorithm to estimate the unknown intensity of relay distribution, which is critical to properly engage cooperating nodes. The convergence and accuracy of the estimation algorithm have been theoretically and numerically justified. Although the backoff-based scheme can save considerable energy consumption when compared to the centralized schemes and probability-based schemes, we found that many relays may be active unnecessarily. Hence, we further proposed a distributed energy saving scheme to minimize energy consumption while maintaining satisfactory transmission success probability. To evaluate the performance of the proposed cooperative scheme with energy saving, we analyzed the collision probability and derived an upper bound. Moreover, the simulation results showed that the energy saving scheme can significantly reduce the energy consumption.
- Extending the widely studied single S-D pair scenario, we considered a new framework where multiple S-D pairs share a group of relays with energy constraint. To satisfy the QoS requirement of multimedia services in a green manner, we proposed an energy-aware distributed cooperative scheme. Besides, we derived the theoretical performance bounds for the proposed scheme with respect to the collision probability and transmission success probability. Extensive simulations were conducted to compare the performance of different distributed schemes and the analytical bounds. As shown in simulation results, by adjusting the weighting parameter ρ, we can achieve good performance in the high traffic load condition through energy balance. Moreover, the theoretical and simulation results demonstrated that our proposed scheme can achieve much energy saving.
- Finally, we proposed a feasible and truthful auction mechanism ICAM for cooperative communications,

where S-D pairs are service users (buyers) and relays are service providers (sellers). It has been proved that ICAM has the desirable properties, including computational efficiency, individual rationality, budget balance, and truthfulness for both buyers and sellers. With computational efficiency, ICAM is guaranteed to be implemented in a polynomial time. With individual rationality, ICAM can benefit both the S-D pairs and the relays. With budget balance, the auctioneer can host and run the auction without a deficit. As seen, these three properties together guarantee the feasibility of ICAM. Besides, with the property of truthfulness, ICAM is free of market manipulation, and ensures auction fairness. Moreover, simulation results confirmed our analysis, and demonstrated that ICAM can achieve the desirable properties while maintaining a reasonable system efficiency.

6.2 Future Work

In this thesis, we have proposed two energy-efficient cooperative MAC schemes to accommodate green communications in wireless networks, and designed a feasible and truthful auction mechanism to stimulate the wireless devices to serve as relays. There are still many open issues and this research can be extended in the following aspects:

- The proposed energy-efficient scheme in Chapter 3 is not optimal, since we set bias for the relays close to destination due to their high transmission success probability. If we take into account the transmission success probability over the relay-destination channel, the energy consumption can be further reduced. To determine the optimal active probability for each relay, global information of the relays is prerequisite, and more complex reasoning is required.
- Extending the widely studied single S-D pair to multiple S-D pairs, we focused on the energy perspective, and thus defined the cooperation capability based on the energy level and the distance metric. Actually, depending on the design objective for the multiple S-D pairs scenario, the cooperation capability can be adapted accordingly. For example, to maximize the throughput of each source, the instantaneous channel state information should be incorporated into the cooperation capability.
- In addition to the three properties (computational efficiency, individual rationality and budget balance) that guarantee the feasibility of an auction mechanism, the proposed ICAM emphasizes the property of truthfulness, which prevents market manipulation and eliminates the strategic overhead of the participants. However, there are few works on incentive design to improve the system efficiency, which is another crucial property of auction mechanisms. Here, in cooperative communications, the system efficiency can be measured in terms of the number of successful trades (i.e., the number of final matchings between S-D pairs and relays) or the social welfare (i.e., the total valuation of S-D pairs that get relaying services).To improve the system efficiency of an incentive mechanism for cooperative communications while maintaining other desirable properties, more efforts are required in future study.

Appendix A

A.1 Extended Proof of Lemma 3.2 with m Relays

Let $p_1, p_2, \ldots, p_m$ be the probabilities that m relays correctly receive a packet from S, and $\zeta_1, \zeta_2, \ldots, \zeta_m$ be the active probabilities of the m relays, respectively. Any unknown ζ_i ($2 \leq i \leq m$) can be determined according to known $\zeta_1, \ldots, \zeta_{i-1}$. Thus, $\zeta_1, \zeta_2, \ldots, \zeta_m$ can be obtained sequentially so as to minimize the overall energy consumption of these m relays.

The average energy consumption of a packet transmission is given by

$$E = \mathcal{P}_1 \cdot E_t + \mathcal{P}_2 \cdot E_r + \mathcal{P}_3 \cdot E$$

where $\mathcal{P}_1$ is the probability that at least one active relay correctly overhears the packet from the source, $\mathcal{P}_2$ is the average number of relays that are active during the packet transmission, and $\mathcal{P}_3$ is the probability that none of the active relays successfully overhears the packet from the source. For m relays, we have

$$\mathcal{P}_1 = 1 - \prod_{i=1}^{m}(1 - p_i\zeta_i), \quad \mathcal{P}_2 = \sum_{i=1}^{m}\zeta_i, \quad \mathcal{P}_3 = 1 - \mathcal{P}_1.$$

Thus, we have

$$E = E_t + \frac{\zeta_1 + \zeta_2 + \cdots + \zeta_m}{1 - (1 - p_1\zeta_1)(1 - p_2\zeta_2)\cdots(1 - p_m\zeta_m)} \cdot E_r.$$

Similar to (3.21)-(3.23), it can be easily inferred that, given known $\zeta_1, \ldots, \zeta_{m-1}$, the active probability ζ_m should be either 0 or 1, so as to minimize the average energy consumption E. The setting of 0 or 1 to ζ_m depends on the successful receiving probability p_m and the status of the other relays.

A.2 Proof of (3.34) and (3.35)

The conditional collision probability P_c is given by (A.1):

$$\begin{aligned}
P_c &= \Pr[r_2 \le r_1 + \varpi] = 1 - \Pr[r_2 > r_1 + \varpi] = 1 - \int_0^{L_0 - w} \int_{r_1+\varpi}^{L_0} g(r_1, r_2) \mathrm{d}r_2 \mathrm{d}r_1 \\
&= 1 - \frac{1}{P_{2^+}} \int_0^{L_0-\varpi} \Bigg\{ \Big[2\lambda r_1 e^{-K(L^2+r_1^2)} \int_0^{\arccos(\frac{r_1}{L})} e^{2KLr_1\cos\theta} \mathrm{d}\theta \Big] \\
&\qquad\qquad \int_{r_1+\varpi}^{L_0} \Big[e^{-\Lambda_{r_2}} \Big(2\lambda r_2 e^{-K(L^2+r_2^2)} \int_0^{\arccos(\frac{r_2}{L})} e^{2KLr_2\cos\theta} \mathrm{d}\theta \Big) \Big] \mathrm{d}r_2 \Bigg\} \mathrm{d}r_1 \\
&= 1 - \frac{1}{P_{2^+}} \int_0^{L_0-\varpi} \Bigg\{ \Big[2\lambda r_1 e^{-K(L^2+r_1^2)} \int_0^{\arccos(\frac{r_1}{L})} e^{2KLr_1\cos\theta} \mathrm{d}\theta \Big] \cdot \Big(e^{-\Lambda_{r_1}} \cdot e^{-\Lambda_{\Delta\varpi}} - e^{-\Lambda_{L_0}} \Big) \Bigg\} \mathrm{d}r_1 \\
&= 1 - \frac{1}{P_{2^+}} \int_0^{\Lambda_{L_0-\varpi}} \Big(e^{-\Lambda_{r_1}} \cdot e^{-\Lambda_{\Delta\varpi}} - e^{-\Lambda_{L_0}} \Big) \mathrm{d}\Lambda_{r_1} \\
&= 1 + \frac{\Lambda_{L_0-\varpi} \cdot e^{-\Lambda_{L_0}}}{P_{2^+}} - \frac{1}{P_{2^+}} \int_0^{\Lambda_{L_0-\varpi}} e^{-\Lambda_{r_1}} \cdot e^{-\Lambda_{\Delta\varpi}} \mathrm{d}\Lambda_{r_1}.
\end{aligned} \tag{A.1}$$

Therefore, (3.34) is proved.

Since $\Lambda_{\Delta\varpi} \le \Gamma$, according to (A.1), we have

$$\begin{aligned}
P_c &\le 1 + \frac{\Lambda_{L_0-\varpi} \cdot e^{-\Lambda_{L_0}}}{P_{2^+}} - \frac{1}{P_{2^+}} \int_0^{\Lambda_{L_0-\varpi}} e^{-\Lambda_{r_1}} \cdot e^{-\Gamma} \mathrm{d}\Lambda_{r_1} \\
&= 1 + \frac{\Lambda_{L_0-\varpi} \cdot e^{-\Lambda_{L_0}}}{P_{2^+}} - \frac{e^{-\Gamma}}{P_{2^+}} \int_0^{\Lambda_{L_0-\varpi}} e^{-\Lambda_{r_1}} \mathrm{d}\Lambda_{r_1} \\
&= 1 + \frac{\Lambda_{L_0-\varpi} \cdot e^{-\Lambda_{L_0}}}{P_{2^+}} - \frac{e^{-\Gamma}}{P_{2^+}} \Big[\big(- e^{-\Lambda_{r_1}} \big) \big|_0^{\Lambda_{L_0-\varpi}} \Big] \\
&= 1 + \frac{\Lambda_{L_0-\varpi} \cdot e^{-\Lambda_{L_0}}}{P_{2^+}} - \frac{e^{-\Gamma}}{P_{2^+}} \big(1 - e^{-\Lambda_{L_0-\varpi}} \big)
\end{aligned} \tag{A.2}$$

which gives the result in (3.35).

Appendix B

B.1 Proof of (4.17)

According to (4.14), when $\rho > c$, we have

$$I_c \;=\; N(N-1)(I_{c_1} + I_{c_2} + I_{c_3}) \tag{B.1}$$

where I_{c_1}, I_{c_2} and I_{c_3} are given by

$$I_{c_1} = \int_c^{\rho} \frac{t}{\rho(1-\rho)} \left[1 - \frac{t^2/2}{\rho(1-\rho)}\right]^{N-2} \frac{(t-c)^2/2}{\rho(1-\rho)} \mathrm{d}t \tag{B.2}$$

$$I_{c_2} = \int_{\rho}^{1-\rho} \frac{1}{1-\rho} \left[1 - \frac{t-\rho/2}{1-\rho}\right]^{N-2} \frac{t-c-\rho/2}{1-\rho} \mathrm{d}t \tag{B.3}$$

$$I_{c_3} = \int_{1-\rho}^{1} \frac{1-t}{\rho(1-\rho)} \left[\frac{(1-t)^2}{2\rho(1-\rho)}\right]^{N-2} \left[1 - \frac{(1-t+c)^2}{2\rho(1-\rho)}\right] \mathrm{d}t. \tag{B.4}$$

As a closed-form expression is not tractable for I_{c_1}, we take $t \leq \rho$ and have

$$\begin{aligned} I_{c_1} \;&\geq\; \int_c^{\rho} \frac{t}{\rho(1-\rho)} \left[1 - \frac{\rho^2/2}{\rho(1-\rho)}\right]^{N-2} \frac{(t-c)^2/2}{\rho(1-\rho)} \mathrm{d}t \\ &=\; \Big(\frac{1}{1-\rho}\Big)^N \Big(1 - \frac{3}{2}\rho\Big)^{N-2} \Big(\rho - c\Big)^3 \Big(\frac{1}{8\rho} + \frac{c}{24\rho^2}\Big). \end{aligned} \tag{B.5}$$

The closed-form expressions of I_{c_2} and I_{c_3} can be obtained as

$$\begin{aligned} I_{c_2} = \Big(\frac{1}{1-\rho}\Big)^N \Bigg\{ &\frac{1-\rho-c}{N-1} \Big[\Big(1 - \frac{3}{2}\rho\Big)^{N-1} - \Big(\frac{\rho}{2}\Big)^{N-1}\Big] \\ &- \frac{1}{N}\Big[\Big(1 - \frac{3}{2}\rho\Big)^{N} - \Big(\frac{\rho}{2}\Big)^{N}\Big] \Bigg\} \end{aligned} \tag{B.6}$$

$$I_{c_3} = \Big(\frac{\rho/2}{1-\rho}\Big)^N \Big(\frac{2}{\rho}\Big) \Big[\frac{2(1-\rho) - c^2/\rho}{2N-2} - \frac{2c}{2N-1} - \frac{\rho}{2N}\Big]. \tag{B.7}$$

The last three equations conclude the proof to (4.17).

B.2 Proof of (4.25)

According to (4.2), we obtain the transmission success probability over the relay-to-destination channel with $\nu = 2$ as

$$P_{RD} \;=\; e^{-Kd^2} \tag{B.8}$$

where $K = T_0 N_0 / P_0$. Given the PDF of d in (4.10), we derive the CDF of P_{RD} by

$$\begin{aligned}
\Pr[P_{RD} \le p] = \Pr[e^{-Kd^2} \le p] &= 1 - \Pr\left[d \le \sqrt{-\frac{\ln p}{K}}\right] \\
&= 1 - \int_0^{\sqrt{-\frac{1}{K}\ln p}} f(x)\mathrm{d}x = 1 - \frac{d^2}{l^2}\Big|_0^{\sqrt{-\frac{1}{K}\ln p}} \\
&= 1 + \frac{P_0}{N_0 T_0 l^2}\ln p.
\end{aligned}$$

Thus, it is easy to show that the probability that a relay has the maximum transmission success probability over the relay-to-destination channel among N candidates is given by (4.25).

Appendix C

C.1 Proof of Lemma 5.1

Given the ask vector of all sellers in $\mathcal{S}$, $\mathbf{A} = (A_1, \ldots, A_m)$, the kth smallest value of $\mathbf{A}$ is denoted by A_{j_k}. Let $\mathbf{A}_{-j} = (A_1, \ldots, A_{j-1}, A_{j+1}, \ldots, A_m)$ be the ask vector excluding the ask A_j of s_j. The $(k-1)$th smallest value of $\mathbf{A}_{-j}$ is denoted by A^{s}. Let $\mathcal{S}_{<k}$ denote the subset of sellers whose asks are less than A_{j_k}.

A truthful ask $(A_j = C_j)$ of seller s_j or any general ask A_j of s_j result in different ask vectors $\mathbf{A} = \mathbf{A}_{-j} \cup \{C_j\}$ or $\mathbf{A} = \mathbf{A}_{-j} \cup \{A_j\}$, respectively. To distinguish A_{j_k} of the ask vector $\mathbf{A}$ with a different ask of s_j, we use A_{j_k} to specifically denote the kth smallest value of $\mathbf{A}_{-j} \cup \{C_j\}$ and $\widetilde{A}_{j_k}$ for the kth smallest value of $\mathbf{A}_{-j} \cup \{A_j\}$. The utilities of s_j with a truthful ask and a general ask are then denoted by U_j^{s} and $\widetilde{U}_j^{\mathrm{s}}$, respectively.

Proposition C.1. *If every seller $s_j \in \mathcal{S}_{<k}$ receives payment A_{j_k} at cost C_j, and every seller $s_j \in \mathcal{S} \setminus \mathcal{S}_{<k}$ receives payment zero at zero cost, then telling truth $(A_j = C_j)$ is a weakly dominant strategy for each seller $s_j \in \mathcal{S}$.*

Proof. We first consider the case with $1 < k < m$, which is further divided into three cases.

- $C_j < A_{j_k}$: We have $C_j < A^{\mathrm{s}}$. If s_j bids truthfully with $A_j = C_j$, its utility is given by $U_j^{\mathrm{s}} = A^{\mathrm{s}} - C_j > 0$. For any general ask A_j, we have
  - If $A_j < \widetilde{A}_{j_k}$, $\widetilde{U}_j^{\mathrm{s}} = A^{\mathrm{s}} - C_j = U_j^{\mathrm{s}}$;
  - If $A_j \geq \widetilde{A}_{j_k}$, $\widetilde{U}_j^{\mathrm{s}} = 0$.
- $C_j = A_{j_k}$: We have $C_j \geq A^{\mathrm{s}}$. Even though s_j bids truthfully, it gains zero utility $(U_j^{\mathrm{s}} = 0)$ since it does not fall within $\mathcal{S}_{<k}$. For any general ask A_j, we have
  - If $A_j < \widetilde{A}_{j_k}$, $\widetilde{U}_j^{\mathrm{s}} = A^{\mathrm{s}} - C_j \leq 0$;
  - If $A_j \geq \widetilde{A}_{j_k}$, $\widetilde{U}_j^{\mathrm{s}} = 0$.
- $C_j > A_{j_k}$: In this case, $C_j > A^{\mathrm{s}}$ and the utility of s_j when asking truthfully is $U_j^{\mathrm{s}} = 0$. For any general ask A_j, we have
  - If $A_j < \widetilde{A}_{j_k}$, $\widetilde{U}_j^{\mathrm{s}} = A^{\mathrm{s}} - C_j < 0$;
  - If $A_j \geq \widetilde{A}_{j_k}$, $\widetilde{U}_j^{\mathrm{s}} = 0$.

As seen in all three cases when $1 < k < m$, telling truth is a weakly dominant strategy for seller s_j since the utility of s_j with a truthful ask (U_j^{s}) is always no less than the utility with any general ask ($\widetilde{U}_j^{\mathrm{s}}$). It can be shown similarly that this conclusion also applies to the cases with $k = 1$ and $k = m$. This completes the proof of Proposition C.1. □

Proposition C.2. *Let $\mathcal{S}_{l_1} \subseteq \mathcal{S}_{<k}$ be the subset of sellers that no buyers bid for them with a price of at least A_{j_k}. If every seller $s_j \in \mathcal{S}_{<k} \setminus \mathcal{S}_{l_1}$ receives payment A_{j_k} at cost C_j, and every seller $s_j \in \mathcal{S}_{l_1} \cup \{\mathcal{S} \setminus \mathcal{S}_{<k}\}$ receives payment zero at zero cost, then telling truth $(A_j = C_j)$ is a weakly dominant strategy for each seller $s_j \in \mathcal{S}$.*

Proof. We can follow a logic similar to the proof of Proposition C.1. If seller s_j asks truthfully and falls into set $\mathcal{S} \setminus \mathcal{S}_{<k}$, it can be easily shown that telling truth is a weakly dominant strategy for seller s_j, according to Proposition C.1.

If seller s_j asks truthfully and falls into set $\mathcal{S}_{<k}$, we have $C_j < A^{\mathrm{s}}$ and $A_{j_k} = A^{\mathrm{s}}$. Then, there are two cases in the following.

- $s_j \in \mathcal{S}_{l_1}$ when asking truthfully: s_j achieves utility $U_j^{\mathrm{s}} = 0$. Then, a general ask of s_j may result in two possible subcases.
  - $A_j < A^{\mathrm{s}}$: We still have $\widetilde{A}_{j_k} = A_{j_k} = A^{\mathrm{s}}$ and $s_j \in \mathcal{S}_{l_1}$. Thus, $\widetilde{U}_j^{\mathrm{s}} = 0$.
  - $A_j \geq A^{\mathrm{s}}$: We have $s_j \in \mathcal{S} \setminus \mathcal{S}_{<k}$ and $\widetilde{U}_j^{\mathrm{s}} = 0$.
- $s_j \in \mathcal{S}_{<k} \setminus \mathcal{S}_{l_1}$ when asking truthfully: s_j achieves utility $U_j^{\mathrm{s}} = A^{\mathrm{s}} - C_j > 0$. Similar to the preceding case, there are two subcases with a general ask of s_j.
  - $A_j < A^{\mathrm{s}}$: We still have $\widetilde{A}_{j_k} = A_{j_k} = A^{\mathrm{s}}$. Thus, s_j stays in $\mathcal{S}_{<k} \setminus \mathcal{S}_{l_1}$ and its utility $\widetilde{U}_j^{\mathrm{s}} = A^{\mathrm{s}} - C_j = U_j^{\mathrm{s}}$.
  - $A_j \geq A^{\mathrm{s}}$: We have $s_j \in \mathcal{S} \setminus \mathcal{S}_{<k}$ and $\widetilde{U}_j^{\mathrm{s}} = 0$.

As seen from both cases, telling truth is a weakly dominant strategy for seller s_j because $U_j^{\mathrm{s}} \geq \widetilde{U}_j^{\mathrm{s}}$.

Therefore, Proposition C.2 is proved. □

Proposition C.3. *Let $\mathcal{S}_{l_2} \subseteq \{\mathcal{S}_{<k} \setminus \mathcal{S}_{l_1}\}$ be the subset of sellers, so that for each seller $s_j \in \mathcal{S}_{l_2}$, buyer b_i with the highest bid for s_j chooses a seller, $s_{j'} \in \{\mathcal{S}_{<k} \setminus \mathcal{S}_{l_1}\} \setminus \mathcal{S}_{l_2}$, to achieve utility $U_{ij'}^{\mathrm{b}} \geq U_{ij}^{\mathrm{b}}$. Besides, the utility U_{ij}^{b} of buyer b_i on seller s_j depends on a bid $D_{i'}^j$ $(D_{i'}^j \geq A_{j_k})$. If every seller $s_j \in \{\mathcal{S}_{<k} \setminus \mathcal{S}_{l_1}\} \setminus \mathcal{S}_{l_2}$ receives payment A_{j_k} at cost C_j, and every seller $s_j \in \mathcal{S}_{l_2} \cup \mathcal{S}_{l_1} \cup \{\mathcal{S} \setminus \mathcal{S}_{<k}\}$ receives payment zero at zero cost, then telling truth $(A_j = C_j)$ is a weakly dominant strategy for each seller $s_j \in \mathcal{S}$.*

Proof. For the case that seller $s_j \in \mathcal{S} \setminus \mathcal{S}_{<k}$ when asking truthfully, Proposition C.1 already shows that telling truth is a weakly dominant strategy for seller s_j. On the other hand, if $s_j \in \mathcal{S}_{<k}$, it implies that $C_j < A^{\mathrm{s}}$ and $A_{j_k} = A^{\mathrm{s}}$. Then, there are three cases in the following.

- $s_j \in \mathcal{S}_{l_1}$ with a truthful ask: Proposition C.2 can be referred to easily show that telling truth is a weakly dominant strategy for seller s_j.

- $s_j \in \mathcal{S}_{l_2}$ with a truthful ask: s_j achieves utility $U_j^{\mathrm{s}} = 0$. In contrast, there are two subcases resulting from a general ask of s_j.
  - $A_j < A^{\mathrm{s}}$: We still have $\widetilde{A}_{j_k} = A_{j_k} = A^{\mathrm{s}}$, and $\widetilde{U}_{ij}^{\mathrm{b}}$ remains unchanged, since $\widetilde{U}_{ij}^{\mathrm{b}}$ depends on a bid $D_{i'}^j$ ($D_{i'}^j \geq A_{j_k}$). Thus, b_i still chooses $s_{j'}$ with $\widetilde{U}_{ij'}^{\mathrm{b}} \geq \widetilde{U}_{ij}^{\mathrm{b}}$. Then, $s_j \in \mathcal{S}_{l_2}$ and $\widetilde{U}_j^{\mathrm{s}} = 0$.
  - $A_j \geq A^{\mathrm{s}}$: We have $s_j \in \mathcal{S} \setminus \mathcal{S}_{<k}$ and $\widetilde{U}_j^{\mathrm{s}} = 0$.
- $s_j \in \{\mathcal{S}_{<k} \setminus \mathcal{S}_{l_1}\} \setminus \mathcal{S}_{l_2}$ with a truthful ask: s_j achieves utility $U_j^{\mathrm{s}} = A^{\mathrm{s}} - C_j > 0$. On the other hand, there are two subcases with a general ask of s_j.
  - $A_j < A^{\mathrm{s}}$: We still have $\widetilde{A}_{j_k} = A_{j_k} = A^{\mathrm{s}}$. Thus, $s_j \in \{\mathcal{S}_{<k} \setminus \mathcal{S}_{l_1}\} \setminus \mathcal{S}_{l_2}$ and $\widetilde{U}_j^{\mathrm{s}} = A^{\mathrm{s}} - C_j = U_j^{\mathrm{s}}$.
  - $A_j \geq A^{\mathrm{s}}$: We have $s_j \in \mathcal{S} \setminus \mathcal{S}_{<k}$ and $\widetilde{U}_j^{\mathrm{s}} = 0$.

Comparing the utilities of truthful asks to those of general asks which may deviate from true costs, we can conclude that telling truth is a weakly dominant strategy for seller s_j. This completes the proof of Proposition C.3. □

C.2 Proof of Lemma 5.2

Based on the original buyer set $\mathcal{B} = \{b_1, b_2, \ldots, b_n\}$, we construct a new buyer set $\mathcal{B}' = \{b_{ij} : D_i^j > 0, b_i \in \mathcal{B}\}$, where D_i^j is the bid of b_i on s_j. Obviously, $b_{ij} \in \mathcal{B}'$ corresponds to $b_i \in \mathcal{B}$. Let $\mathcal{B}_\varphi \subseteq \mathcal{B}'$ be the subset of buyers that have bids of at least D_φ, where D_φ is *independent* of the overall bidding matrix $\mathbf{D}$ of all buyers. Similar to Appendix C.1, we use U_{ij}^{b} and $\widetilde{U}_{ij}^{\mathrm{b}}$ to denote the utility of buyer b_i with a truthful bid for seller s_j and the corresponding utility with a general bid, respectively. We have the following four propositions related to truthfulness of buyers.

Proposition C.4. *If every buyer, $b_{ij} \in \mathcal{B}_\varphi$, pays D_φ to use the service from seller s_j, and every buyer, $b_{ij} \in \mathcal{B}' \setminus \mathcal{B}_\varphi$, pays zero for not having the service from s_j, then telling truth ($D_i^j = V_i^j$) is a weakly dominant strategy for every buyer $b_{ij} \in \mathcal{B}'$.*

Proof. There are two cases for buyer b_{ij}, depending on how its true valuation V_i^j is related to D_φ.

- $V_i^j < D_\varphi$: If b_{ij} submits a truthful bid V_i^j, it receives utility $U_{ij}^{\mathrm{b}} = 0$ because $b_{ij} \in \mathcal{B}' \setminus \mathcal{B}_\varphi$ with a bid less than D_φ. For any general bid D_i^j, there are two subcases.
  - $D_i^j < D_\varphi$: We still have $b_{ij} \in \mathcal{B}' \setminus \mathcal{B}_\varphi$ and $\widetilde{U}_{ij}^{\mathrm{b}} = 0$.
  - $D_i^j \geq D_\varphi$: We have $b_{ij} \in \mathcal{B}_\varphi$, and buyer b_{ij} wins the service from s_j at price D_φ. The utility becomes $\widetilde{U}_{ij}^{\mathrm{b}} = V_i^j - D_\varphi < 0$.
- $V_i^j \geq D_\varphi$: A truthful bid of b_{ij} results in utility $U_{ij}^{\mathrm{b}} = V_i^j - D_\varphi \geq 0$, because b_{ij} wins the service from s_j and thus $b_{ij} \in \mathcal{B}_\varphi$. There are also two subcases with a general bid D_i^j.

- $D_i^j < D_\varphi$: We have $b_{ij} \in \mathcal{B}' \setminus \mathcal{B}_\varphi$ and $\widetilde{U}_{ij}^{\mathrm{b}} = 0$.
- $D_i^j \geq D_\varphi$: In this situation, b_{ij} wins the service from s_j at price D_φ. Thus, $\widetilde{U}_{ij}^{\mathrm{b}} = V_i^j - D_\varphi = U_{ij}^{\mathrm{b}}$.

As seen, telling truth is a weakly dominant strategy for buyer b_{ij} since the utility is always maximized with a truthful bid. This completes the proof of Proposition C.4. □

Proposition C.5. *Let $B_{l_1} \subseteq \mathcal{B}_\varphi$ be the subset of buyers, such that for each buyer $b_{ij} \in \mathcal{B}_{l_1}$, the ask of seller s_j is at least A_φ, where A_φ is independent of $\mathbf{D}$. If every buyer, $b_{ij} \in \mathcal{B}_\varphi \setminus \mathcal{B}_{l_1}$, pays D_φ to use the service from s_j, and every buyer, $b_{ij} \in \mathcal{B}_{l_1} \cup \{\mathcal{B}' \setminus \mathcal{B}_\varphi\}$, pays zero for not having the service from s_j, telling truth $(D_i^j = V_i^j)$ is a weakly dominant strategy for each buyer $b_{ij} \in \mathcal{B}'$.*

Proof. If buyer b_{ij} bids truthfully and falls into set $\mathcal{B}' \setminus \mathcal{B}_\varphi$, i.e., $V_i^j < D_\varphi$, it can be easily shown by Proposition C.4 that telling truth is a weakly dominant strategy for buyer b_{ij}. On the other hand, if a truthful buyer belongs to set $\mathcal{B}_\varphi$, i.e., $V_i^j \geq D_\varphi$, there are two cases.

- $b_{ij} \in \mathcal{B}_{l_1}$ with a truthful bid: b_{ij} receives utility $U_{ij}^{\mathrm{b}} = 0$ without winning the service from s_j. A general bid of b_{ij} may result in two subcases.
  - $D_i^j \geq D_\varphi$: We still have $b_{ij} \in \mathcal{B}_{l_1}$ and $\widetilde{U}_{ij}^{\mathrm{b}} = 0$.
  - $D_i^j < D_\varphi$: We have $b_{ij} \in \mathcal{B}' \setminus \mathcal{B}_\varphi$ and $\widetilde{U}_{ij}^{\mathrm{b}} = 0$.
- $b_{ij} \in \mathcal{B}_\varphi \setminus \mathcal{B}_{l_1}$ with a truthful bid: b_{ij} receives utility $U_{ij}^{\mathrm{b}} = V_i^j - D_\varphi \geq 0$. Similarly, there are two subcases with a general bid of b_{ij}.
  - $D_i^j \geq D_\varphi$: We still have $b_{ij} \in \mathcal{B}_\varphi \setminus \mathcal{B}_{l_1}$ and $\widetilde{U}_{ij}^{\mathrm{b}} = V_i^j - D_\varphi = U_{ij}^{\mathrm{b}}$.
  - $D_i^j < D_\varphi$: We have $b_{ij} \in \mathcal{B}' \setminus \mathcal{B}_\varphi$ and $\widetilde{U}_{ij}^{\mathrm{b}} = 0$.

Therefore, telling truth is a weakly dominant strategy for buyer $b_{ij} \in \mathcal{B}'$ because its utility U_{ij}^{b} with a truthful bid is always no less than its utility $\widetilde{U}_{ij}^{\mathrm{b}}$ with any general bid. This completes the proof of Proposition C.5. □

Proposition C.6. *Let $\mathcal{B}_{l_2} \subseteq \{\mathcal{B}_\varphi \setminus \mathcal{B}_{l_1}\}$ be the subset of buyers, such that for each buyer, $b_{ij} \in \mathcal{B}_{l_2}$, there is a buyer $b_{i'j} \in \{\mathcal{B}_\varphi \setminus \mathcal{B}_{l_1}\} \setminus \mathcal{B}_{l_2}$ with $D_{i'}^j \geq D_i^j$. If every buyer, $b_{ij} \in \{\mathcal{B}_\varphi \setminus \mathcal{B}_{l_1}\} \setminus \mathcal{B}_{l_2}$, pays P_{ij}^{b} $(D_\varphi \leq P_{ij}^{\mathrm{b}} \leq D_i^j$, and P_{ij}^{b} is the smallest value that is no less than any other buyer's bid on $s_j)$ to use the service from s_j, and every buyer $b_{ij} \in \mathcal{B}_{l_2} \cup \mathcal{B}_{l_1} \cup \{\mathcal{B}' \setminus \mathcal{B}_\varphi\}$ pays zero without having the service from s_j, then telling truth $(D_i^j = V_i^j)$ is a weakly dominant strategy for each buyer $b_{ij} \in \mathcal{B}'$.*

Proof. If buyer b_{ij} belongs to set $\mathcal{B}' \setminus \mathcal{B}_\varphi$ when bidding truthfully, i.e., $V_i^j < D_\varphi$, telling truth is a weakly dominant strategy for buyer b_{ij} according to Proposition C.4. On the other hand, if $b_{ij} \in \mathcal{B}_\varphi$ with a truthful bid, i.e., $V_i^j \geq D_\varphi$, there are three cases.

- $b_{ij} \in \mathcal{B}_{l_1}$ with a truthful bid: According to Proposition C.5, telling truth is a weakly dominant strategy for buyer b_{ij}.

- $b_{ij} \in \mathcal{B}_{l_2}$ with a truthful bid: b_{ij} achieves utility $U^{\mathrm{b}}_{ij} = 0$. This also implies that there exists a buyer $b_{i'j} \in \{\mathcal{B}_\varphi \setminus \mathcal{B}_{l_1}\} \setminus \mathcal{B}_{l_2}$, who wins the service from s_j with $D^j_{i'} \geq V^j_i \geq D_\varphi$. Next, consider three subcases with a general bid of b_{ij}.
  - $b_{ij} \in \{\mathcal{B}_\varphi \setminus \mathcal{B}_{l_1}\} \setminus \mathcal{B}_{l_2}$: Since b_{ij} wins the service and pays P^{b}_{ij}, it means that P^{b}_{ij} should be no less than any other buyer's bid on s_j. Thus, $P^{\mathrm{b}}_{ij} \geq D^j_{i'} \geq V^j_i$. This results in utility $\widetilde{U}^{\mathrm{b}}_{ij} = V^j_i - P^{\mathrm{b}}_{ij} \leq 0$.
  - $b_{ij} \in \mathcal{B}_{l_2}$: We still have $\widetilde{U}^{\mathrm{b}}_{ij} = 0$.
  - $b_{ij} \in \mathcal{B}' \setminus \mathcal{B}_\varphi$: We have $\widetilde{U}^{\mathrm{b}}_{ij} = 0$.
- $b_{ij} \in \{\mathcal{B}_\varphi \setminus \mathcal{B}_{l_1}\} \setminus \mathcal{B}_{l_2}$ with a truthful bid: Because $V^j_i = D^j_i \geq P^{\mathrm{b}}_{ij}$, b_{ij} achieves utility $U^{\mathrm{b}}_{ij} = V^j_i - P^{\mathrm{b}}_{ij} \geq 0$. Similarly, three subcases exist with a general bid of b_{ij}.
  - $b_{ij} \in \{\mathcal{B}_\varphi \setminus \mathcal{B}_{l_1}\} \setminus \mathcal{B}_{l_2}$: Since the price P^{b}_{ij} charged to b_{ij} is not affected and remains the same, we still have $\widetilde{U}^{\mathrm{b}}_{ij} = V^j_i - P^{\mathrm{b}}_{ij} = U^{\mathrm{b}}_{ij}$.
  - $b_{ij} \in \mathcal{B}_{l_2}$: We have $\widetilde{U}^{\mathrm{b}}_{ij} = 0$.
  - $b_{ij} \in \mathcal{B}' \setminus \mathcal{B}_\varphi$: We have $\widetilde{U}^{\mathrm{b}}_{ij} = 0$.

As seen above, it always holds that $U^{\mathrm{b}}_{ij} \geq \widetilde{U}^{\mathrm{b}}_{ij}$. Therefore, telling truth is a weakly dominant strategy for buyer $b_{ij} \in \mathcal{B}'$. This completes the proof of Proposition C.6. □

Proposition C.7. *For a buyer $b_i \in \mathcal{B}$ with $b_{i\alpha} \in \{\mathcal{B}_\varphi \setminus \mathcal{B}_{l_1}\} \setminus \mathcal{B}_{l_2}$ and $b_{i\beta} \in \{\mathcal{B}_\varphi \setminus \mathcal{B}_{l_1}\} \setminus \mathcal{B}_{l_2}$, if b_i can only obtain service from the seller which provides b_i a higher utility (or a randomly selected seller when there is a tie), telling truth with $(D^\alpha_i, D^\beta_i) = (V^\alpha_i, V^\beta_i)$ is a weakly dominant strategy for the buyer $b_i \in \mathcal{B}$.*

Proof. Let $P^{\mathrm{b}}_{i\alpha}$ be the payment of $b_{i\alpha}$ to use the service from s_α, and $P^{\mathrm{b}}_{i\alpha}$ be the payment of $b_{i\beta}$ to use the service from s_β. Then, we have the utilities of buyer b_i with respect to seller s_α and seller s_β: $U^{\mathrm{b}}_{i\alpha} = V^\alpha_i - P^{\mathrm{b}}_{i\alpha}$ and $U^{\mathrm{b}}_{i\beta} = V^\beta_i - P^{\mathrm{b}}_{i\beta}$, respectively. Without loss of generality, assuming that $U^{\mathrm{b}}_{i\alpha} \geq U^{\mathrm{b}}_{i\beta}$, we have $U^{\mathrm{b}}_i = U^{\mathrm{b}}_{i\alpha}$ if b_i bids truthfully. On the other hand, a general bid of b_i may lead to four possible cases.

- $b_{i\alpha} \in \{\mathcal{B}_\varphi \setminus \mathcal{B}_{l_1}\} \setminus \mathcal{B}_{l_2}$ and $b_{i\beta} \in \{\mathcal{B}_\varphi \setminus \mathcal{B}_{l_1}\} \setminus \mathcal{B}_{l_2}$: $b_{i\alpha}$ still needs to pay $P^{\mathrm{b}}_{i\alpha}$ to use the service from s_α, while $b_{i\beta}$ still needs to pay $P^{\mathrm{b}}_{i\beta}$ to use the service from s_β. Thus, $U^{\mathrm{b}}_{i\alpha}$ and $U^{\mathrm{b}}_{i\beta}$ remain unchanged. According to the bids D^α_i and D^β_i, there are three subcases.
  - If $D^\alpha_i - P^{\mathrm{b}}_{i\alpha} > D^\beta_i - P^{\mathrm{b}}_{i\beta}$, we have $\widetilde{U}^{\mathrm{b}}_i = U^{\mathrm{b}}_{i\alpha}$.
  - If $D^\alpha_i - P^{\mathrm{b}}_{i\alpha} = D^\beta_i - P^{\mathrm{b}}_{i\beta}$, we have $\widetilde{U}^{\mathrm{b}}_i = U^{\mathrm{b}}_{i\alpha}$ or $U^{\mathrm{b}}_i = U^{\mathrm{b}}_{i\beta}$.
  - If $D^\alpha_i - P^{\mathrm{b}}_{i\alpha} < D^\beta_i - P^{\mathrm{b}}_{i\beta}$, we have $\widetilde{U}^{\mathrm{b}}_i = U^{\mathrm{b}}_{i\beta}$.
- $b_{i\alpha} \in \{\mathcal{B}_\varphi \setminus \mathcal{B}_{l_1}\} \setminus \mathcal{B}_{l_2}$ and $b_{i\beta} \notin \{\mathcal{B}_\varphi \setminus \mathcal{B}_{l_1}\} \setminus \mathcal{B}_{l_2}$: $U^{\mathrm{b}}_{i\alpha}$ remains unchanged since buyer $b_{i\alpha}$ still needs to pay $P^{\mathrm{b}}_{i\alpha}$ to use the service from s_α, whereas $U^{\mathrm{b}}_{i\beta}$ becomes 0. Thus, we still have $\widetilde{U}^{\mathrm{b}}_i = U^{\mathrm{b}}_{i\alpha}$.

- $b_{i\alpha} \notin \{\mathcal{B}_\varphi \setminus \mathcal{B}_{l_1}\} \setminus \mathcal{B}_{l_2}$ and $b_{i\beta} \in \{\mathcal{B}_\varphi \setminus \mathcal{B}_{l_1}\} \setminus \mathcal{B}_{l_2}$: This is an opposite of the above subcase. Here, $U_{i\alpha}^{\mathrm{b}}$ becomes 0, while $U_{i\beta}^{\mathrm{b}}$ remains unchanged since buyer $b_{i\beta}$ still needs to pay $P_{i\beta}^{\mathrm{b}}$ to use the service from s_β. Thus, we have $\widetilde{U}_i^{\mathrm{b}} = U_{i\beta}^{\mathrm{b}}$.
- $b_{i\alpha} \notin \{\mathcal{B}_\varphi \setminus \mathcal{B}_{l_1}\} \setminus \mathcal{B}_{l_2}$ and $b_{i\beta} \notin \{\mathcal{B}_\varphi \setminus \mathcal{B}_{l_1}\} \setminus \mathcal{B}_{l_2}$: Both $U_{i\alpha}^{\mathrm{b}}$ and $U_{i\beta}^{\mathrm{b}}$ become 0, so we have $\widetilde{U}_i^{\mathrm{b}} = 0$.

When selecting a seller which provides a higher utility to a buyer b_i, we can see that telling truth is a weakly dominant strategy for buyer b_i since $U_i^{\mathrm{b}} \geq \widetilde{U}_i^{\mathrm{b}}$ for all the cases. This concludes our proof of Proposition C.7. □

Bibliography

[1] B. P. Crow, I. Widjaja, L. G. Kim, and P. T. Sakai, "IEEE 802.11 wireless local area networks," *IEEE Communications Magazine*, vol. 35, pp. 116–126, 1997.

[2] D. Gesbert, M. Shafi, D. shan Shiu, P. J. Smith, and A. Naguib, "From theory to practice: An overview of MIMO space-time coded wireless systems," *IEEE J. Select. Areas Communications*, vol. 21, no. 3, pp. 281–302, 2003.

[3] S. Cui, A. J. Goldsmith, and A. Bahai, "Energy-efficiency of MIMO and cooperative MIMO techniques in sensor networks," *IEEE J. Select. Areas Communications*, vol. 22, no. 6, pp. 1089–1098, 2004.

[4] J. N. Laneman, D. N. C. Tse, and G. W. Wornell, "Cooperative diversity in wireless networks: Efficient protocols and outage behavior," *IEEE Trans. Information Theory*, vol. 50, pp. 3062–3080, Dec. 2004.

[5] A. Nosratinia, T. E. Hunter, and A. Hedayat, "Cooperative communication in wireless networks," *IEEE Communications Magazine*, vol. 42, pp. 74–80, Oct. 2004.

[6] S. Alamouti, "A simple transmit diversity technique for wireless communications," *IEEE J. Select. Areas Communications*, vol. 16, no. 8, pp. 1451–1458, 1998.

[7] W. Zhuang and M. Ismail, "Cooperation in wireless communication networks," *IEEE Wireless Communications*, vol. 19, no. 2, pp. 10–20, Apr. 2012.

[8] P. Liu, Z. Tao, S. Narayanan, T. Korakis, and S. S. Panwar, "CoopMAC: A cooperative MAC for wireless LANs," *IEEE J. Select. Areas Communications*, vol. 25, no. 2, pp. 340–354, Feb. 2007.

[9] H. Shan, W. Zhuang, and Z. Wang, "Distributed cooperative MAC for multihop wireless networks," *IEEE Communications Magazine*, vol. 47, pp. 126–133, Feb. 2009.

[10] Y. Li, P. Wang, D. Niyato, and W. Zhuang, "A hierarchical framework of dynamic relay selection for mobile users and profit maximization for service providers in wireless relay networks," *Wireless Communications and Mobile Computing*, 2013, to appear.

[11] Q. Du and X. Zhang, "QoS-aware base-station selections for distributed MIMO links in broadband wireless networks," *IEEE J. Select. Areas Communications*, vol. 29, no. 6, pp. 1123–1138, May 2011.

[12] C. Zhai, W. Zhang, and G. Mao, "Uncoordinated cooperative communications with spatially random relays," *IEEE Trans. Wireless Communications*, vol. 11, no. 9, pp. 3126–3135, Sep. 2012.

[13] L. Xiong, L. Libman, and G. Mao, "Uncoordinated cooperative communications in highly dynamic wireless networks," *IEEE J. Select. Areas Communications*, vol. 30, no. 2, pp. 280–288, Feb. 2012.

[14] W. Song and W. Zhuang, "Performance analysis and enhancement of cooperative retransmission strategy for delay-sensitive real-time services," in *Proc. IEEE GLOBECOM*, Dec. 2009.

[15] H. Shan, H. Cheng, and W. Zhuang, "Cross-layer cooperative MAC protocol in distributed wireless networks," *IEEE Trans. Wireless Communications*, vol. 10, no. 8, pp. 2603–2615, Aug. 2011.

[16] A. Bletsas, A. Khisti, D. P. Reed, and A. Lippman, "A simple cooperative diversity method based on network path selection," *IEEE J. Select. Areas Communications*, vol. 24, no. 3, pp. 659–672, Mar. 2006.

[17] F. R. Yu, X. Zhang, and V. C. M. Leung, *Green Communications and Networking*. CRC Press, 2012.

[18] M. Gursoy, D. Qiao, and S. Velipasalar, "Analysis of energy efficiency in fading channels under QoS constraints," *IEEE Trans. Wireless Communications*, vol. 8, no. 8, pp. 4252–4263, Aug. 2009.

[19] V. Krishna, *Auction Theory*, 2nd ed. Academic Press, Aug. 2009.

[20] Y. Zhang, C. Lee, D. Niyato, and P. Wang, "Auction approaches for resource allocation in wireless systems: A survey," *IEEE Communications Surveys & Tutorials*, vol. 15, no. 3, pp. 1020–1041, 2013.

[21] L. M. Ausubel, "An efficient dynamic auction for heterogeneous commodities," *American Economic Review*, vol. 96, no. 3, pp. 602–629, 2006.

[22] G. Demange, D. Gale, and M. Sotomayor, "Multi-item auctions," *Journal of Political Economy*, vol. 94, pp. 863–872, 1986.

[23] D. Mishra and R. Garg, "Descending price multi-item auctions," *Journal of Mathematical Economics*, vol. 42, pp. 161–179, 2006.

[24] R. P. McAfee, "A dominant strategy double auction," *Journal of Economic Theory*, vol. 56, pp. 434–450, Apr. 1992.

[25] D. Parkes, J. Kalagnanam, and M. Eso, "Achieving budget-balance with Vickrey-based payment schemes in exchanges," in *Proc. International Joint Conference on Artificial Intelligence*, 2001, pp. 1161–1168.

[26] R. B. Myerson and M. A. Satterthwaite, "Efficient mechanisms for bilateral trading," *Journal of Economic Theory*, vol. 29, no. 2, pp. 265–281, Apr. 1983.

[27] D. Yang, X. Fang, and G. Xue, "Truthful auction for cooperative communications," in *Proc. MobiHoc*, 2011, http://inside.mines.edu/~djyang/doc/MOBIHOC2011-TASC.pdf.

[28] P. Ju, W. Song, and D. Zhou, "Survey on cooperative medium access control protocols," *IET Communications*, vol. 7, no. 9, pp. 893–902, Jun. 2013.

[29] Y. Li, P. Wang, D. Niyato, and W. Zhuang, "A dynamic relay selection scheme for mobile users in wireless relay networks," in *Proc. IEEE INFOCOM Workshop*, 2011.

[30] K. Vardhe, D. Reynolds, and B. Woerner, "Joint power allocation and relay selection for multiuser cooperative communication," *IEEE Trans. Wireless Communications*, vol. 9, no. 4, pp. 1255–1260, Apr. 2010.

[31] A. Ribeiro, N. Sidiropoulos, and G. Giannakis, "Optimal distributed stochastic routing algorithms for wireless multihop networks," *IEEE Trans. Wireless Communications*, vol. 7, no. 11, pp. 4261–4272, 2008.

[32] B. Chen, K. Jamieson, H. Balakrishnan, and R. Morris, "Span: An energy-efficient algorithm for topology maintenance in ad hoc wireless networks," *ACM Wireless Networks*, vol. 8, no. 5, Sep. 2002.

[33] Y. Xu, J. Heidemann, and D. Estrin, "Geography-informed energy conservation for ad hoc routing," in *Proc. ACM MOBICOM*, 2001.

[34] M. Zorzi and R. R. Rao, "Geographic random forwarding (GeRaF) for ad hoc and sensor networks: Energy and latency performance," *IEEE Trans. Mobile Computing*, vol. 2, no. 4, pp. 349–365, Oct. 2003.

[35] W. Vickrey, "Counterspeculation, auctions, and competitive sealed tenders," *The Journal of Finance*, vol. 16, pp. 8–37, 1961.

[36] E. H. Clarke, "Multipart pricing of public goods," *Public Choice*, vol. 11, pp. 17–33, 1971.

[37] T. Groves, "Incentives in teams," *Econometrica*, vol. 41, no. 4, pp. 617–631, Jul. 1973.

[38] Y. Shi, S. Sharma, Y. T. Hou, and S. Kompella, "Optimal relay assignment for cooperative communications," in *Proc. MobiHoc*, 2008.

[39] D. West, *Introduction to Graph Theory*, 2nd ed. Prentice Hall, 1999.

[40] L. Xiong, L. Libman, and G. Mao, "Optimal strategies for cooperative MAC-layer retransmission in wireless networks," in *Proc. IEEE WCNC*, Mar. 2008.

[41] R. K. Ganti and M. Haenggi, "Analysis of uncoordinated opportunistic two-hop wireless ad hoc systems," in *Proc. IEEE ISIT*, Jun. 2009.

[42] G. Carofiglio, C. Chiasserini, M. Garetto, and E. Leonardi, "Route stability in MANETs under the random direction mobility model," *IEEE Trans. Mobile Computing*, vol. 8, no. 9, pp. 1167–1179, Sep. 2009.

[43] G. Mao, B. Fidan, and B. Anderson, "Wireless sensor network localization techniques," *Computer Networks*, vol. 51, pp. 2529–2553, Jul. 2007.

[44] Z. Chen, G. Gokeda, and Y. Yu, *Introduction to Direction-of-Arrival Estimation*. Artech House, 2010.

[45] D. Stoyan, W. Kendall, and J. Mecke, *Stochastic Geometry and Its Applications*, 2nd ed. John Wiley and Sons, 1996.

[46] S. Narayanan and S. S. Panwar, "To forward or not to forward – That is the question," *Wireless Personal Communications*, vol. 43, no. 1, pp. 65–87, 2007.

[47] P. Nain, D. Towsley, B. Liu, and Z. Liu, "Properties of random direction models," in *Proc. IEEE INFOCOM*, vol. 3, Mar. 2005.

[48] Y. Cheng, X. Ling, L. Cai, W. Song, W. Zhuang, X. Shen, and A. Leon-Garcia, "Statistical multiplexing, admission region, and contention window optimization in multiclass wireless LANs," *ACM Wireless Networks*, vol. 15, no. 1, pp. 73–86, 2009.

[49] Y. Zhao, R. Adve, and T. J. Lim, "Improving amplify-and-forward relay networks: Optimal power allocation versus selection," *IEEE Trans. Wireless Communications*, vol. 6, no. 8, pp. 3114–3123, Aug. 2007.